Discovery of QUARK-GLUON PLASMA

Johann Rafelski
Department of Physics, University of ARIZONA, Tucson

REPORTING WORK CARRIED OUT WITH

Mike Fromerth, Giorgio Torrieri, and Jean Letessier (Paris)

Landek Zdrój, February 2-12, 2003

[I] INTRODUCTION: RHI-collisions and facilities, observables, strangeness, spectra, statistical hadronization (32)

[II] EQUATIONS OF STATE: Statistical physics, quark-gluon gas, QCD interactions, QGP, hadron gas, supercooling (64)

[III] STRANGENESS: kinetic strangeness production, hadronization, particle yields, $m_\perp$ spectra, resonances (97)

[I] QUARK-HADRON UNIVERSE: time constant, constraints and potentials, particle abundances, distillation, baryon-antibaryon

supported by a grant from the U.S. Department of Energy, DE-FG03-95ER40937.
Some reprints available.

WHAT YOU NEED TO REVIEW

This is a very interdisciplinary subject matter:

attempt to answer the test questions quantitatively:

- **Relativity:** is Lorentz-contraction of space or body of matter; what is proper time, rapidity?
- **Relativistic Statistical Physics:** Is $3P \geq \varepsilon$ or $3P \leq \varepsilon$?
- **Nuclear Physics:** what is quark content of a hyperon?
- **Particle Physics:**
  what is evidence that gluons are charged, confined particles?
- **Quantum Field Theory (for pedestrians):**
  How strong is strong interaction α_s in quark-gluon plasma?
- **Cosmology:**
  when did quark Universe hadronize – what fixes the time scale!
- **Astrophysics:** why is not every neutron star a quark star, and conversely are any quark stars around?

TWO REASONS FOR THIS NEW NUCLEAR-PARTICLE FIELD:

Short History of the Universe

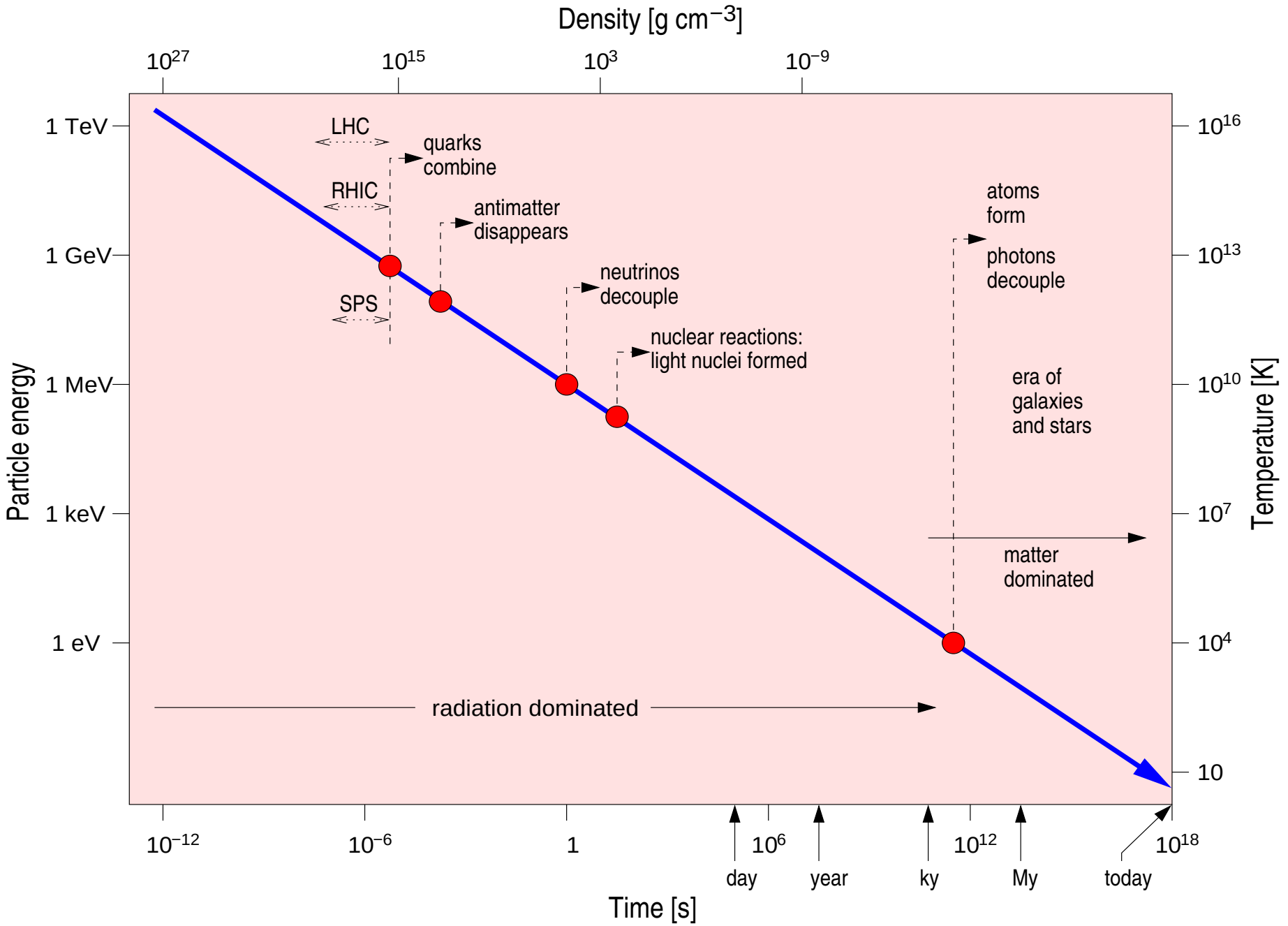

RECREATING THE EARLY UNIVERSE IN LABORATORY

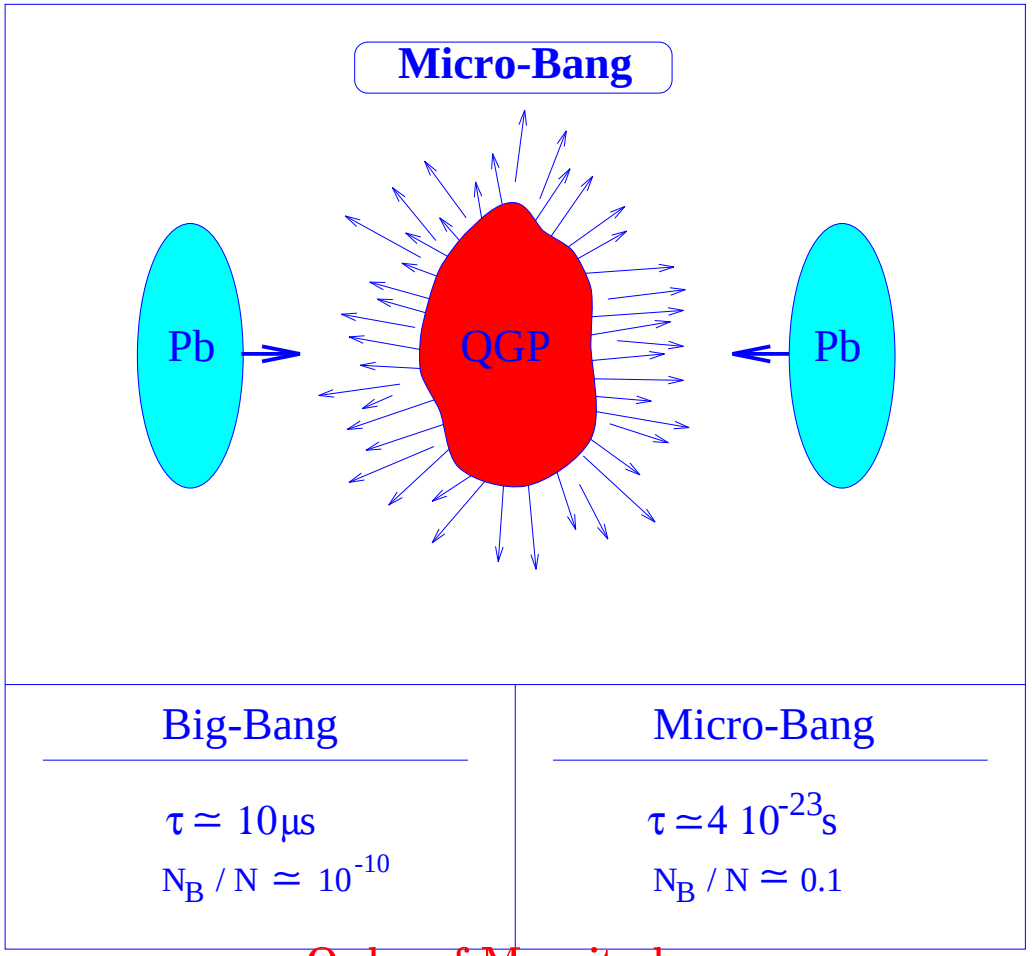

Big-Bang	Micro-Bang
$\tau \simeq 10\mu s$	$\tau \simeq 4\ 10^{-23} s$
$N_B / N \simeq 10^{-10}$	$N_B / N \simeq 0.1$

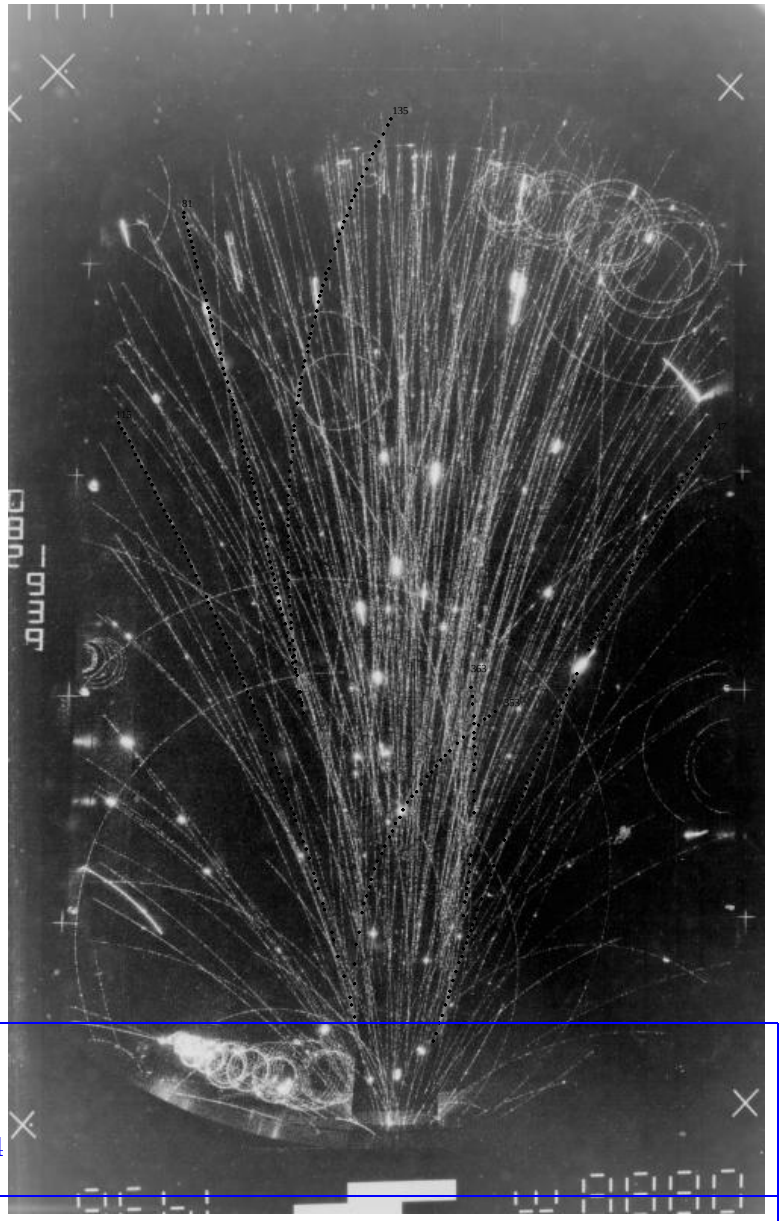

S–Ag Reaction at 200AGeV (by NA35)

Order of Magnitude

ENERGY density	ϵ	$\simeq$ 1–**5GeV/fm**^{3} = 1.8–9 10^{15}**g/cc**
Latent vacuum heat	B	$\simeq$ 0.1–**0.4GeV/fm**^{3} $\simeq$ (166–234**MeV**)^4
PRESSURE	P	$= \frac{1}{3}\epsilon = 0.52\ 10^{30}$ **barn**
TEMPERATURE	T_0, T_f	**300–250, 175–145 MeV; 300MeV$\simeq$3.5** 10^{12}**K**

Beyond Nuclear Matter: QGP

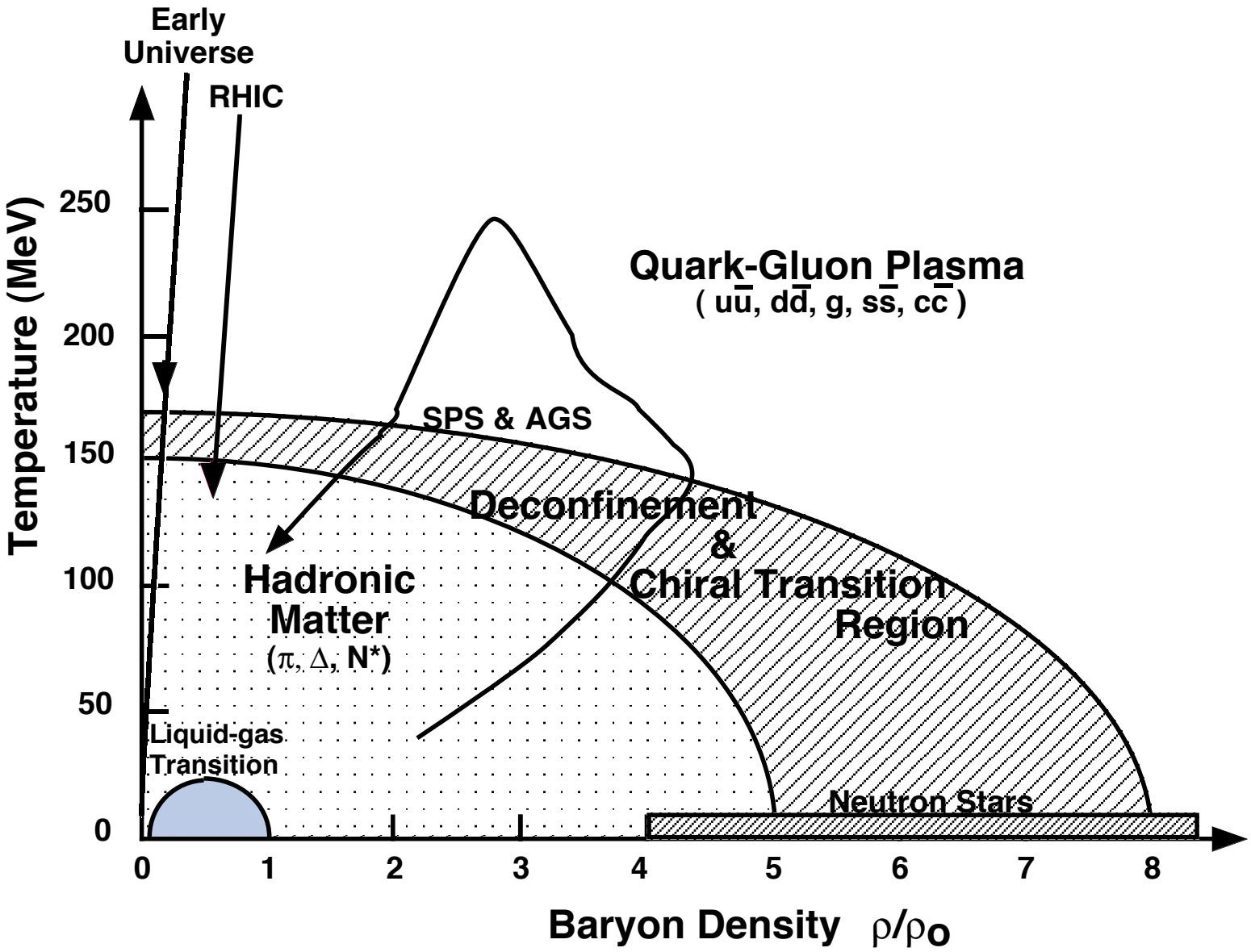

HOW we do this: Experimental Facilities

- **Study of compressed nuclear matter:**
  DUBNA, LBL-BEVELAC, GSI-SIS
- **Study of hadronic matter: matter comprising a significant fraction of hadrons other than nucleons:**
  BNL–AGS (Alternate Gradient Synchrotron)
- **Beyond the threshold to quark matter:**
  CERN-SPS (Super-Proton-Synchrotron)
  International Facility proposed at Darmstadt
- **Study of quark-gluon matter:**
  RHIC (Relativistic Heavy Ion Collider) at BNL
- **Exploring conditions close to those seen in early Universe:**
  CERN-LHC (Large Hadron Collider)

DUBNA, LBL and GSI: nuclear matter studies

DUBNA had capacity to accelerate only light ions. LBL-Berkeley closed the BEVALAC around the time GSI/Darmstadt turned on the **SIS (SchwerIonenSynchrotron).**

GSI A new international project is being proposed, with GSI-SIS being the injector. A double-ring synchrotron will provide ion beams of unprecedented intensities as well as of considerably increased energy, rivaling CERN SPS. Thereby intense beams of secondary beams – unstable nuclei or antiprotons – can also be produced. A total of 4 research programs is envisaged.

Construction of a Clinical Therapy Facility for Cancer Treatment with Ion Beams in progress in Heidelberg in partnership with Cancer Research Center and Uni Heidelberg

CERN

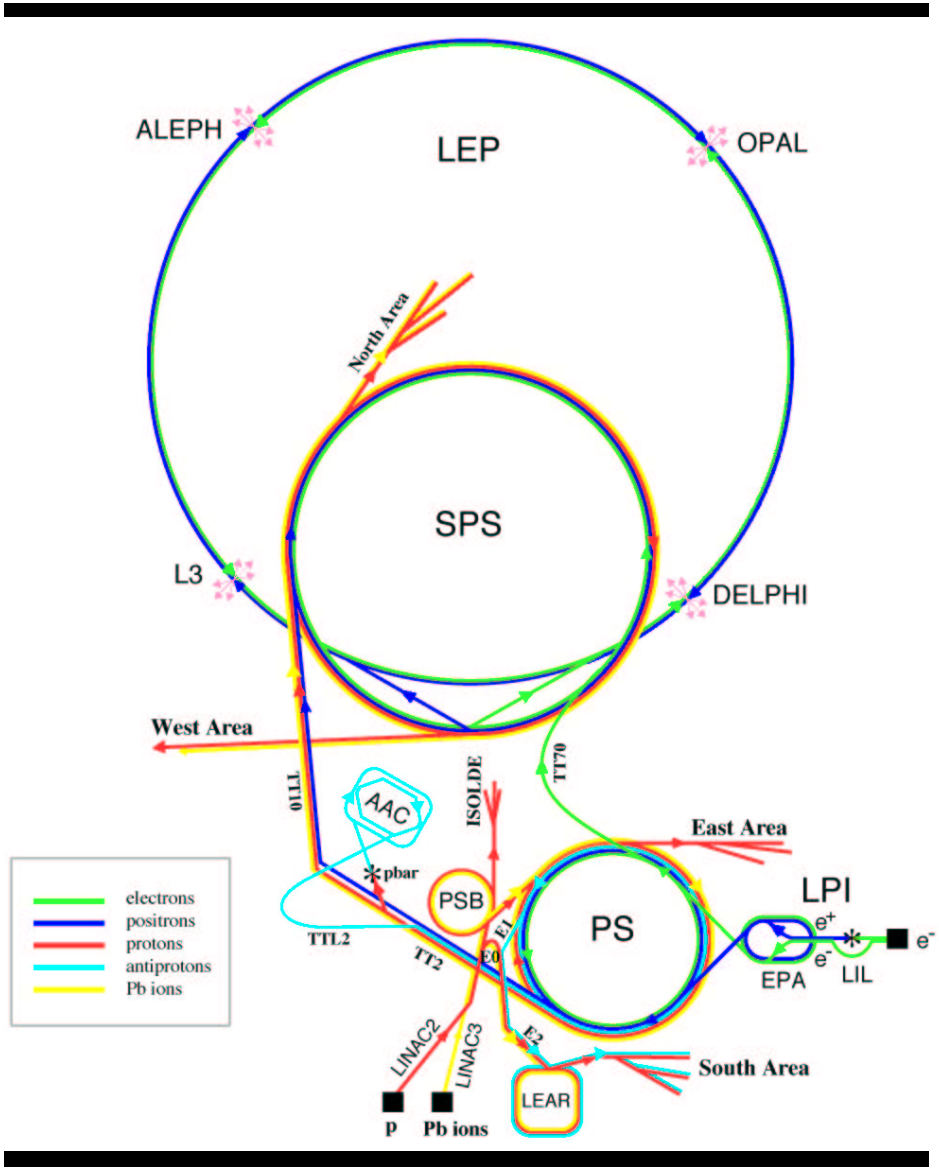

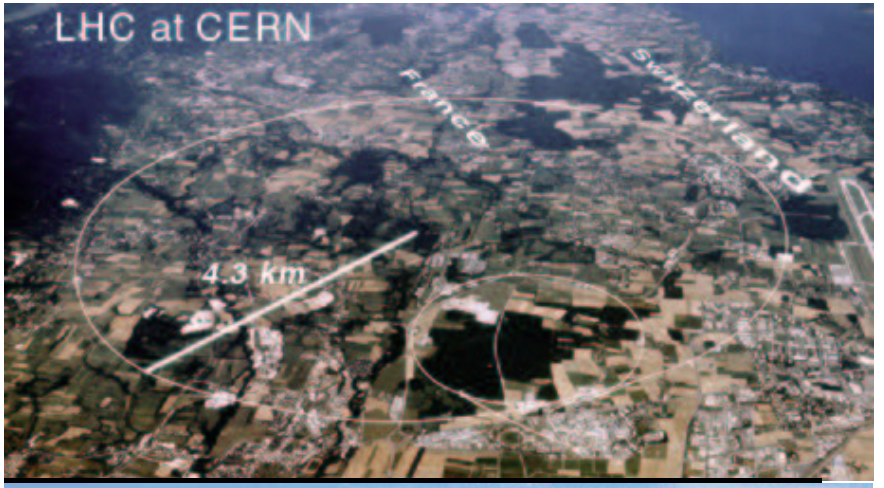

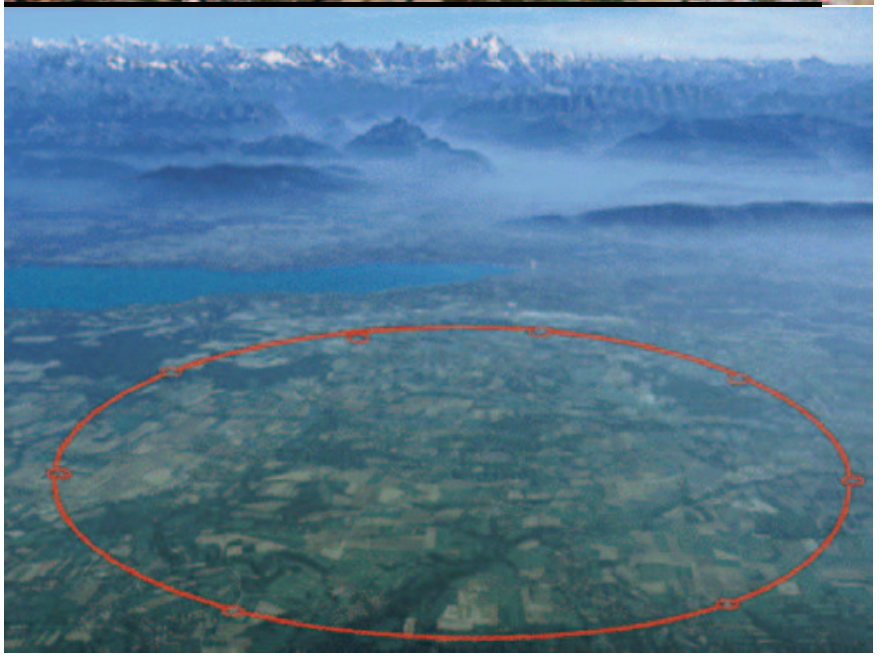

SPS and in future LHC

BROOKHAVEN NATIONAL LABORATORY

Relativistic Heavy Ion Collider

BROOKHAVEN NATIONAL LABORATORY

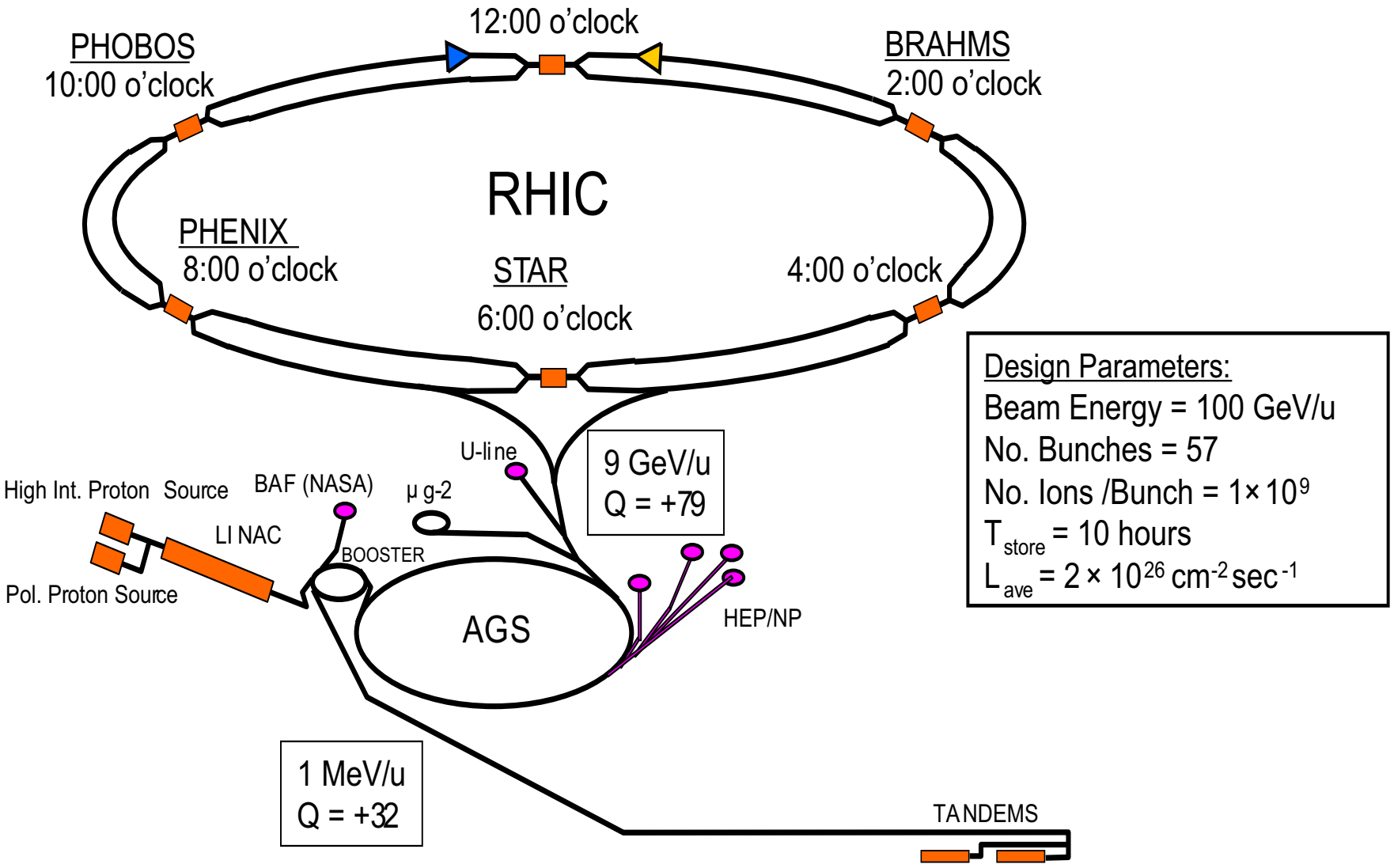

Design Parameters:
Beam Energy = 100 GeV/u
No. Bunches = 57
No. Ions /Bunch = 1×10^9
T_{store} = 10 hours
$L_{ave} = 2 \times 10^{26}\ cm^{-2}\ sec^{-1}$

Relativistic Heavy Ion Collider

ABC of relativistic kinematics

$$E = \sqrt{m^2+\vec{p}_\perp^{\,2}+p_L^2} = \sqrt{m_\perp^2+p_L^2},$$

$$m_\perp = \sqrt{m^2+\vec{p}_\perp^{\,2}},$$

$$p_L \equiv m_\perp \sinh y, \rightarrow E = m_\perp \cosh y,$$

$$\rightarrow v_L \equiv \frac{cp_L}{E} = c\,\tanh y$$

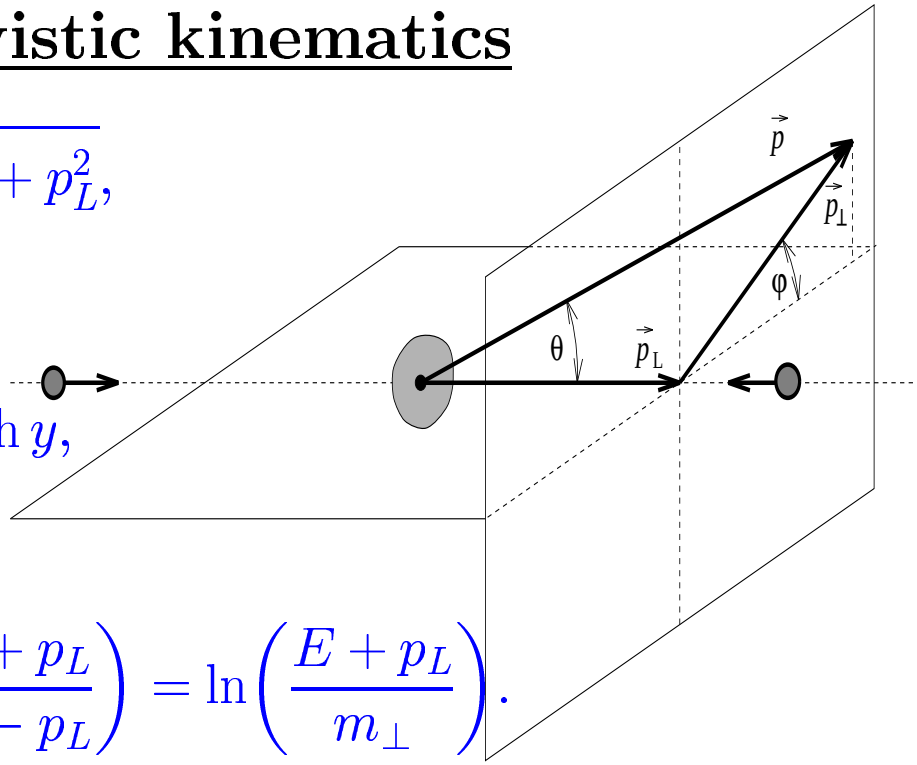

$$y = \frac{1}{2}\ln\left(\frac{1+v_L}{1-v_L}\right) = \frac{1}{2}\ln\left(\frac{E+p_L}{E-p_L}\right) = \ln\left(\frac{E+p_L}{m_\perp}\right).$$

$$\cosh y = \frac{1}{\sqrt{1-v_L^2}} \equiv \gamma_L, \qquad \sinh y = \gamma_L\, v_L$$

The longitudinal momentum p_L of a particle is an inconvenient variable, since it depends in a nonlinear way on the velocity of the CM frame with reference to the laboratory frame. The rapidity y is defined to be additive under successive Lorentz transformations along the same direction. It can be understood as the 'angle' of the (hyperbolic) rotation in (3 + 1)-dimensional space.

With $\cosh y_c = \gamma_c, \quad \sinh y_c = \gamma_c\, v_c$**,**

$$E' = \gamma_c(E + v_c\, p_L), \quad p'_L = \gamma_c(p_L + v_c\, E). \quad \rightarrow \quad E' = m_T\,\cosh(y+y_c), \quad p'_L = m_T\,\sinh(y+y_c).$$

Experimental Program: Energy – Rapidity Range

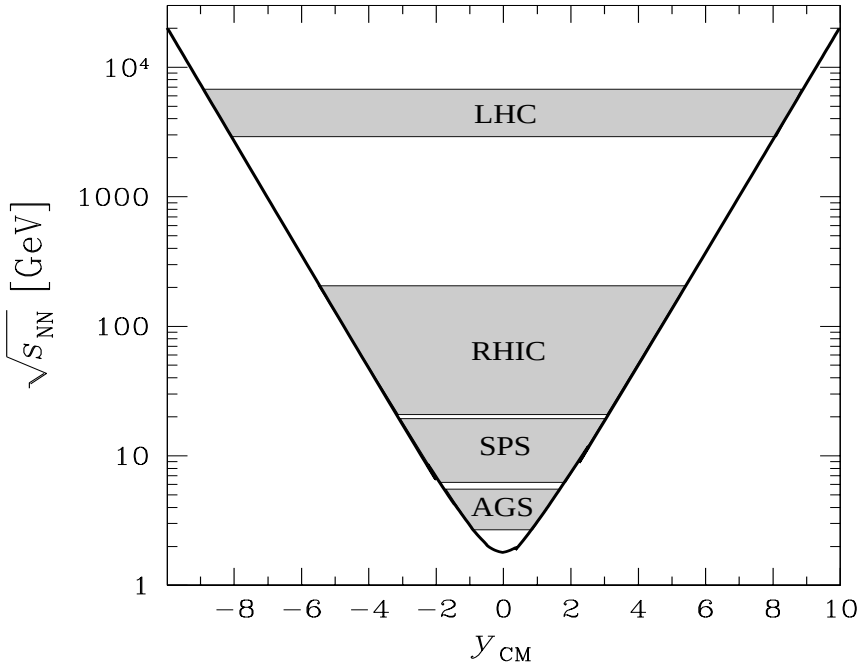

Rest energy content per PARTICIPATING nucleon pair :

$$\sqrt{s_{\rm NN}} = \frac{2}{A_p + A_t}\sqrt{(E_p + E_t)^2 - (p_p + p_t)^2}$$

just like

$$m = \sqrt{E^2 - p^2}$$

Why is high energy important?

	AGS	AGS	SPS	SPS	SPS	RHIC	RHIC	LHC
Start year	1986	1992	1986	1994	1999+	2000	2001+	2007
$A_{\rm max}$	^{28}Si	^{197}Au	^{32}S	^{208}Pb	^{208}Pb	^{197}Au	^{197}Au	^{208}Pb
$E_{\rm P}^{\rm max}[A$ GeV]	14.6	11	200	158	30–80	0.91×10^4	2.1×10^4	1.9×10^7
$\sqrt{s_{\rm NN}}$ [GeV]	5.4	4.7	19.2	17.2	7.5–12	130	200	6000
$\sqrt{s_{\rm AA}}$ [GeV]	151	934	614	3.6×10^3	1.5–2.5×10^3	2.6×10^4	4×10^4	1.2×10^6
$\Delta y/2$	1.72	1.58	2.96	2.91	2.08–2.57	4.94	5.37	8.77

Experimental Output

Experiments deliver single particle SPECTRA of particles in rapidity y and $m_\perp$. Typically today these are spectra of HADRONS, spectra of photons, dileptons , are not yet accessible. We also study two particle correlations which offer through quantum interference opportunity to image the geometry of the particle source (HBT).

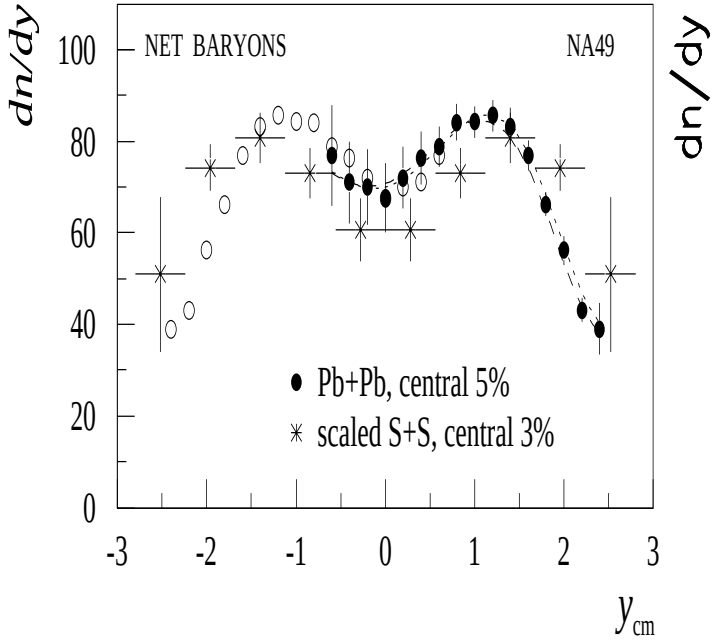

158 A GeV Pb on Pb
200 A GeV S on S
scaled with 352/52

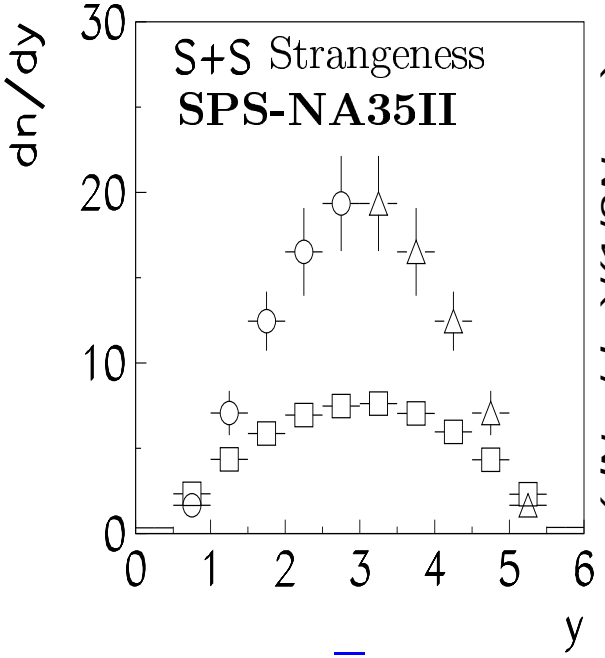

$1.6\Lambda + 1.6\overline{\Lambda} + 4\mathrm{K}s$
200 A GeV S on S
200 A GeV p on p
multiplicity scaled

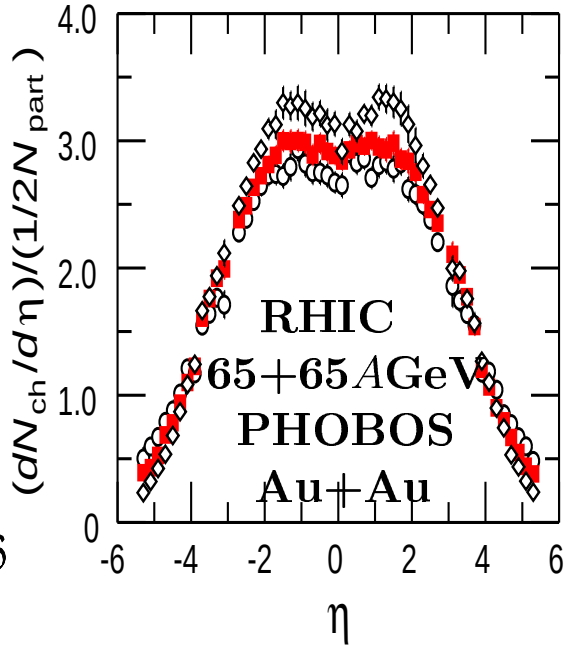

Centralities:
$\langle N \rangle = 102, 216, 354$

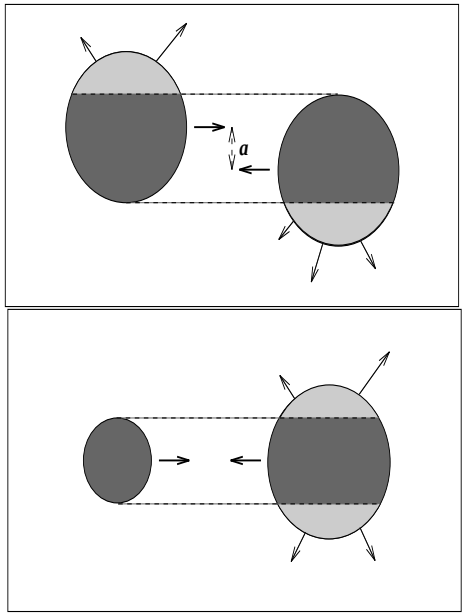

Two centralities

Geometrically central collisions: for symmetric systems rare but nearly all nucleons participate, asymmetric collisions have an edge but are more difficult to interpret.

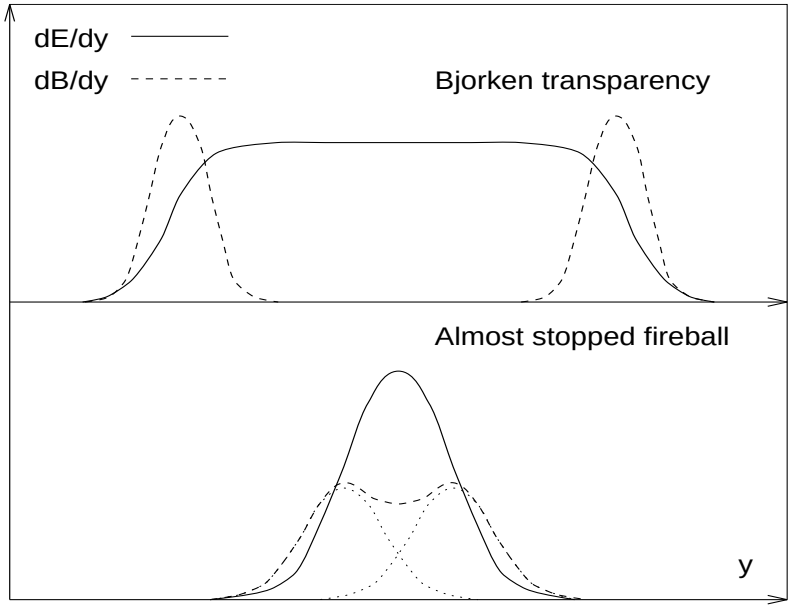

Central in rapidity particle spectra: those emitted near to the center of momentum condition, for collider, that is laboratory frame, for fixed target experiments shift by $y_{\rm CM}$.

Rapidity distributions of energy (solid lines) and baryon number (dashed lines) (in a qualitative representation): (a) for a 'Transparent' reaction mechanism; and (b) for full stopping in the collision

Non-identified particles and (π)-pseudorapidity

Often we do not know what is the mass of the particle observed. For relativistic particles $E = \sqrt{p^2 + m^2} \to p$, so often the value of m will not matter. When m is 'small' we introduce pseudorapidity η:

$$p = p_\perp \cosh\eta, \qquad p_L = p_T \sinh\eta,$$

$$y(m \to 0) \to \eta = \frac{1}{2}\ln\left(\frac{p + p_L}{p - p_L}\right) = \frac{1}{2}\ln\left(\frac{1+\cos\theta}{1-\cos\theta}\right) = \ln\left(\cot\frac{\theta}{2}\right).$$

θ is the particle-emission angle relative to the beam axis. Thus we obtain a remarkably simple way to measure pseudorapidity spectra: for charged particles in magnetic field we obtain momentum p from the curvature (rigidity) and angle of emission θ. Since most particles produced are pions it is customary to do as if this was the case for all charged particles, so $m \to m_\pi$. Errors are understood, not always negligible. From definition:

$$p_L = \sqrt{m^2 + p_\perp^2}\,\sinh y = \sqrt{m_\pi^2 + p_\perp^2}\,\sinh\eta_\pi,$$

we find for the true m (kaon, nucleon) what error we are making.

Deconfinement Signatures

PROBLEM: when all is over, we have just many hadrons, some rare direct photons, some rare direct 'dileptons'. How can we tell there was deconfinement? Early ideas about direct γ, e^+e^-, $\mu^+\mu^-$ not yet practical (maybe never). Two hadronic observables are well studied, the J/Ψ suppression (mention), and strangeness next topic.

Illustration of suppression idea.

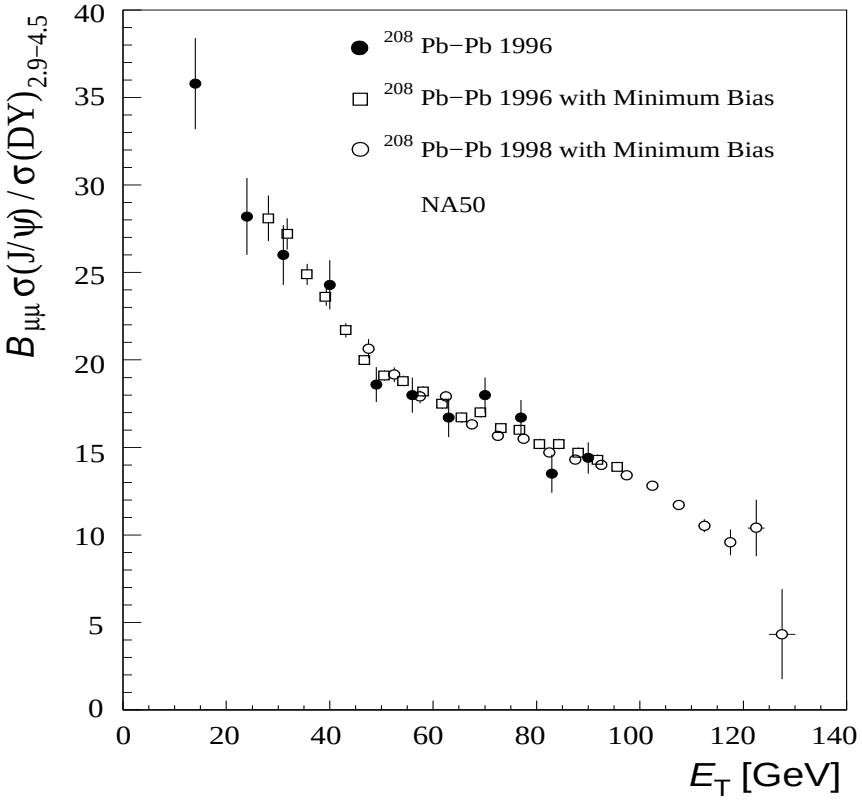

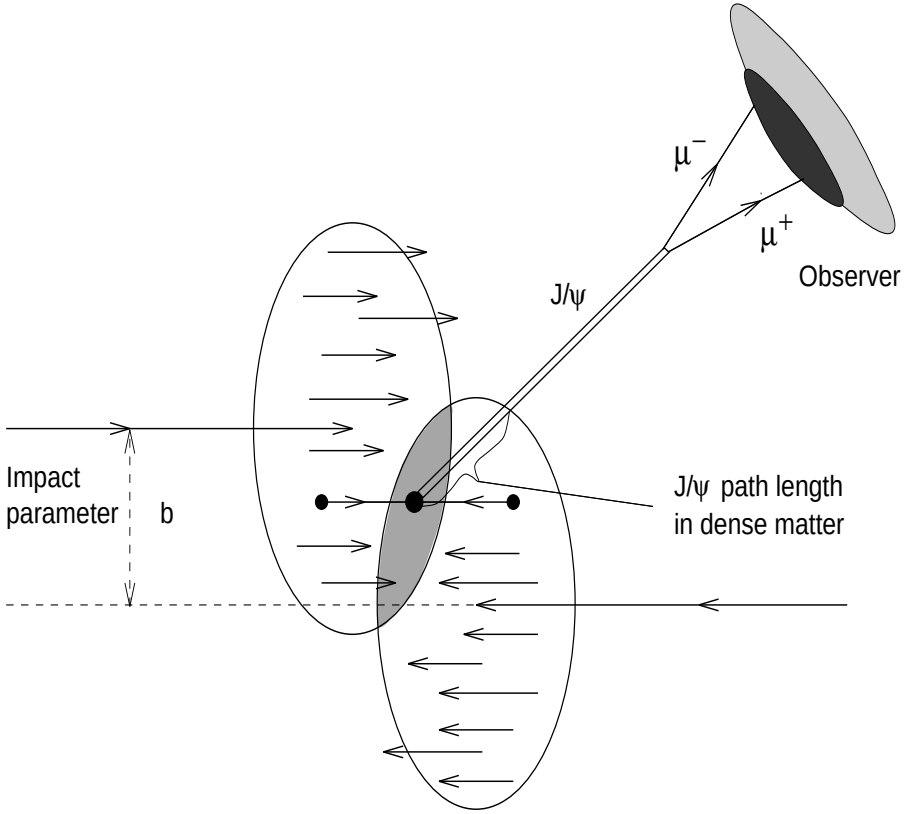

Suppression of production of J/Ψ as a function of AA-collision centrality, characterized in terms of the transverse energy $E_{\rm T}$ produced in the reaction. Results of experiment NA50.

Strangeness – a popular QGP diagnostic tool

EXPERIMENTAL REASONS

- There are many strange particles allowing to study different physics questions ($q = u, d$):

$$\phi(s\bar{s}), \quad K(q\bar{s}), \quad \overline{K}(\bar{q}s), \quad \Lambda(qqs), \quad \overline{\Lambda}(\bar{q}\bar{q}\bar{s}),$$

$$\Xi(qss), \quad \overline{\Xi}(\bar{q}\bar{s}\bar{s}), \quad \Omega(sss), \quad \overline{\Omega}(\bar{s}\bar{s}\bar{s})$$

- Strange hadrons are subject to a self analyzing decay within a few cm from the point of production;

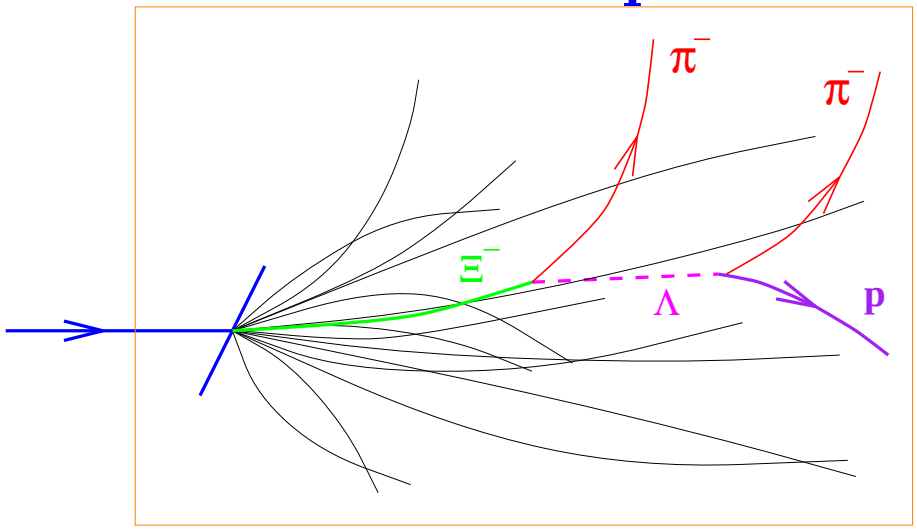

- Production rates hence statistical significance is high;

'CROSS-TALK' HADRON FORMATION MECHANISM IN QGP

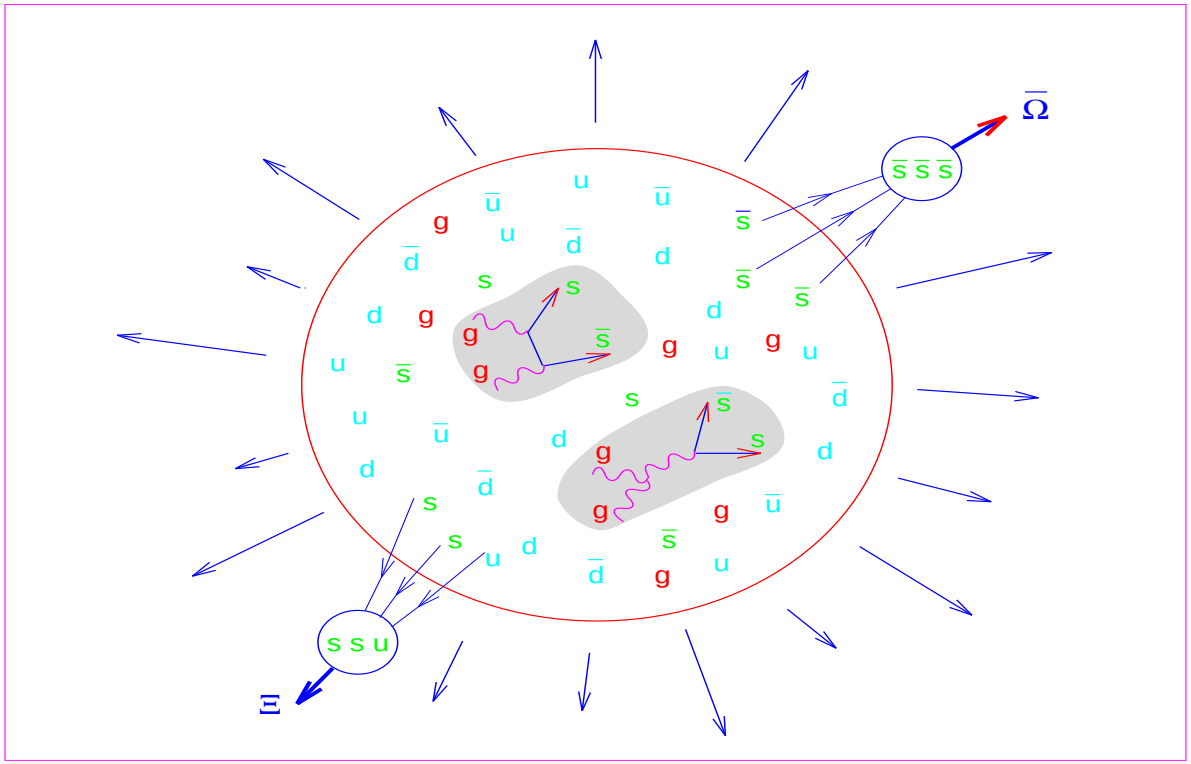

In quark-gluon plasma we have a reservoir of strange and anti-quarks. Hence formation of complex rarely produced multi strange (anti)particles possible which are difficult to make otherwise – requires 'cross talk' between quarks made in different microscopic reactions = deconfinement. We study strange antibaryons which have small background from direct N–N reactions.

THEORETICAL CONSIDERATIONS

- **production of strangeness in gluon fusion** $\boxed{GG \to s\bar{s}}$ **strangeness linked to gluons from QGP;**

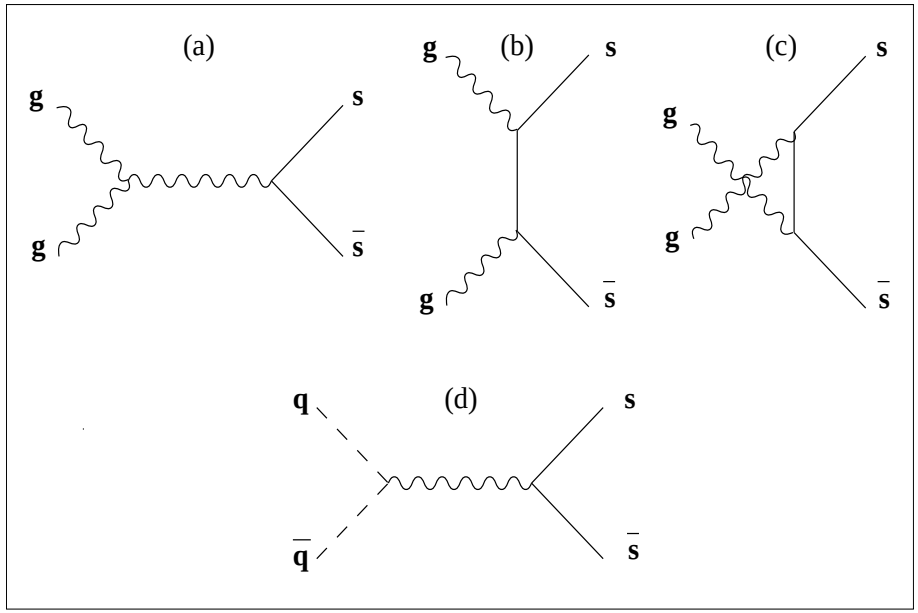

- **coincidence of scales:**

$$\boxed{m_s \simeq T_c} \to \boxed{\tau_s \simeq \tau_{\rm QGP}} \to$$

strangeness a clock for reaction

- **Often** $\boxed{\bar{s} > \bar{q}} \to$
strange antibaryon enhancement and
at RHIC also (anti)hyperon dominance of (anti)baryons.

Strangeness as Deconfinement Signatures

1. **TOTAL Strangeness YIELD:** $s$strangeness/$b$baryon depends primarily on initial conditions and evolution dynamics
(how long the system is at which T)

$\gamma_{\rm s}^{\rm QGP}$: is QGP near chemical equilibrium?

$$\gamma_{\rm s,q}^{\rm QGP} = \left.\frac{n_{\rm s,q}(t,T(t))}{n_{\rm s,q}(\infty,T(t))}\right|_{\rm QGP} \to 1?$$

---

2. **Strangeness overpopulation at QGP BREAK-UP:**
QGP phase space is squeezed into
a smaller number of HG phase space cells: $\gamma_{\rm s}^{HG} \simeq 3\gamma_{\rm s}^{\rm QGP}$

---

3. **TO BE SENSITIVE WE NEED ALSO TO CONSIDER** $\gamma_q^{\rm HG} > 1$
over population of pion phase space is ENTROPY enhancement

---

4. **STRANGENESS MOBILITY IN QGP IMPLIES**
s–$\bar{s}$ phase space symmetry, within baryon rich (SPS) environment
IMPRINTED ON HADRONS AT HADRONIZATION
λ_s = strange quark fugacity

Retrospective: Strangeness Discoveries
MULTISTRANGE HYPERON ENHANCEMENT

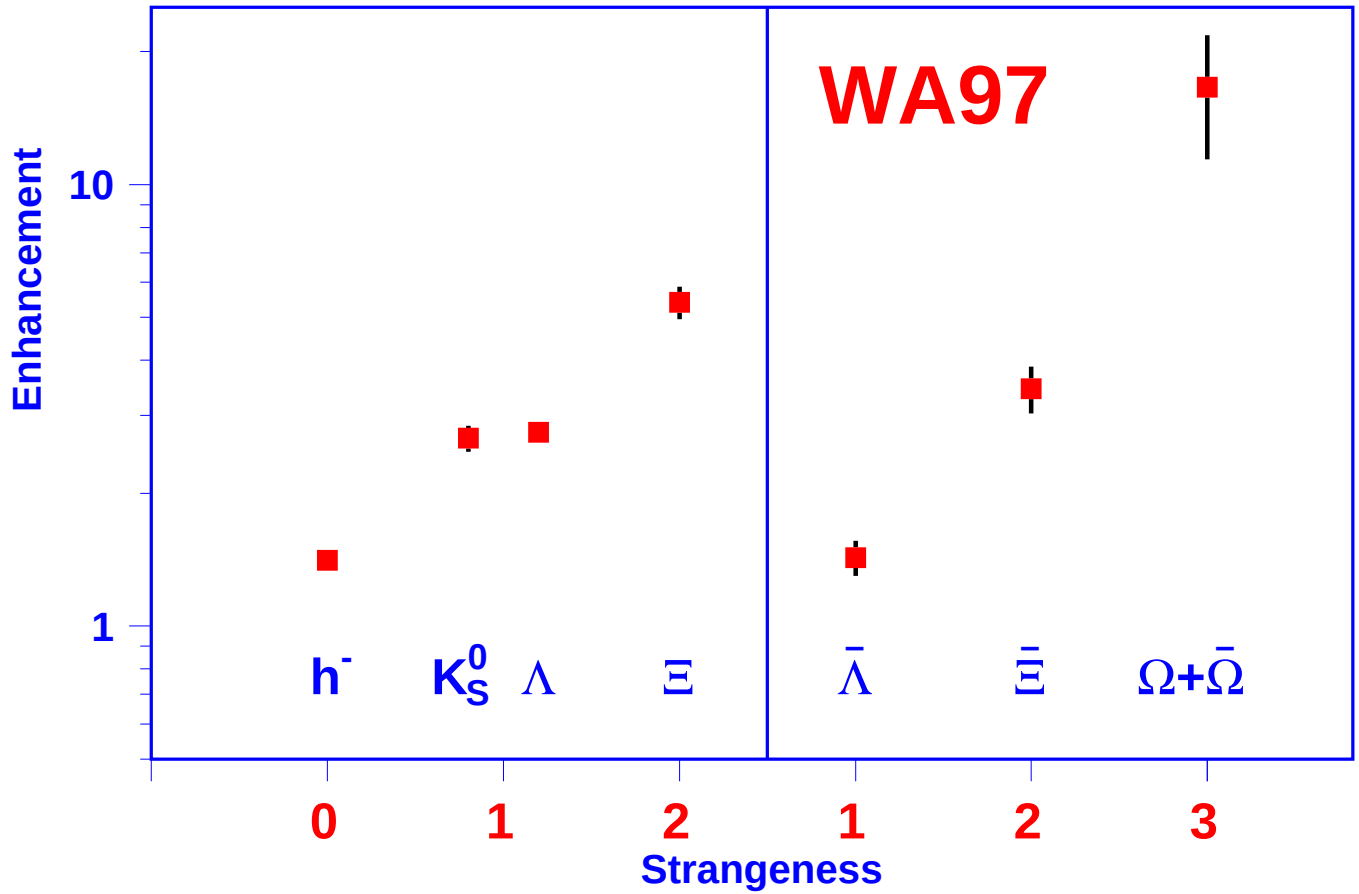

Results of WA97/NA57 collaboration. Enhancement GROWS with a) strangeness b) antiquark content as predicted. Enhancement is defined with respect toyield in p–Be collisions, scaled up with the number of 'wounded' nucleons.

Antibaryon excess at central CM rapidity

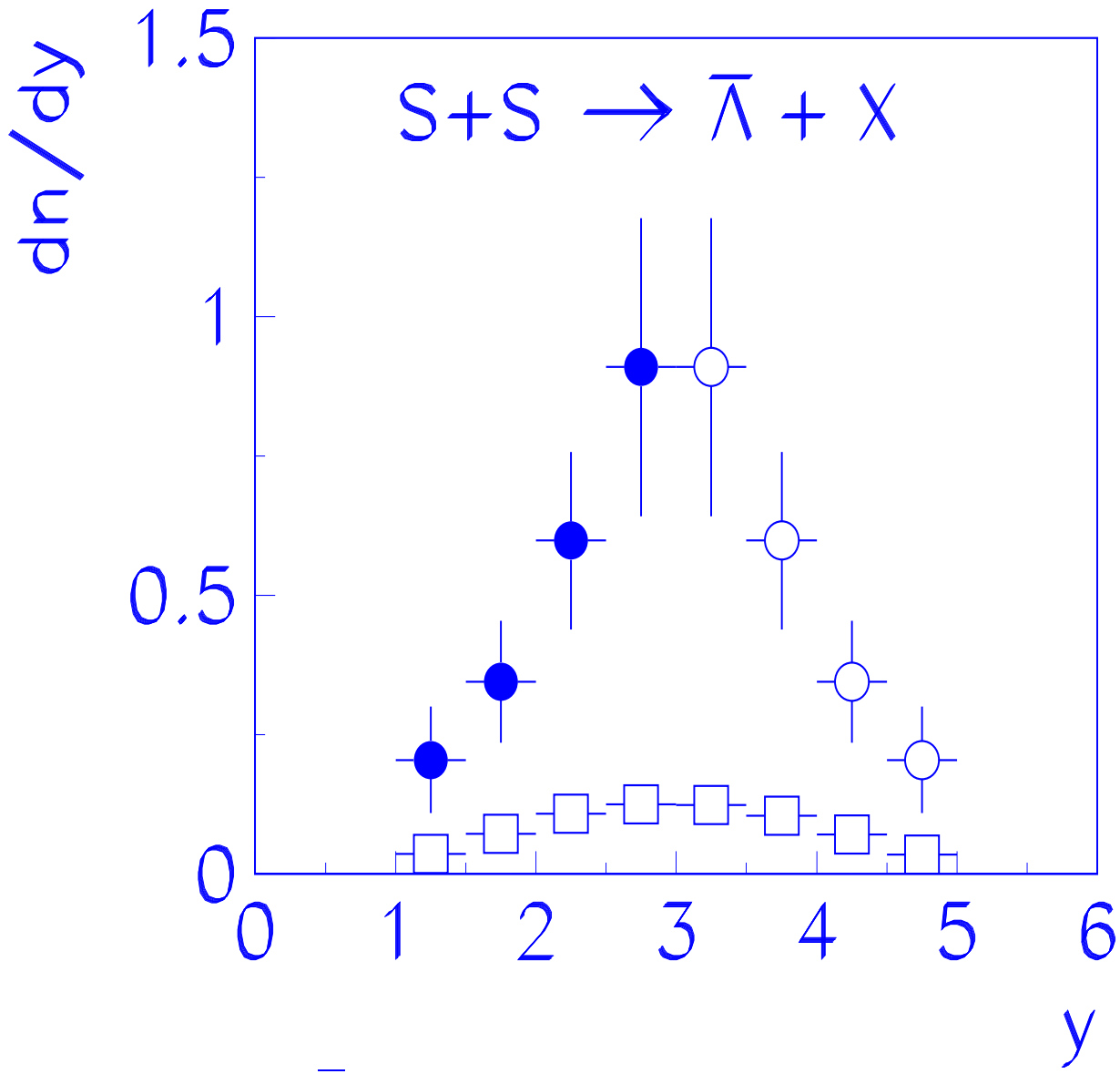

NA35II EXCESS $\bar{\Lambda}$ emitted from a central well localized source.
Background (squares) from multiplicity scaled NN reactions

MORE EFFECTIVE CONVERSION OF ENERGY INTO STRANGE MATTER

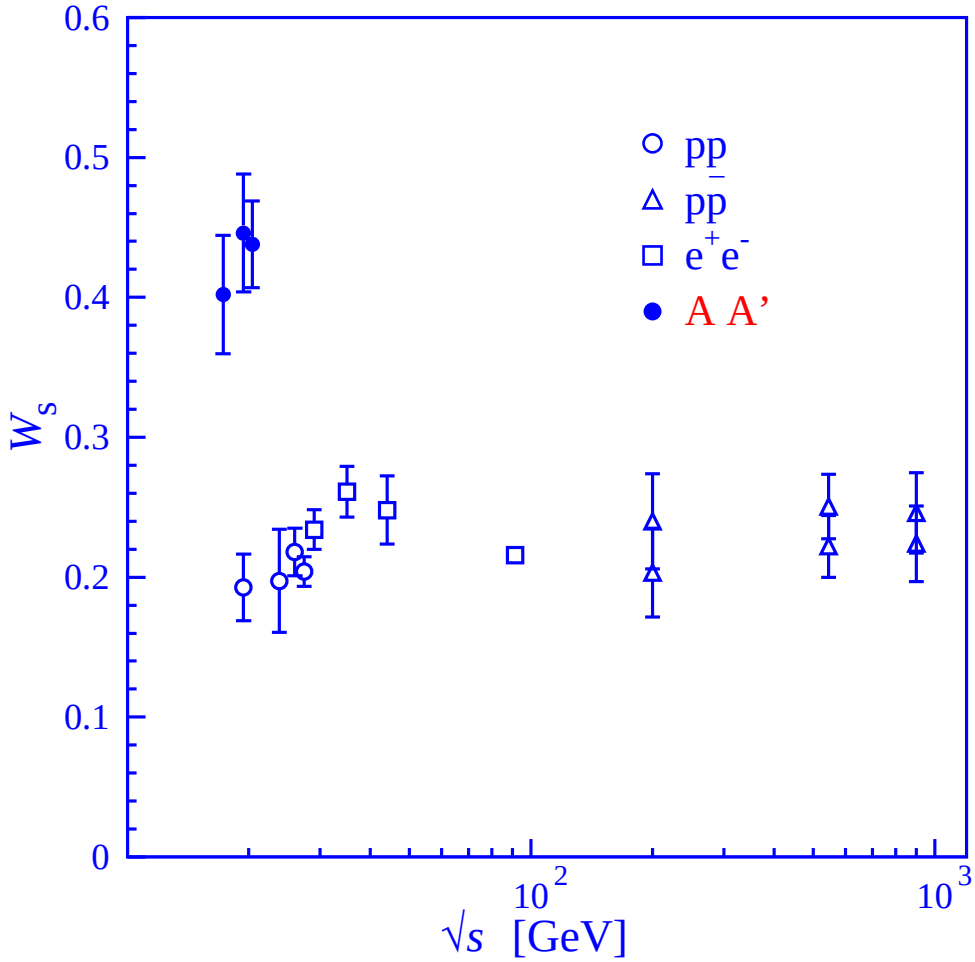

Enhancement of strangeness pair production compared to light quarks due to onset of thermal glue fusion processes – seen most clearly in Wróblewski ratio in which only newly made s- and q-pairs are counted:

$$W = \frac{2\langle s\bar{s}\rangle}{\langle d\bar{d} + u\bar{u}\rangle}$$

High $m_\perp$ slope universality

Discovered in S-induced collisions, very pronounced in Pb-Pb Interactions.

Why is the slope of baryons and antibaryons precisely the same?

Why is the slope of different particles in same m_t range the same?

Analysis+Hypothesis 1991: QGP quarks coalescing in SUDDEN hadronization

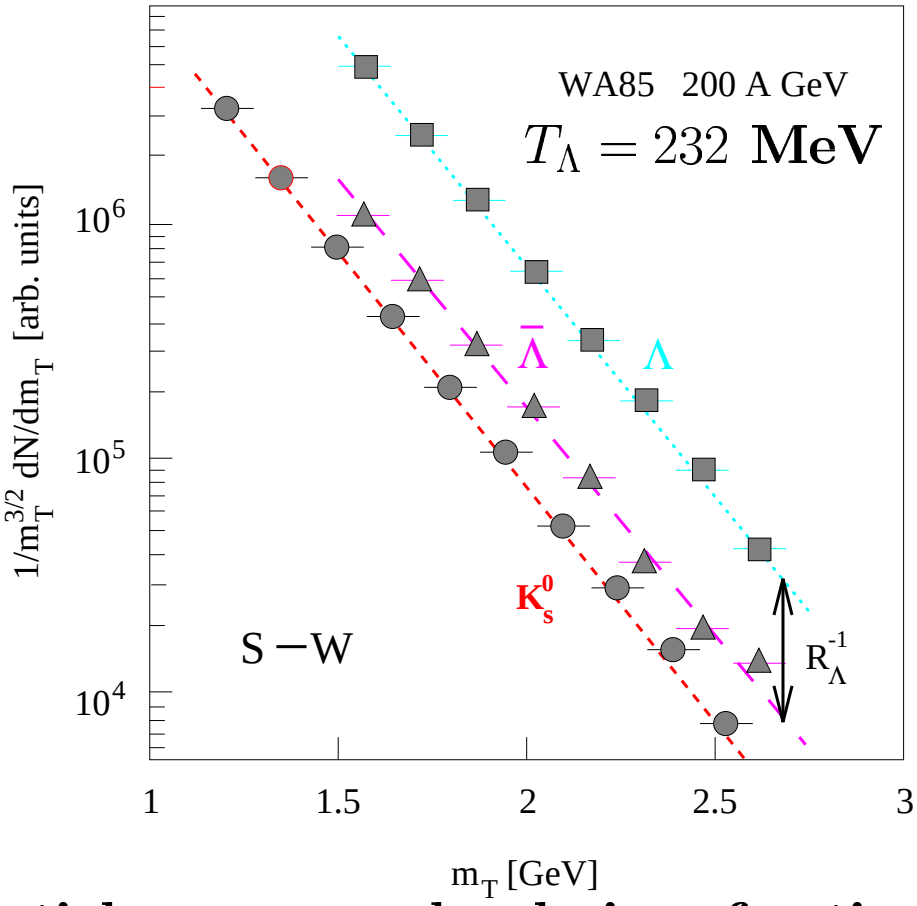

This allows to study ratios of particles measured only in a fraction of phase space

WA97	$T_\perp^{\rm Pb}$ **[MeV]**
$T^{\rm K^0}$	**230 ± 2**
T^{Λ}	**289 ± 3**
$T^{\overline{\Lambda}}$	**287 ± 4**
T^{Ξ}	**286 ± 9**
$T^{\overline{\Xi}}$	**284 ± 17**
$T^{\Omega+\overline{\Omega}}$	**251 ± 19**

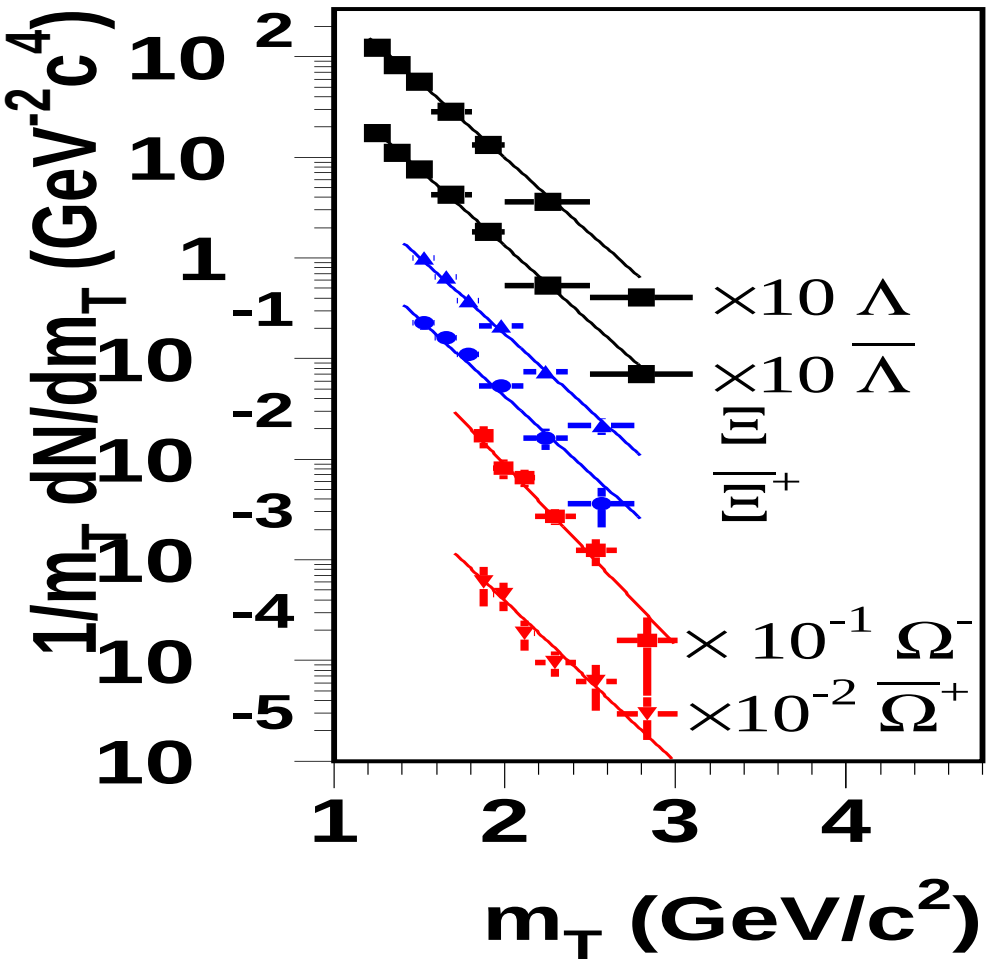

Λ **within 1% of** $\overline{\Lambda}$

Kaon – hyperon difference:

EXPLOSIVE FLOW effect

Difference between $\Omega + \overline{\Omega}$**:**

presence of an excess of low $p_\perp$ **particles**

we will return to study this in spectral analysis

FIRST (XI-)RESULTS FROM RHIC:

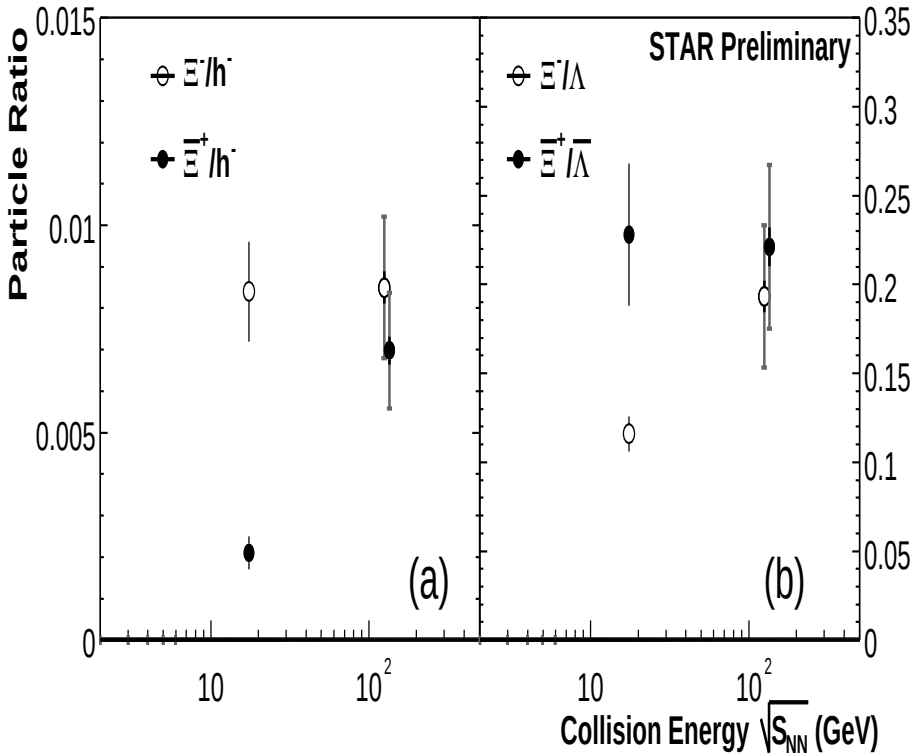

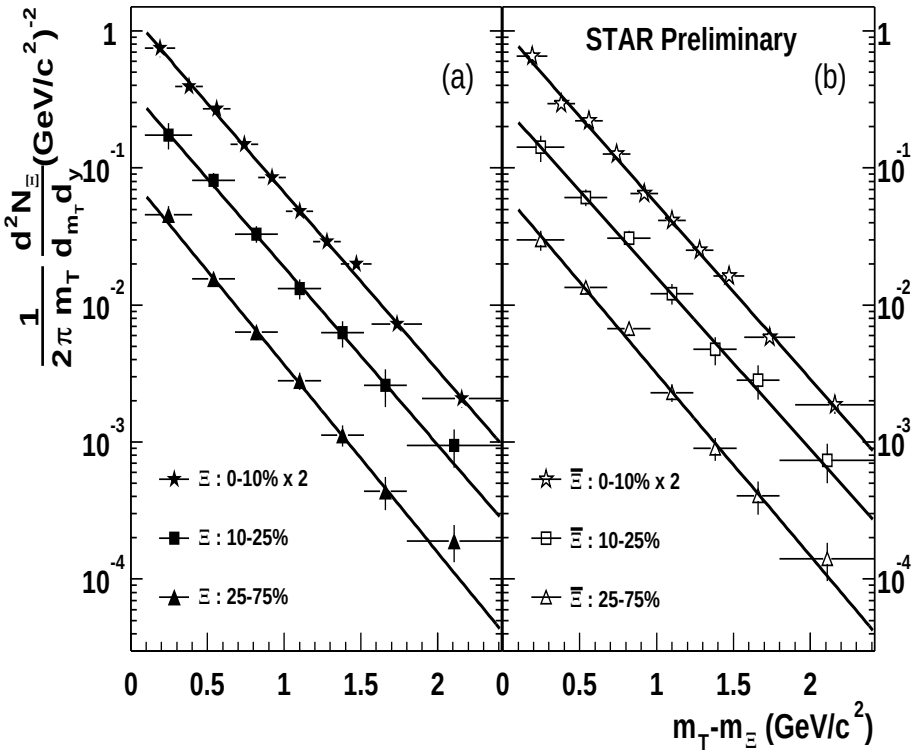

COMPARISON SLOPES AT RHIC and CERN

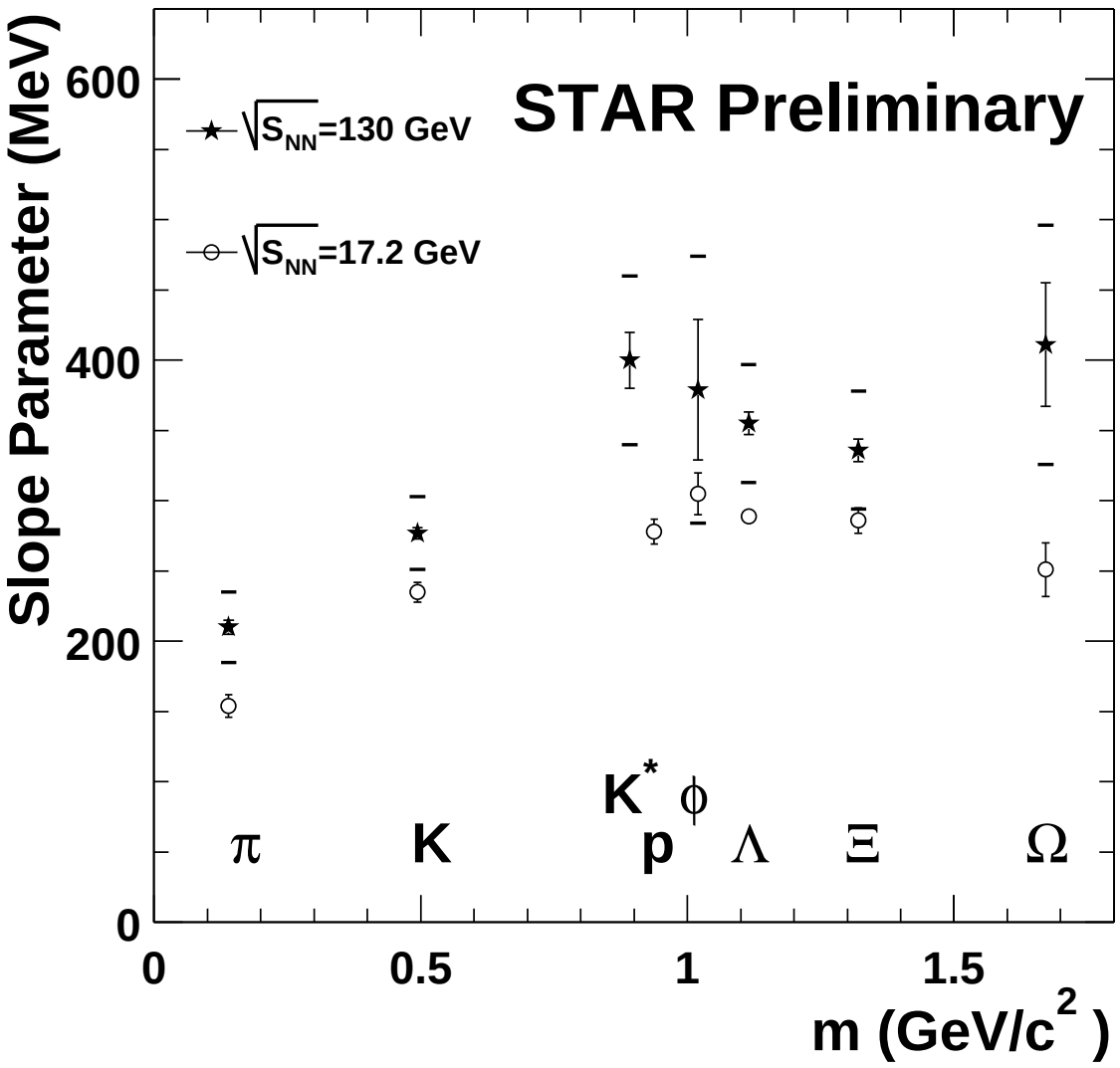

PARTICLE SLOPES IMPLY SUDDEN HADRONIZATION

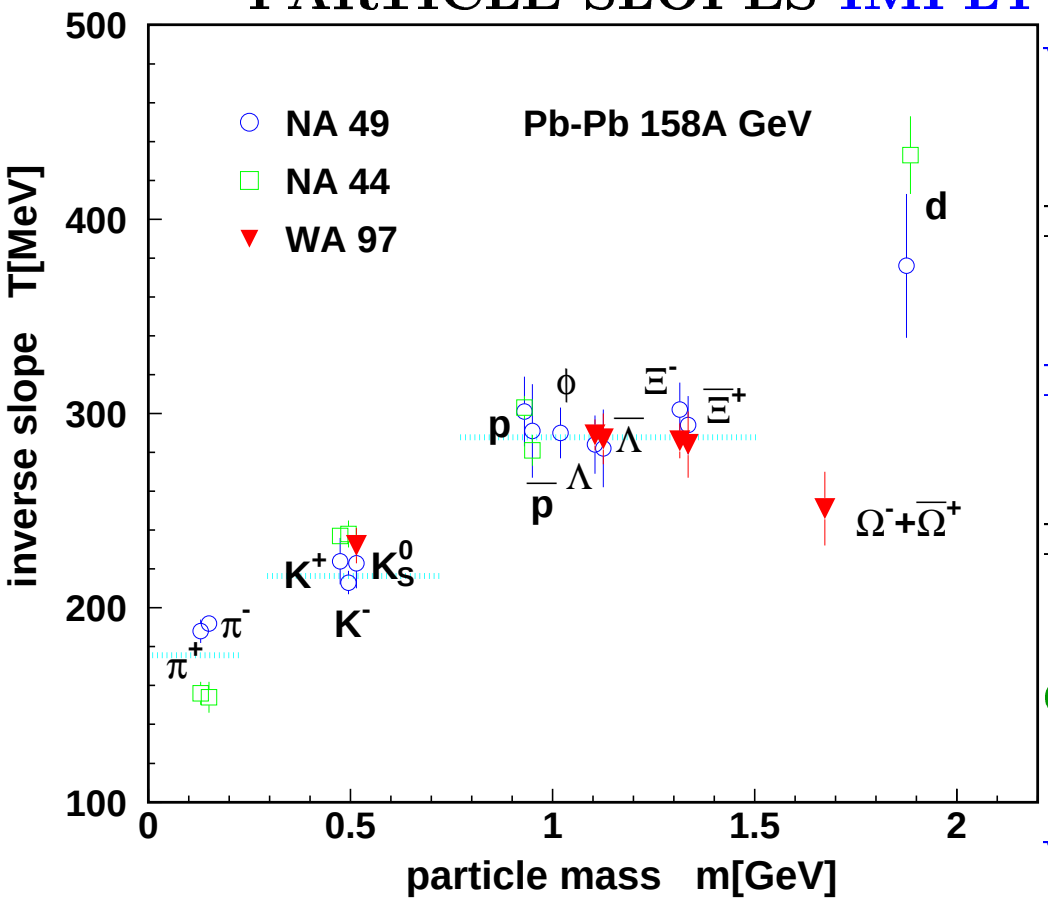

Why are the slopes rising in value?
→ **EXPLOSIVE FLOW** $v > 0.5c$

Figure reflects similar range p_T thus a very different m_T range

Diff. mass HYPERONS: SLOPES include resonance decays

Deuterons from final state interactions, disregard!

Omegas remain enigmatic and thus most interesting

Why is slope of baryons and antibaryons precisely the same?

EVAPORATION: inverse slope T related to $T_{\rm tf}$ the intrinsic temperature of the source which explodes with local flow velocity $v_{\rm tf}$:

$$T \simeq \frac{1+\vec{n}\cdot\vec{v}_{\rm tf}}{\sqrt{1-\vec{v}_{\rm tf}^2}} T_{\rm tf} \to \sqrt{\frac{1+v_{\rm tf}}{1-v_{\rm tf}}} T_{\rm tf}.$$

Caution – does not apply in the same fashion to all particles, precision rarely better than ±10%.

QGP PHASE $\Longrightarrow$ HADRON PHASE SPACE

EXPERIMENTAL SIGNATURE: Symmetry in $m_\perp$ spectra of strange baryons with antibaryons $\rightarrow$ production ('evaporation') into vacuum by a common (deconfined) source.

No hadronic 'phase'!
No 'mixed phase' either!
Direct emission of free-streaming hadrons from exploding QGP

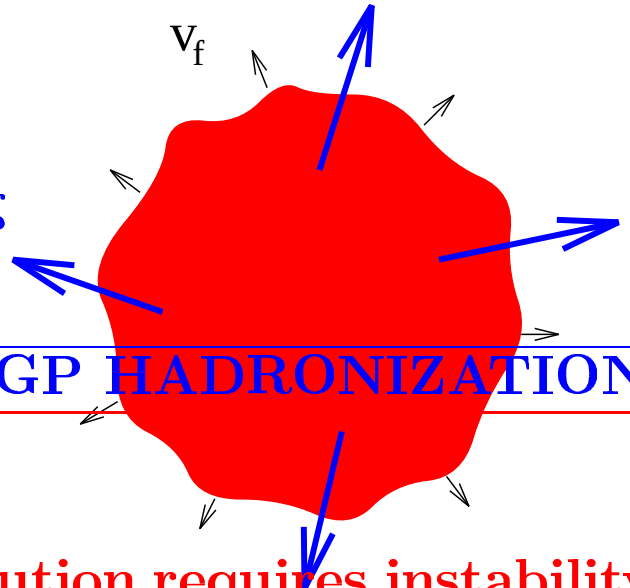

Orient analysis toward SUDDEN QGP HADRONIZATION reaction

NO slow transformation

contradiction to experiment – resolution requires instability in time evolution which leads $\rightarrow$ phase NONEQUILIBRIUM

STATISTICAL HADRONIZATION

OBJECTIVE: describe particle yields, spectra exploiting the simplicity of statistical physics methods, without need to address the microscopic interactions between particles. We replace microscopic bulk variables such as energy, particle density by:

temperature T

chemical potentials μ (equivalently fugacity $\lambda = e^{\mu/T}$)

time evolving quark occupancy γ (chemical 'non'-equilibrium),

There are at least two relevant 'temperatures':

1. Chemical freeze-out (T_f):

this is the decoupling condition at which particle number stops changing similar to early universe nucleosynthesis abundance freeze-out

2. and at equal time, or later Thermal (kinetic) freeze-out (T_t):

where particle momentum distribution stops evolving, similar to decoupling of cosmic background photons at $T = 3000K$

Primary hypothesis of STATISTICAL HADRONIZATION

We assume that within a 'family', particle yields with same valance quark content are thermally equilibrated, e.g. the relative yield of $\Delta(1230)$ and N completely controlled by the ratio m/T:

$$\frac{n_\Delta}{n_N} = \frac{g_\Delta (m_\Delta T)^{3/2} e^{-m_\Delta/T}}{g_N (m_N T)^{3/2} e^{-m_N/T}}$$

Resonances often as important as gound state in counting of produced particles. Yields of particles are obtained summing over all resonances (recall Hagedorn's exponentially growing spectrum!) and compared with experiment in order to check if in principle this approach is valid.

Statistical particle abundances at CERN and AGS

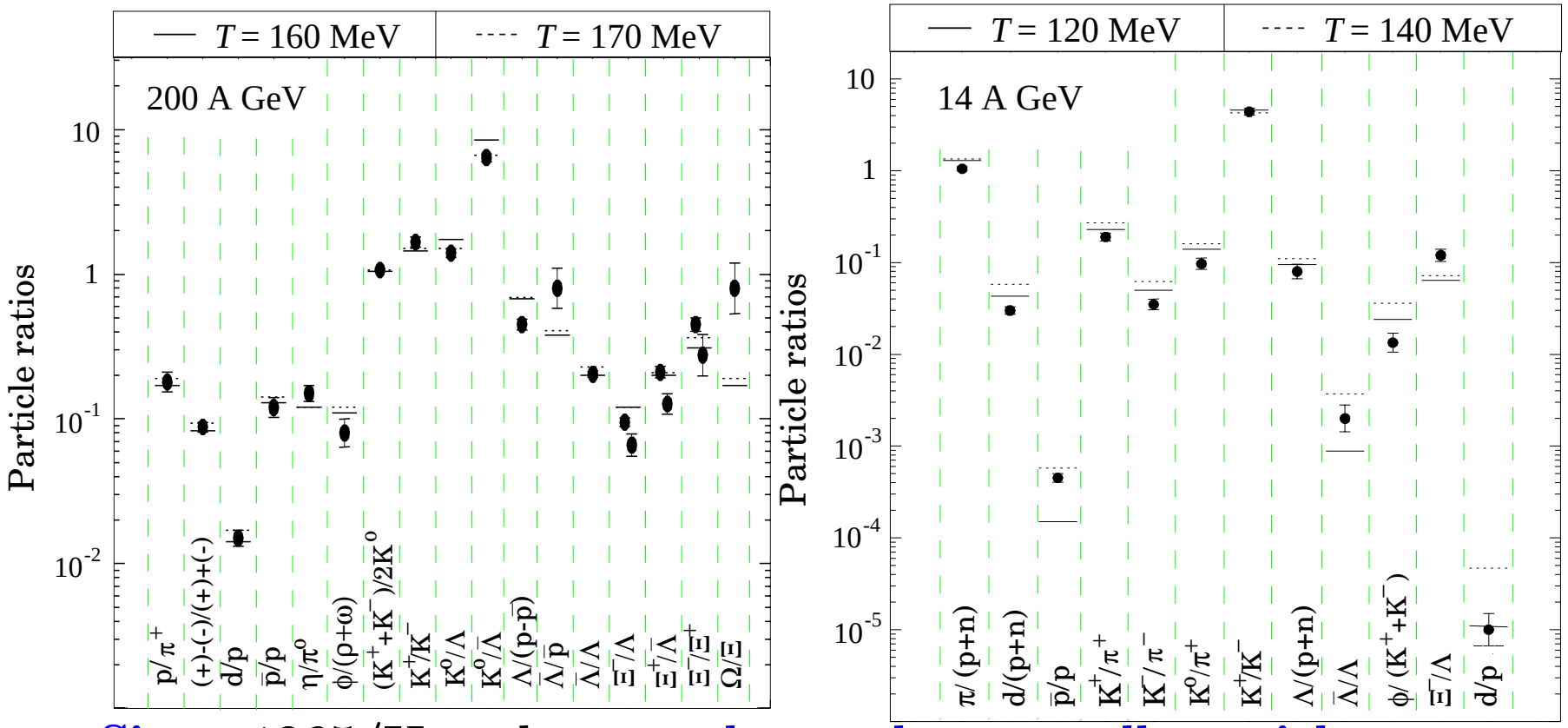

Since 1965/Hagedorn we know that overall particle spectra and yields in p–p reactions can be described within a factor 2 by the integrated statistically yields. It is quite impressive to see that this also works VERY WELL in A–A reactions.

WHAT DOES THIS MEAN?

END LECTURE 1

Statistical Physics Tutorial

The distribution $n = \{n_i\}$ of $N = \sum n_i$ elements having the same energy $E^{(N)} = \sum n_i E_i$ can be achieved in many different ways. To find how many, consider:

$$K^N = (x_1 + x_2 + \cdots + \cdots x_K)^N|_{x_i=1} = \sum_n \frac{N!}{n_1! n_2! \cdots n_K!} x_1^{n_1} x_2^{n_2} \cdots x_K^{n_K}|_{x_i=1}.$$

The normalized coefficients are the relative probabilities of realizing each state in the ensemble n, with n_i equivalent elements. To find the most probable distribution $\overline{n}$ subject to the constraints of fixed total particle number and energy we introduce two Lagrange multipliers a and β and look for an extremum of:

$$A(n_1, n_2, \ldots, n_K) = \ln W(n) + \ln\gamma \sum_i n_i - \beta \sum_i n_i E_i,$$

$$\frac{\partial}{\partial n_i}[-\ln(n_i!) + \ln\gamma n_i - \beta n_i E_i]\Big|_{\bar{n}_m} = 0. \qquad \frac{d}{dk}[\ln(k!)] \approx \frac{\ln(k!) - \ln[(k-1)!]}{(k) - (k-1)} = \ln k.$$

We find the most probable distribution: $\bar{n}_i = \gamma e^{-\beta E_i}$, the inverse of the slope parameter β can be shown to be temperature.
The particle number $\sum_i \bar{n}_i = \gamma \sum_{i=1}^K e^{-\beta E_i} = N$ is fixed by the chemical fugacity γ.
The energy $E^{(N)} = \sum_i \bar{n}_i E_i = \gamma \sum_i E_i e^{-\beta E_i}$. divided by N,

$$\frac{E^{(N)}}{N} \equiv \overline{E^{(N)}} = \frac{\gamma \sum_i E_i\, e^{-\beta E_i}}{\gamma \sum_i e^{-\beta E_i}} \equiv -\frac{d}{d\beta} \ln Z; \qquad Z = \sum_i \gamma e^{-\beta E_i}.$$

motivates the introduction of the partition function Z. $\beta = 1/T$

Statistical and thermal physics relations

$$\beta P = \frac{\partial \ln \mathcal{Z}(V,\beta,\mu)}{\partial V}, \qquad E = -\frac{\partial \ln \mathcal{Z}(V,\beta,\mu)}{\partial \beta},$$

$$\mathcal{F}(V,T,\mu) \equiv EI(S,b) - ST - \mu b = -P(T,\mu)V,$$

$$S = -\frac{d}{dT}\mathcal{F}(V,T,\mu) = \frac{d}{dT}T\ln\tilde{\mathcal{Z}}(V,T,\mu) = \frac{dP}{dT}\,|_{\mu}$$

Statistical physics Gibbs–Duham relation

$$P = T\sigma + \mu\nu - \epsilon, \quad \sigma = \frac{S}{V}, \quad \nu = \frac{b}{V}, \quad \epsilon = \frac{E}{V},$$

is more powerful than the 1st law of thermodynamics:

$$dE(V,S,b) = -P\,dV + T\,dS + \mu\,db, \qquad d\mathcal{F} = -P\,dV - S\,dT - b\,d\mu,$$

Chemical Potentials Tutorial

particle fugacity: $\Upsilon_i \equiv e^{\sigma_i/T} \Longleftrightarrow \sigma_i$ **particle 'i' chemical potential**

Phase space density is:

$$\frac{d^6N_i}{d^3pd^3x} = g_i\frac{\Upsilon_i}{(2\pi)^3}e^{-E_i/T}, \qquad \frac{d^6N_i^{\rm F/B}}{d^3pd^3x} = \frac{g_i}{(2\pi)^3}\frac{1}{\Upsilon_i^{-1}e^{E_i/T}\pm 1}, \qquad \Upsilon_i^{\rm B} \leq e^{m_i/T},$$

each hadron comprise two chemical factors associated with the two different chemical equilibria, example of NUCLEONS:

$$\Upsilon_N = \gamma_N e^{\mu_b/T}, \qquad \Upsilon_{\overline{N}} = \gamma_N e^{-\mu_b/T};$$

$$\sigma_N \equiv \mu_b + T\ln\gamma_N, \qquad \sigma_{\overline{N}} \equiv -\mu_b + T\ln\gamma_N.$$

γ determines the number of nucleon-antinucleon pairs, $\gamma_i(t)$ rises from 0 (initially absent) to 1 for chemical equilibrium. The (baryo)chemical potential μ_b, controls the particle difference = baryon number.

This can be seen looking at the first law of thermodynamics:

$$dE + P\,dV - T\,dS = \sigma_N\,dN + \sigma_{\overline{N}}\,d\overline{N}$$
$$= \mu_b(dN - d\overline{N}) + T\ln\gamma_N(dN + d\overline{N}).$$

To characterize a particle we follow the valance quark content of a hadron forming a product of factors $\gamma_{u,d,s}$, and $\lambda_{u,d,s}$, e.g. for $p(uud)$:

$$\Upsilon_p = \gamma_u^2\gamma_d\,\lambda_u^2\lambda_d, \qquad \Upsilon_{\bar{p}} = \gamma_u^2\gamma_d\,\lambda_u^{-2}\lambda_d^{-1},$$

note that:

$$\lambda_{u,d,s} = e^{\mu_{u,d,s}/T}, \qquad \mu_q = \frac{1}{2}(\mu_u + \mu_d), \quad \lambda_q^2 = \lambda_u\lambda_d \quad \lambda_b = \lambda_q^3.$$

This implies relations between quark and hadron potential:

$\mu_b = 3\mu_q$ $\mu_s = \frac{1}{3}\mu_b - \mu_{\rm S}$, $\lambda_s = \frac{\lambda_q}{\lambda_{\rm S}}$,

Often forgotten: NEGATIVE strangeness in s-hadrons. e.g. for blu $\Lambda(uds)$:

$$\Upsilon_\Lambda = \gamma_u\gamma_d\gamma_s\,e^{\mu_u+\mu_d+\mu_s}, \qquad \Upsilon_{\overline{\Lambda}} = \gamma_u\gamma_d\gamma_s\,e^{-\mu_u-\mu_d-\mu_s},$$

CHEMICAL (NON)EQUILIBRIUM:

γ_i controls overall abundance of quark 'i' pairs	Absolute chemical equilibrium
λ_i controls difference between strange and non-strange quarks 'i'	Relative chemical equilibrium

EXAMPLE: Strangeness in HG:
Relative chemical equilibrium Absolute chemical equilibrium

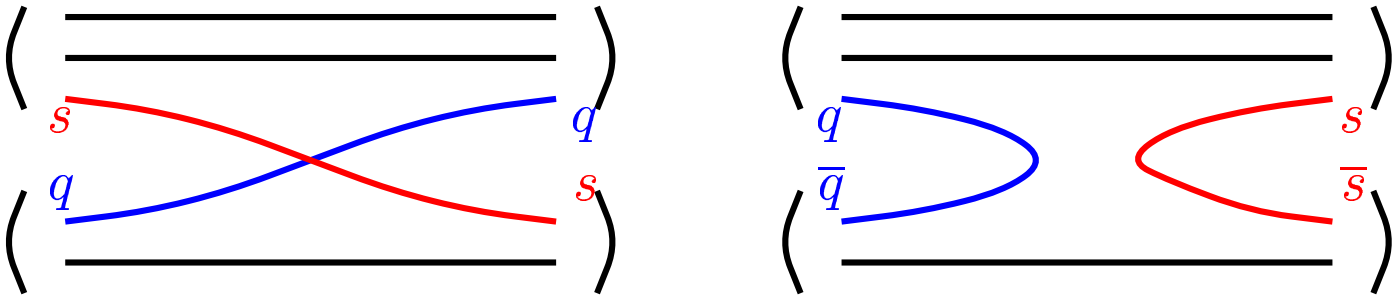

EXCHANGE REACTION **PRODUCTION REACTION**

Absolute equilibrium $\gamma \to 1$ require more rarely occurring truly inelastic collisions with creation of new particles.

Phase Transition Tutorial

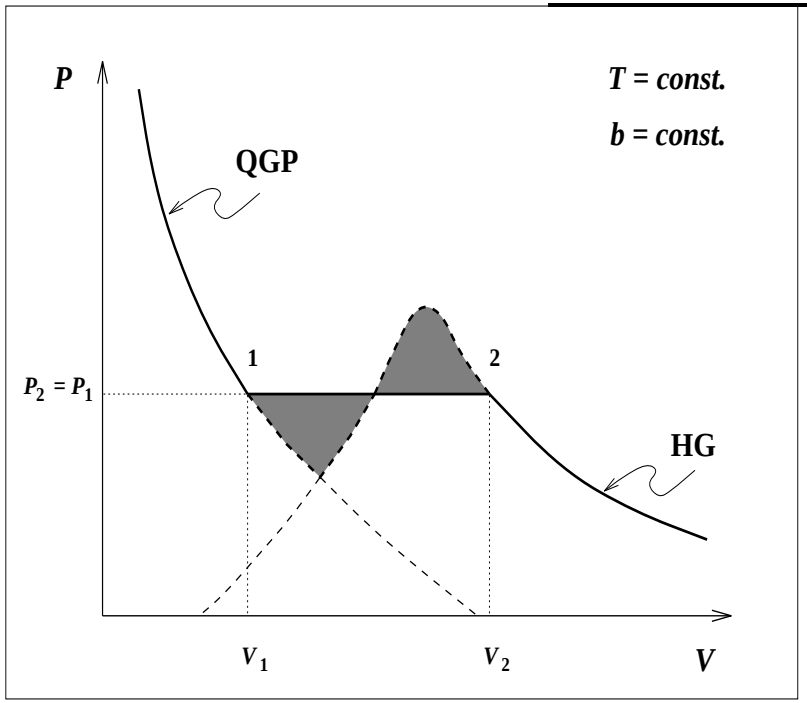

The P–V diagram for the QGP–HG system, shown at fixed temperature and baryon number; dashed lines indicate unstable domains of overheated and undercooled phases. Darkened area: Maxwell construction, connecting the volumes $V_1 = b/\rho_1$ and $V_2 = b/\rho_2$, such that work done along the metastable branches vanishes:

$$\int_{V_1}^{V_2} (P - P_{12})\, dV = 0.$$

Construction can be repeated for different values of b and T, the set of resulting points 1 and 2 forms then two phase-boundary lines.

Between V_1 and V_2 is the mixed phase comprising a mixture of hadrons and drops of QGP. Such a phase formed in early Universe but probably NOT in laboratory experiments.

In a second order phase transition, a discontinuity in e.g. energy density or baryon density is not present, higher order derivatives of partition function are discontinuous.

Independent quantum (quasi)particles

$$\hat{H}|i\rangle = E_i|i\rangle; \qquad [\hat{b},\hat{H}] = 0; \qquad \hat{b}|i,b\rangle = b|i,b\rangle$$

The grand-canonical partition function, can be written as:

$$\mathcal{Z} \equiv \sum_{i,b}\langle i,b|\gamma e^{-\beta(\hat{H}-\mu\hat{b})}|i,b\rangle = \mathbf{Tr}\,\gamma\, e^{-\beta(\hat{H}-\mu\hat{b})} \equiv \sum_{n}\langle n|e^{-\beta(\hat{H}-\mu\hat{b}-\beta^{-1}\ln\gamma)}|n\rangle.$$

The trace of a quantum operator is representation-independent; that is, any complete set of microscopic basis states $|n\rangle$ may be used to find the (quantum) canonical or grand-canonical partition function. This allows us to obtain the physical properties of quantum gases in the, often useful, approximation that they consist of independent (quasi)particles, and, eventually, to incorporate any remaining interactions by means of a perturbative expansion.

$$\mathcal{Z} = \sum_{n} e^{-\sum_{i=1}^{\infty} n_i\beta(\varepsilon_i-\mu b_i-\beta^{-1}\ln\gamma)} = \sum_{n}\prod_{i} e^{-n_i\beta(\varepsilon_i-\mu b_i-\beta^{-1}\ln\gamma)} = \prod_{i}\sum_{n_i=0,1\ldots} e^{-n_i\beta(\varepsilon_i-\mu b_i-\beta^{-1}\ln\gamma)}.$$

To show last equality, one considers whether all the terms on the left-hand side are included on the right hand side, where the sum is not over all the sets of occupation numbers n, but over all the allowed values of occupation numbers n_i.For fermions (F,) we can have only $n_i = 0, 1$,whereas for bosons (Bs) $n_i = 0, 1, \ldots, \infty$. The resulting sums are easily carried out analytically:

$$\ln \mathcal{Z}_{\mathrm{F/B}} = \ln \prod_{i}\left(1 \pm \gamma e^{-\beta(\varepsilon_i-\mu b_i)}\right)^{\pm 1} = \pm\sum_{i}\ln(1 \pm \gamma\lambda_i^b e^{-\beta\varepsilon_i}).$$

- **For antiparticles, the eigenvalue of $\hat{b}$ is the negative of the particle value, the fugacity $\lambda_{\bar{\mathrm{f}}}$ for antiparticles $\lambda_{\bar{\mathrm{f}}} = \lambda_{\mathrm{f}}^{-1}$. This implies $\mu_{\mathrm{f}} = -\mu_{\bar{\mathrm{f}}}$.**
- **level sum $\sum_i$: If energy is the only controlling factor then we carry out this summation in terms of the single particle level density $\sigma_1(\varepsilon, V)$. Taking quantum levels in a box in the limit of infinite volume of the system we find the phase-space integral:**

$$\sum_i \to g \int \frac{d^3x\, d^3p}{(2\pi)^3}.$$

- **Independent particle energy $\varepsilon_i = \sqrt{m_i^2 + \vec{p}^2}$.**

$$\ln \mathcal{Z}_{\rm F/B}(V,\beta,\lambda,\gamma) = \pm gV \int \frac{d^3p}{(2\pi)^3} \left[\ln(1 \pm \gamma\lambda e^{-\beta\sqrt{p^2+m^2}}) + \ln(1 \pm \gamma\lambda^{-1} e^{-\beta\sqrt{p^2+m^2}})\right];$$

Boltzmann limit:

$$\ln \mathcal{Z}_{\rm cl}(V,\beta,\lambda,\gamma) = gV \int \frac{d^3p}{(2\pi)^3} \gamma(\lambda+\lambda^{-1}) e^{-\beta\sqrt{p^2+m^2}}.$$ **for Fermi and Bose**

Single particle phase space occupancy:

$$\begin{aligned}
\overline{w_i} \equiv \frac{\bar{n}_i}{N} &= \frac{e^{-\beta E_i}}{\sum_j e^{-\beta E_j}} \\
&= -\frac{1}{\beta}\frac{\partial}{\partial E_i}\left(\ln \sum_j \gamma e^{-\beta E_j}\right) = -\frac{1}{\beta}\frac{\partial}{\partial E_i}\ln Z \to \frac{1}{\gamma^{-1}\lambda^{-1}e^{\beta E_i} \pm 1} \\
&= \pm \sum_{n=1}^{\infty} \left(\pm\gamma\lambda e^{-\beta E_i}\right)^n \to \gamma\lambda e^{-\beta E_i},
\end{aligned}$$

we recognize FERMI, BOSE, BOLTZMANN distributions.
To evaluate a statistical physics property weight a distribution with suitable factor, for example, energy density results using as the weight single particle energy; particle density has weight 1 (integral of distribution).

Classical relativistic gas

Relativistic Boltzmann gas – a useful integral, for $\varepsilon = \sqrt{m^2+p^2}$:

$$W(\beta m) \equiv \beta^3 \int e^{-\beta\varepsilon} p^2\, dp = (\beta m)^2 K_2(\beta m), \quad \to 2, \ \text{for } m \to 0, \quad \to \sqrt{\frac{\pi m^3}{2T^3}} e^{-m/T}, \ \text{for } m \gg T$$

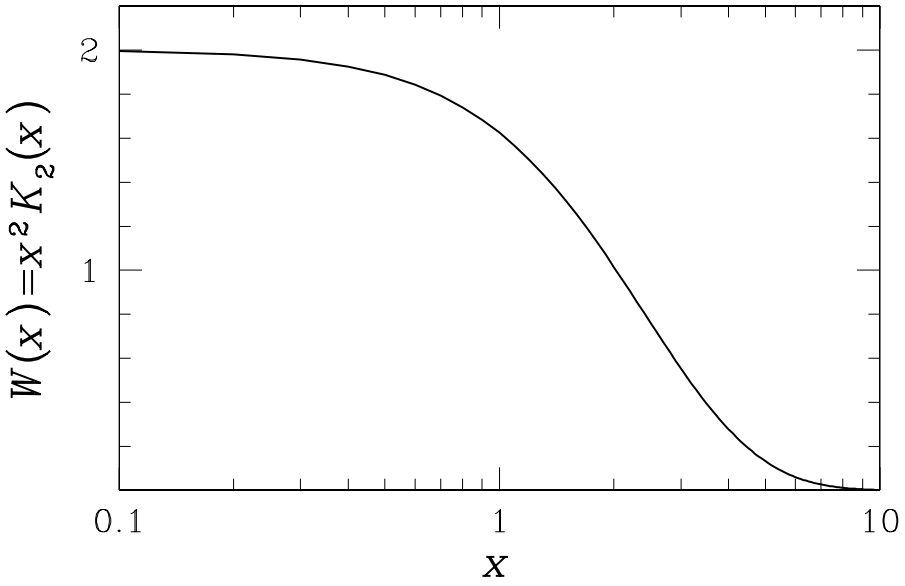

$$\ln \mathcal{Z}_{\rm cl} \equiv Z^{(1)} = \sum_i \gamma_i(\lambda_i + \lambda_i^{-1}) Z_i^{(1)},$$

$$Z_i^{(1)} = g_{\rm f} V \int \frac{d^3p}{(2\pi)^3} e^{-\beta\varepsilon(p)}$$

$$= g_i \frac{\beta^{-3} V}{2\pi^2} W(\beta m_i).$$

Relativistic Bose gas

Relativistic Bose gas, e.g. photon, gluons, pions: exploit the sum:

$$f(\varepsilon) = \frac{1}{\gamma^{-1}e^{\beta\varepsilon} - 1} = \sum_{n=1}^{\infty} \gamma^n e^{-n\beta\varepsilon}, \quad \gamma < e^{\beta m}.$$

or for the partition function

$$\ln \mathcal{Z} = -gV \int \frac{dp^3}{(2\pi)^3} \ln(1 - \gamma e^{-\beta\varepsilon}) = \frac{gV}{2\pi^2} \int_0^{\infty} dp p^2 \sum_{n=1}^{\infty} \frac{\gamma^n}{n} e^{-n\beta\varepsilon}, \quad \gamma < e^{\beta m}.$$

Exchange integral and sum! As we see, each term in the sum differs by $\beta \to n\beta$ and all we have to do it so make sure that we have the right power of $1/n$ in the final expression from substitution. Example: particle density:

$$\rho = \frac{g}{2\pi^2} T^3 \sum_{n=1}^{\infty} \frac{\gamma^n}{n^3} \int_0^{\infty} dx\, x^2 e^{-\sqrt{(nm/T)^2 + x^2}} = \frac{\beta^{-3} g}{2\pi^2} \sum_{n=1}^{\infty} \frac{\gamma^n}{n^3} (n\beta m)^2 K_2(n\beta m) \to \frac{gT^3}{\pi^2} \sum_{n=1}^{\infty} \frac{1}{n^3}.$$

Recall Riemann zeta function:

$$\zeta(k) = \sum_{n=1}^{\infty} \frac{1}{n^k}, \ \zeta(2) = \frac{\pi^2}{6}, \ \zeta(3) \simeq 1.202, \ \zeta(4) = \frac{\pi^4}{90}.$$

For a Fermi occupation function, the signs of the terms in the sums are alternating, which leads to the eta function

$$\eta(k) = \sum_{n=1}^{\infty} (-1)^{n-1} \frac{1}{n^k} = (1 - 2^{1-k})\zeta(k), \ \eta(3) = \frac{3}{4}\zeta(3) = 0.901\,5, \ \eta(4) = \frac{7}{8}\zeta(4) = \frac{7}{720}\pi^4.$$

Quark gas

Fermi gas, (note that we have assumed complete phase space occupancy $\gamma = 1$)

$$\ln \mathcal{Z}_{\rm F} \;=\; g_{\rm F} V \int \frac{d^3p}{(2\pi)^3}[\ln(1+e^{-\beta(\varepsilon-\mu)}) + \ln(1+e^{-\beta(\varepsilon+\mu)})],$$

integrate by parts: $d^3p \to 4\pi p^2 dp$

$$3\frac{T}{V}\ln \mathcal{Z}_{\rm F} \;=\; g_{\rm F}\frac{\beta}{3}\int \frac{d^3p}{(2\pi)^3}\frac{\vec{p}^{\,2}}{\varepsilon}\left(\frac{1}{e^{\beta(\varepsilon-\mu)}+1}+\frac{1}{e^{\beta(\varepsilon+\mu)}+1}\right).$$

Substitute the arguments of f and $\bar{f}$ with $x = \beta(\varepsilon \pm \mu)$:

$$3\frac{T}{V}\ln \mathcal{Z}_{\rm F} = \frac{g_{\rm F}}{2\pi^2}T^4\Big(\int_{\beta(m-\mu)}^{\infty} dx\,\frac{[(x+\mu/T)^2-(m/T)^2]^{3/2}}{e^x+1} + (\mu\to-\mu)\Big).$$

For $m \to 0$ $[(x \pm \mu/T)^2 - (m/T)^2]^{3/2} \to (|x \pm \beta\mu|)^3$, integrals split to be from $\pm\beta\mu \to 0$ and from $0 \to \infty$. The finite-range terms:

$$\int_{-\beta\mu}^{0} dx\,\frac{|x+\beta\mu|^3}{1+e^x} - \int_0^{\beta\mu} dx\frac{(x-\beta\mu)^3}{1+e^x} \;=\; \int_0^{\beta\mu} dx\,\frac{(\beta\mu-x)^3}{1+e^{-x}} + \int_0^{\beta\mu} dx\,\frac{(\beta\mu-x)^3}{1+e^x}$$

$$= \int_0^{\beta\mu} dx\,(\beta\mu-x)^3 = \frac{(\beta\mu)^4}{4},$$

The reminder evaluated expanding $(e^x+1)^{-1} = \sum_{n=1}^{\infty} e^{-nx}$.

$$\ln \mathcal{Z}_{\rm F}|_{m=0} = \frac{g_{\rm F} V \beta^{-3}}{6\pi^2}\left(\frac{7\pi^4}{60}+\frac{\pi^2}{2}\ln^2\lambda+\frac{1}{4}\ln^4\lambda\right).$$

s-QUARK PHASE-SPACE in QGP with Coulomb

For quarks chemical fugacity λ_s;

For antiquarks chemical fugacity λ_s^{-1};

Both quarks and antiquarks subject to pair-abundance factor γ_s

$$\langle s-\bar{s}\rangle = \int g_s \frac{d^3p d^3x}{(2\pi)^3} \frac{1}{1+\gamma_s\lambda_s e^{-(E-\frac{1}{3}V_c)/T}} - \frac{1}{1+\gamma_s\lambda_s^{-1} e^{-(E+\frac{1}{3}V_c)/T}}$$

When Coulomb field is negligible:

deconfinement and $\langle s-\bar{s}\rangle = 0 \Rightarrow$ $\boxed{\lambda_s = 1}$

COULOMB EFFECT on s-QUARK PHASE-SPACE in QGP

Relevant only for CERN Pb–Pb. In Boltzmann approximation:

$$\langle s-\bar{s}\rangle = \int g_s \frac{d^3p}{(2\pi)^3}\gamma_s e^{-E/T} \int_{R_{\rm f}} \frac{d^3r}{V_{R_{\rm f}}} \left[\lambda_s e^{\frac{V_c}{3T}} - \lambda_s^{-1} e^{-\frac{V_c}{3T}}\right] .$$

for $R_{\rm f} = 8\,$fm, $T = 140\,$MeV, $m_s = 200\,$MeV and $Z_{\rm f} = 150 \Rightarrow$ $\boxed{\lambda_s = 1.1}$

PERTURBATIVE EFFECTS

an essential prerequirement for the perturbative theory to be applicable in domain of interest to us, is the relatively small experimental value $\alpha_{\rm s}(M_Z) \simeq 0.118$, experimentally established in recent years.

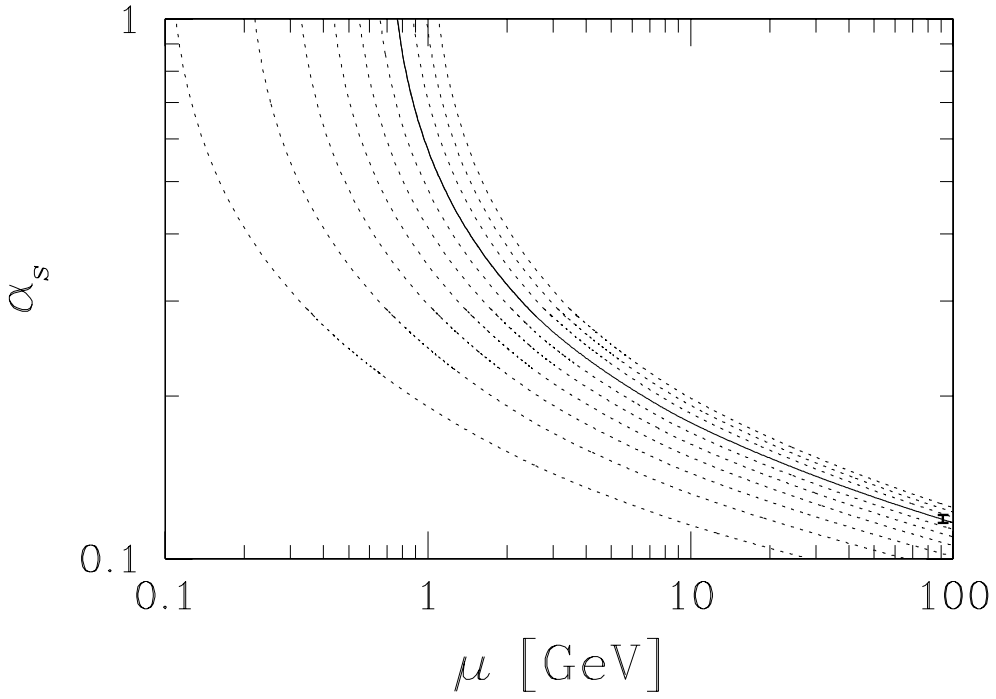

$\alpha_{\rm s}^{(4)}(\mu)$ as function of energy scale μ for a variety of initial conditions. Solid line: $\alpha_{\rm s}(M_Z) = 0.1182$ (experimental point, includes the error bar at $\mu = M_Z$). Result of integration of renormalization group equation.

$$\mu\frac{\partial\alpha_s}{\partial\mu} = -b_0\alpha_s^2 - b_1\alpha_s^3 + \ldots \equiv \beta_2^{\rm pert}\,,$$

note that above μ is scale of energy NOT chemical potential

$$b_0 = \frac{11 - 2n_{\rm f}/3}{2\pi}\,, \qquad b_1 = \frac{51 - 19n_{\rm f}/3}{4\pi^2}\,.$$

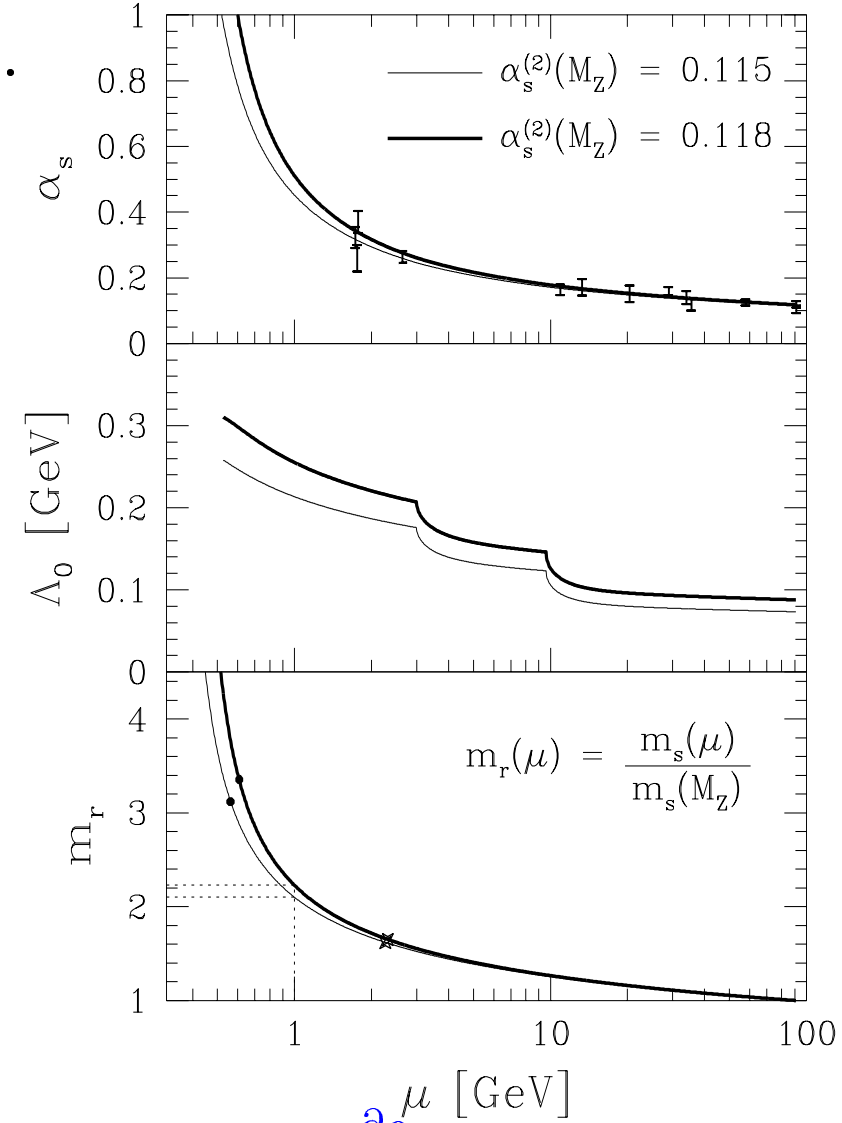

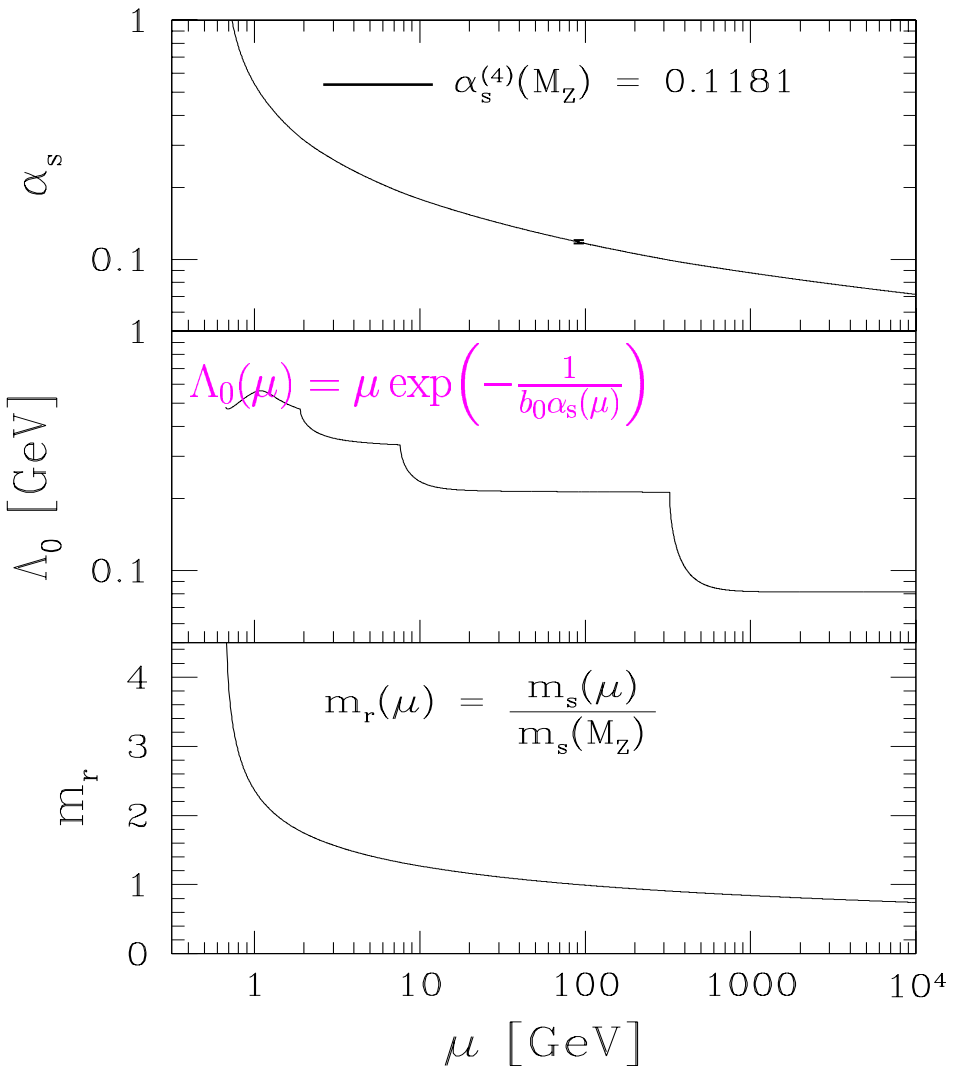

$$\mu \frac{\partial \alpha}{\partial \mu} \equiv \beta(\alpha_s) \qquad \beta^{\rm pert} = -\alpha_s^2 \left[\, b_0 + b_1 \alpha_s + b_2 \alpha_s^2 + \cdots \,\right]$$

$$-\frac{\mu}{m}\frac{\partial m}{\partial \mu} \equiv \gamma(\alpha_s), \qquad \gamma_{\rm m}^{\rm pert} = \alpha_s \left[\, w_0 + w_1 \alpha_s + w_2 \alpha_s^2 + \cdots \,\right]$$

QCD perturbative interaction

QCD perturbative interaction reduce effective degeneracy: for each flavor of quarks (u, d, s) we have 2-spins, 3-colors, so $g_{u,d,s} = 6$, and need to keep in mind the doubling due to particle-antiparticle symmetry. Evaluation in thermal field theory of the Feynman diagrams in order α_s shows that on average this interaction is ATTRACTIVE and some of the many degrees of freedom freeze. Feynman diagrams contributing are of the type:

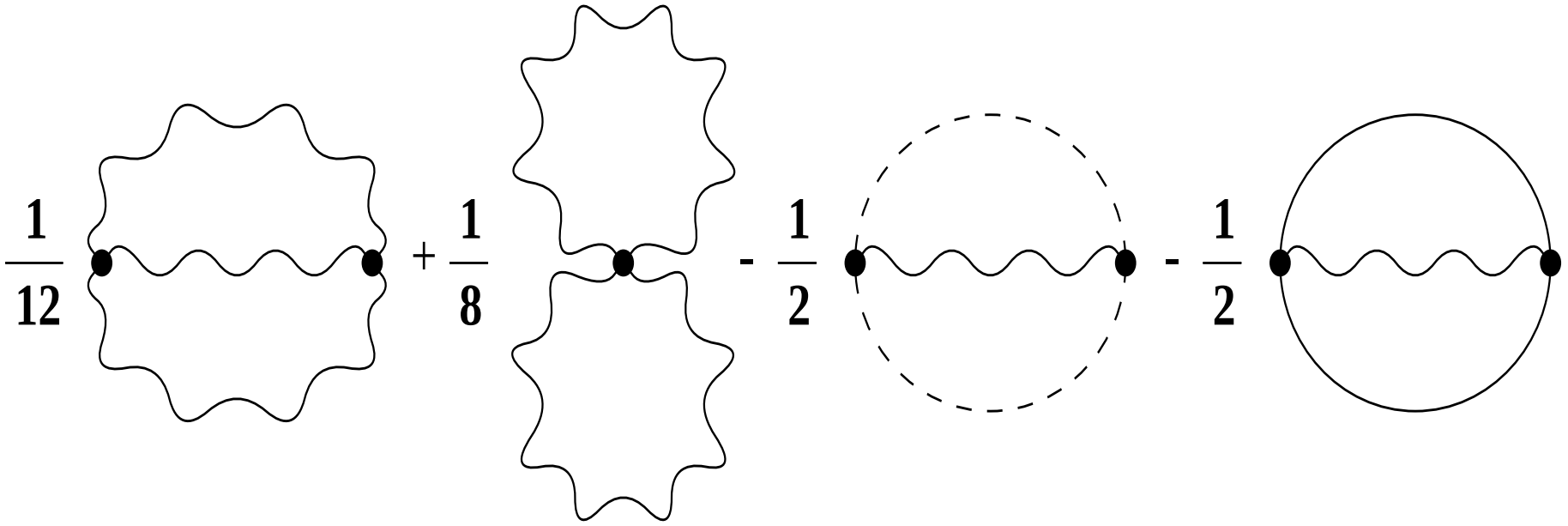

Wavy lines represent gluons, solid lines represent quarks, and dashed lines denote the ghost subtractions of non-physical degrees of freedom. Lecturs by R. Baier

Perturbative QCD and QGP

$$\frac{T}{V}\ln\mathcal{Z}_{QGP}=-\mathcal{B}+\frac{8}{45\pi^2}c_1(\pi T)^4+\sum_{i=u,d,s}\frac{n_i}{15\pi^2}\left[\frac{7}{4}c_2(\pi T)^4+\frac{15}{2}c_3\left(\mu_i^2(\pi T)^2+\frac{1}{2}\mu_i^4\right)\right]$$

$$c_1=1-\frac{15\alpha_s}{4\pi}\,,\quad c_2=1-\frac{50\alpha_s}{21\pi}\,,\quad c_3=1-\frac{2\alpha_s}{\pi}\,.$$

We recall that $\mu_b=3\mu_q$ and $\lambda_q=e^{\mu_q/T}$. The temperature dependence $\alpha_s(T)$ is obtained from $\alpha_s(\mu)$ setting the energy scale $\mu=2\pi T$. $\alpha_s(\mu)$ is obtained integrating the renormalization group equation, where $\alpha_s(\mu=M_Z)=0.1182+0.001-0.0016$. in the domain of relevance $\alpha_s/\pi<0.22$ We cross several flavor mass thresholds, $n_{\rm f}(\mu)\neq$ Const. Error of solution with $n_{\rm f}(\mu)=$ Const. accumulates,

$$\alpha_s^2(\mu)\simeq\frac{2}{b_0\bar{L}}\left[1-\frac{2b_1}{b_0^2}\frac{\ln\bar{L}}{\bar{L}}\right],\quad \bar{L}\equiv\ln(\mu^2/\Lambda^2)\,,$$

with $\Lambda=0.15\,$GeV is not precise enough at scale to interest compared to exact 2-loop numerical solution. This form suitable for $\mu>10\,$GeV.

$\alpha_s(T)$ and Pressure of QGP-Liquid

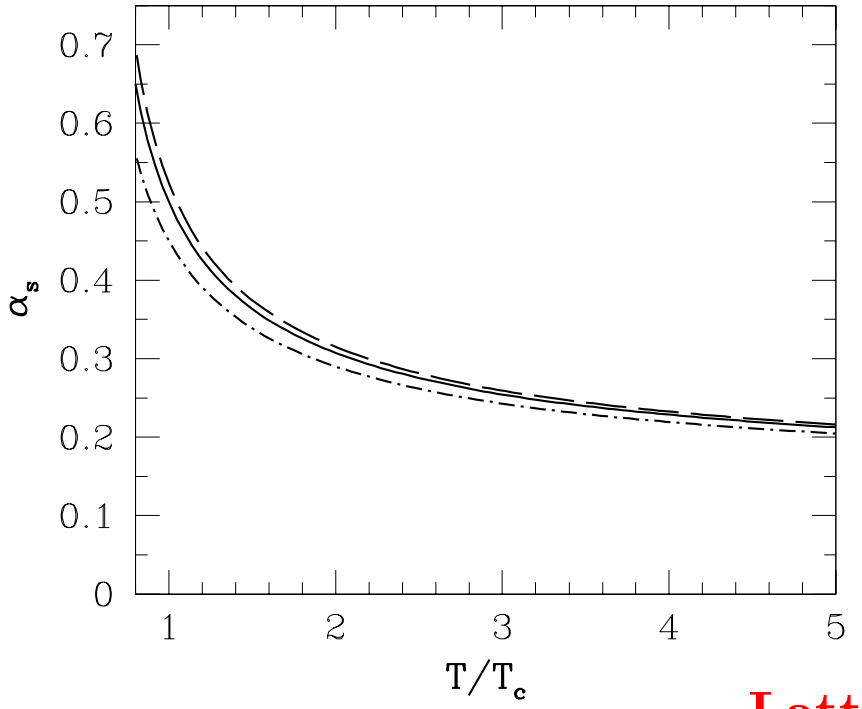

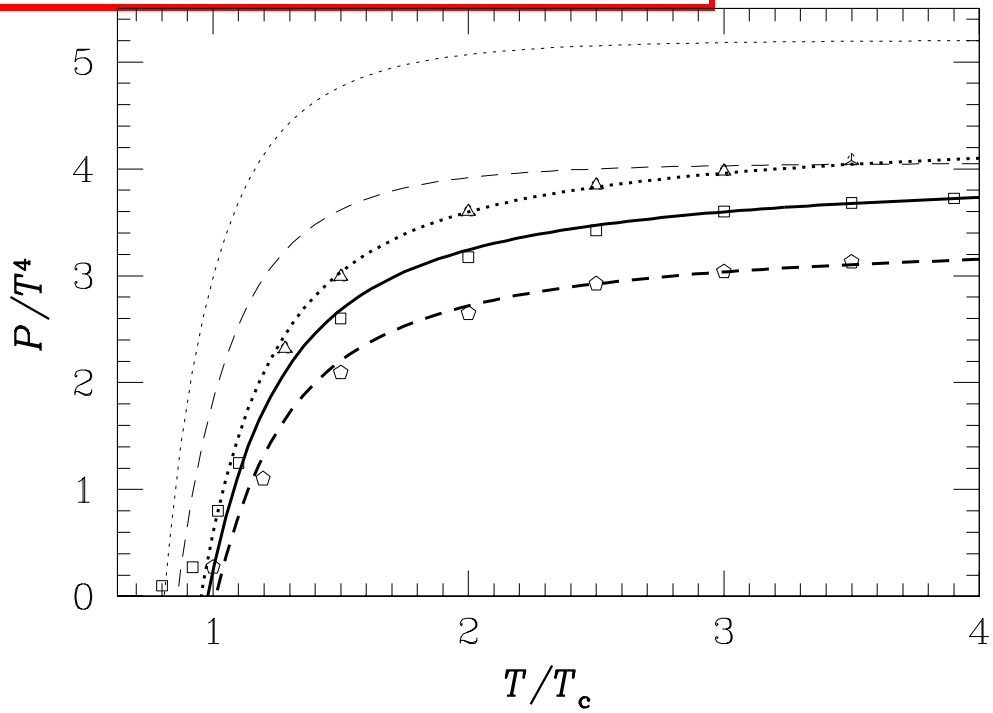

$\alpha_s(2\pi T)$ **for** $T_c = 0.16$ **GeV.**
$\mu = 2\pi T = T/T_c$ **[GeV]**
Dashed line:
$\alpha_s(M_Z) = 0.119$**;**
solid line $= 0.118$**;**
dot-dashed $= 0.1156$**.**
For $T < 5T_c$**:**

$$\alpha_{\rm s}(T) \simeq \frac{\alpha_{\rm s}(T_{\rm c})}{1+C\ln(T/T_{\rm c})}$$

$$\alpha_{\rm s}(T_{\rm c}) = 0.50^{-0.05}_{+0.03}$$

$$C = 0.760 \pm 0.002.$$

Lattice-QCD results F. Karsch, E. Laermann and A. Peikert *Phys. Lett.* **B 478, 447-455, (2000); Quark-gluon liquid model at** $\lambda_q = 1$ **(thick lines) and with** $\mu = 2\pi T = \kappa T/T_c, \kappa = 1$ **GeV.** $\mathcal{B} = 0.19\,\mathbf{GeV/fm^3}$**. Solid line 2+1 flavors** $(m_s/T = 1.7)$
dotted: 3 flavors, dashed: 2 flavors.
Thin lines: without perturbative α_s **effects,which is just the bag model.**

What do Interactions, What does $\mathcal{B}$

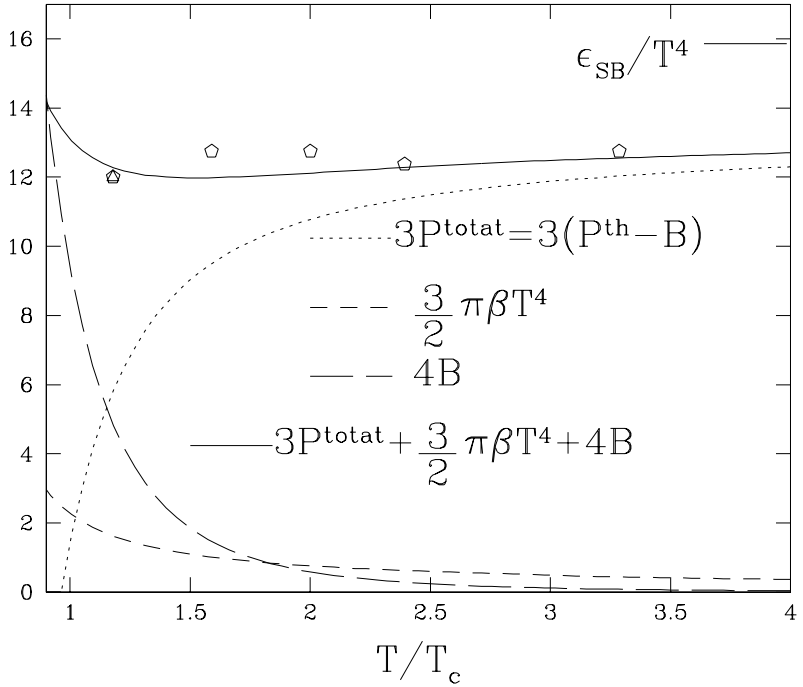

$\kappa=1,\ B=2$

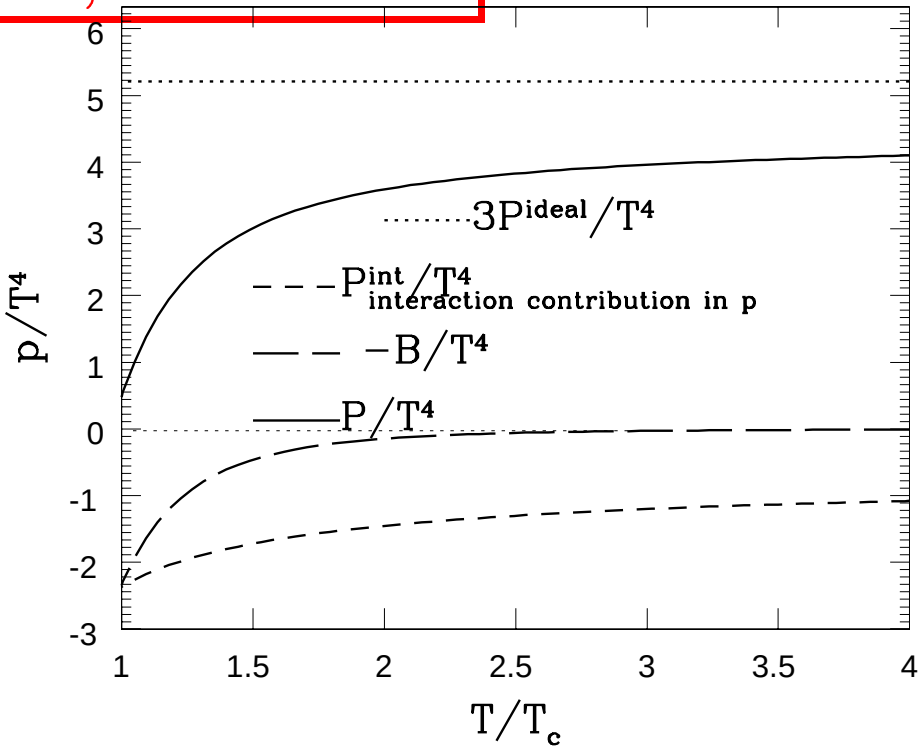

$\kappa=1,\ B=0.2, N_f=3, m/T=0$

$$\epsilon_{\rm QGP} = -\frac{\partial \ln \mathcal{Z}_{QGP}(\beta,\lambda)}{V\partial\beta} = 4\mathcal{B} + 3P_{QGP} + A\,,$$

$$A = (b_0\alpha_s^2 + b_1\alpha_s^3)\left[\frac{2\pi}{3}T^4 + \frac{n_{\rm f}5\pi}{18}T^4 + \frac{n_{\rm f}}{\pi}\left\{\mu_{\rm q}^2T^2 + \frac{1}{2\pi^2}\mu_{\rm q}^4\right\}\right]\,.$$

Extension to finite baryon density

To relate the QCD scale to the temperature $T = 1/\beta$ we use

$$\mu = 2\sqrt{(\pi T)^2 + \mu_q^2} = 2\pi\beta^{-1}\sqrt{1 + \frac{1}{\pi^2}\ln^2\lambda_q}\,.$$

A convenient way to obtain entropy and baryon density uses the thermodynamic potential $\mathcal{F}$:

$$\frac{\mathcal{F}(T,\mu_q,V)}{V} = -\frac{T}{V}\ln\mathcal{Z}(\beta,\lambda_q,V)_{QGP} = -P_{QGP}\,.$$

The entropy density is:

$$s_{QGP} = -\frac{d\mathcal{F}}{V\,dT} = \frac{32\pi^2}{45}c_1T^3 + \frac{n_{\rm f}7\pi^2}{15}c_2T^3 + n_{\rm f}c_3\mu_{\rm q}^2T + A\frac{\pi^2T}{\pi^2T^2+\mu_{\rm q}^2}\,.$$

Noting that baryon density is 1/3 of quark density, we have:

$$\rho_{\rm B} = -\frac{1}{3}\frac{d\mathcal{F}}{V\,d\mu_{\rm q}} = \frac{n_{\rm f}}{3}c_3\left\{\mu_{\rm q}T^2 + \frac{1}{\pi^2}\mu_{\rm q}^3\right\} + \frac{1}{3}A\frac{\mu_{\rm q}}{\pi^2T^2+\mu_{\rm q}^2}\,.$$

$$A = A_g + A_q + A_s; \qquad A_g = (b_0\alpha_s^2 + b_1\alpha_s^3)\frac{2\pi}{3}T^4$$

$$A_{i=q,s} = (b_0\alpha_s^2 + b_1\alpha_s^3)\left[\frac{n_{\rm i}5\pi}{18}T^4 + \frac{n_{\rm i}}{\pi}\left\{\mu_{\rm i}^2T^2 + \frac{1}{2\pi^2}\mu_{\rm i}^4\right\}\right]\,.$$

Extension to finite baryon density works

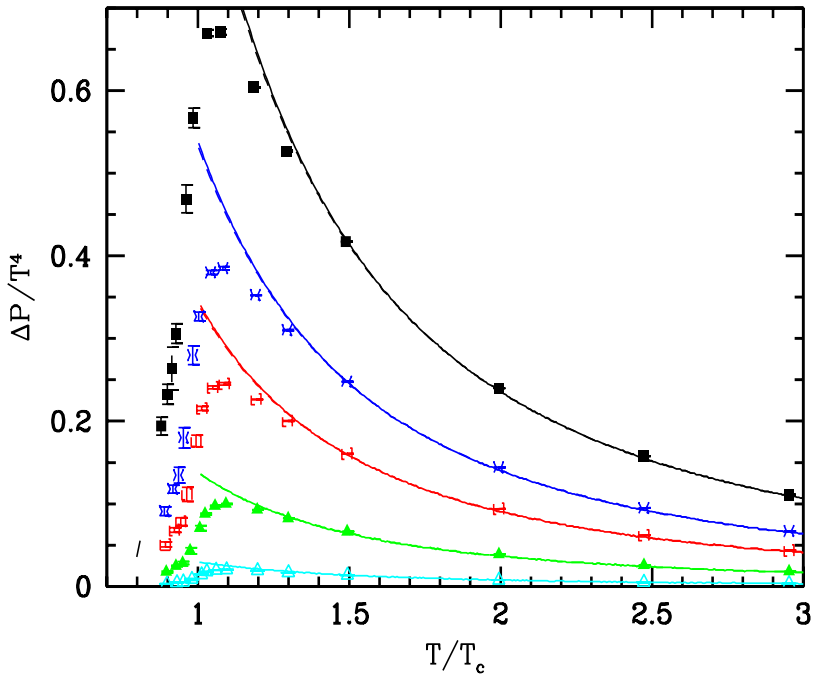

$\Delta P \equiv P(T,\mu_b) - P(T,\mu_b = 0)$ **normalized by** T^4 **as function of** T/T_c **for** $\mu_b =$**, 100, 210, 330, 410 and 530 MeV from bottom to top. Data points from Z. Fodor et al lattice work, solid lines massless liquid of quarks. Dashed (and mostly invisible) results with finite mass correction applied for** $m_q = 65$ **MeV as used in lattice data.**

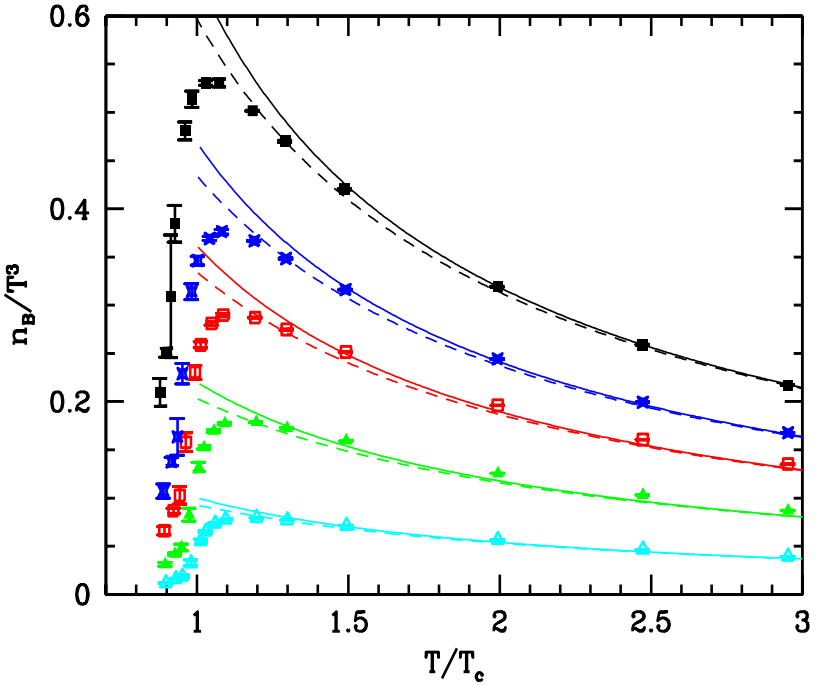

Baryon density $n_{\rm B}$ **normalized by** T^3 **as function of** T/T_c **for** $\mu_b = 100$**, 210, 330, 410 and 530 MeV from bottom to top. Solid lines massless liquid of quarks. Dashed lines: allowance is made for** $m_q = 65$ **MeV as is used to obtain the lattice data.**

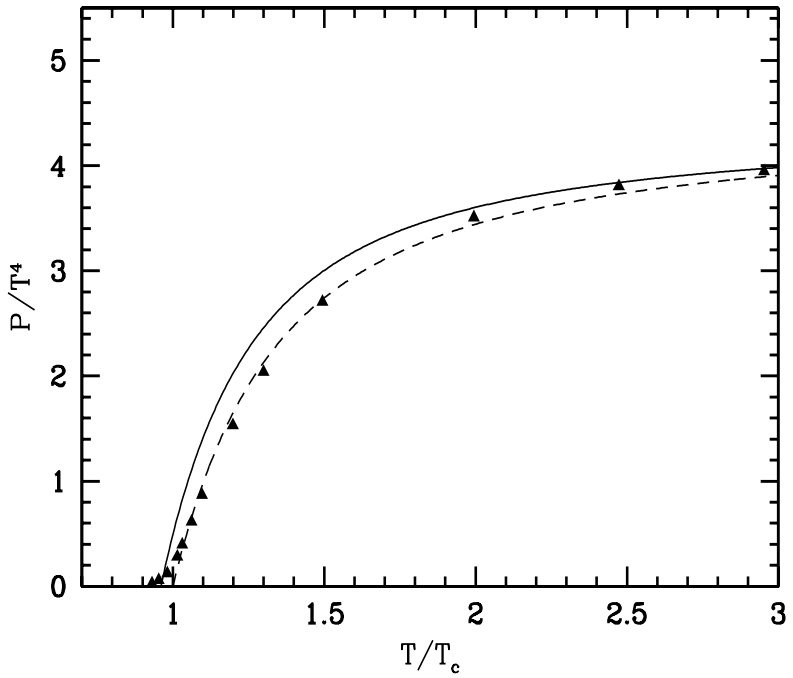

The pressure $P(T,\mu_b=0)$ normalized by T^4 as function of T/T_c. Data points from Z. Fodor et al lattice work. Solid lines: massless gluons with $\mathcal{B}=(0.211\,\mathrm{GeV})^4$. Dashed line allows for a finite mass $m_G=200$ MeV.

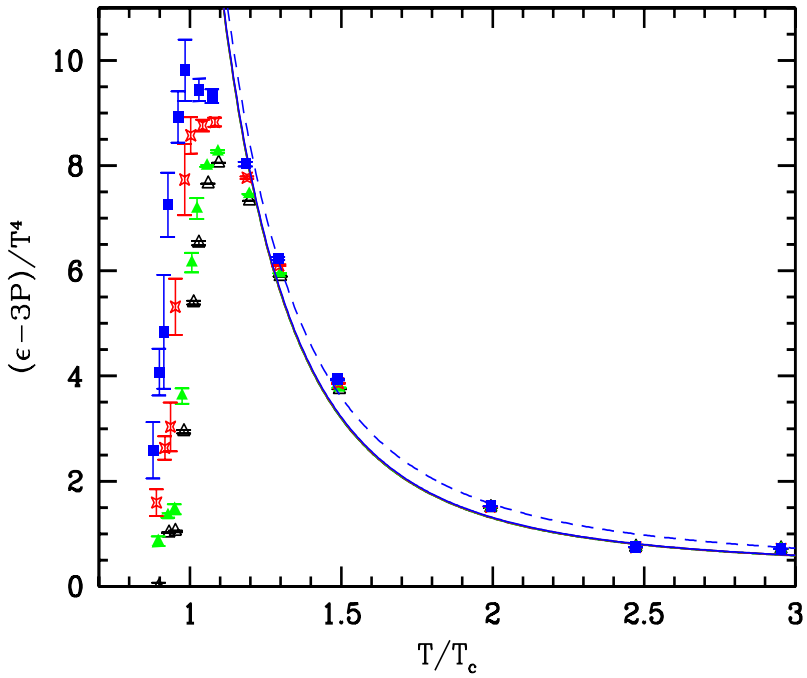

$(\epsilon-3P)/T^4$ as function of T/T_c for $\mu_b=0$, 210, 410 and 530 MeV, for $\mathcal{B}=(0.211\,\mathrm{GeV})^4$ and $T_c=173\,\mathrm{MeV}$. Solid lines: massless gluons. Dashed lines: allowance is made for $m_G=200$ MeV. All chemical potential lines coincide within line-width.

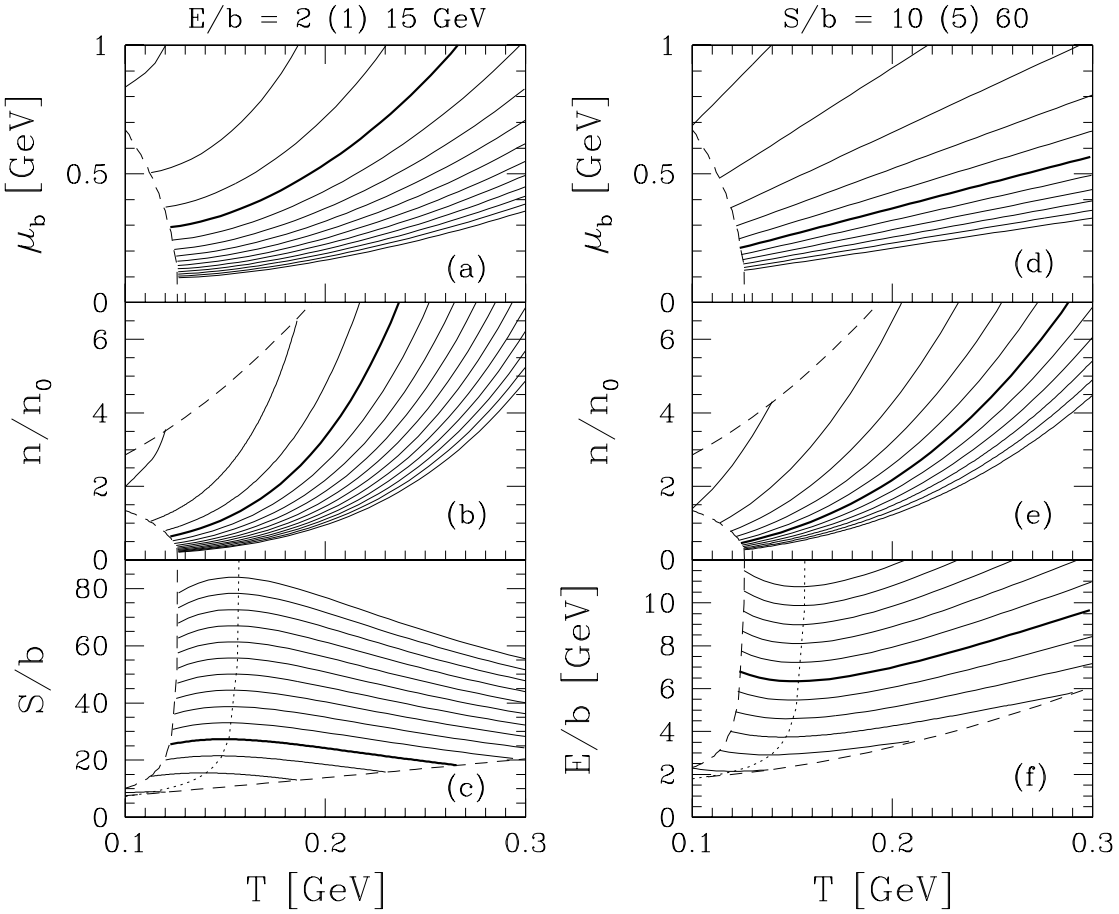

Left: lines corresponding to fixed energy per baryon $E/b = 2$ to 15 GeV in steps of 1 GeV, with $E/b = 5$ highlighted. Right: E/b lines corresponding to fixed entropy per baryon $S/b = 10$ to 60 in steps of 5, with $S/b = 35$ highlighted. (a) and (d) (top section), baryo-chemical potential μ_b , (b) and (e) (middle section), baryon density n/n_0 in units of equilibrium nuclear density, and (c) bottom portion: on left S/b, the entropy per baryon (highest E/b at the top), and (f) on right E/b, (highest S/b at the bottom).

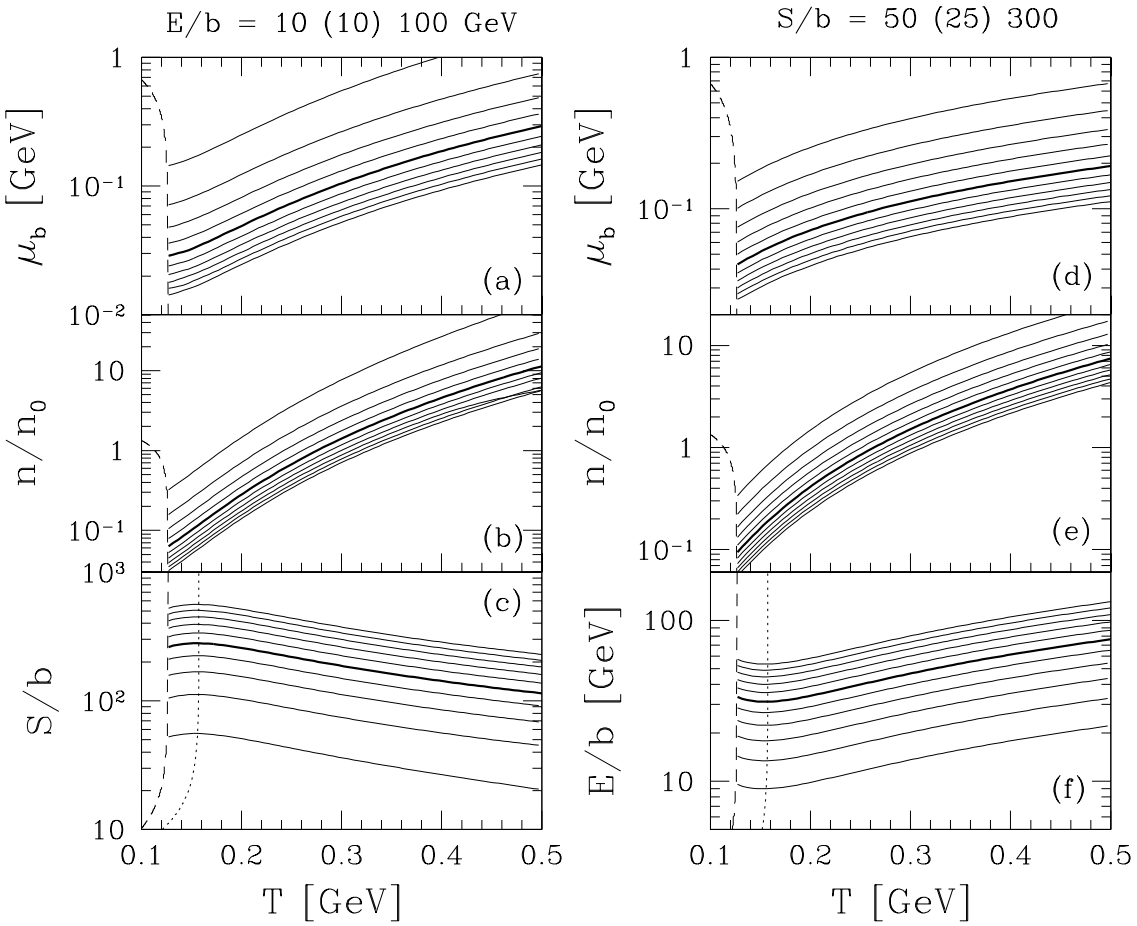

Now for the RHIC energy domain. Left, lines at fixed energy per baryon $E/b = 10$ to 100 GeV in steps of 10 GeV, with $E/b = 50$ GeV highlighted. Right, lines at fixed entropy per baryon $S/b = 50$ to 300 in steps of 25, with $S/b = 175$ hilighted.

Other way: massive quasi-particles

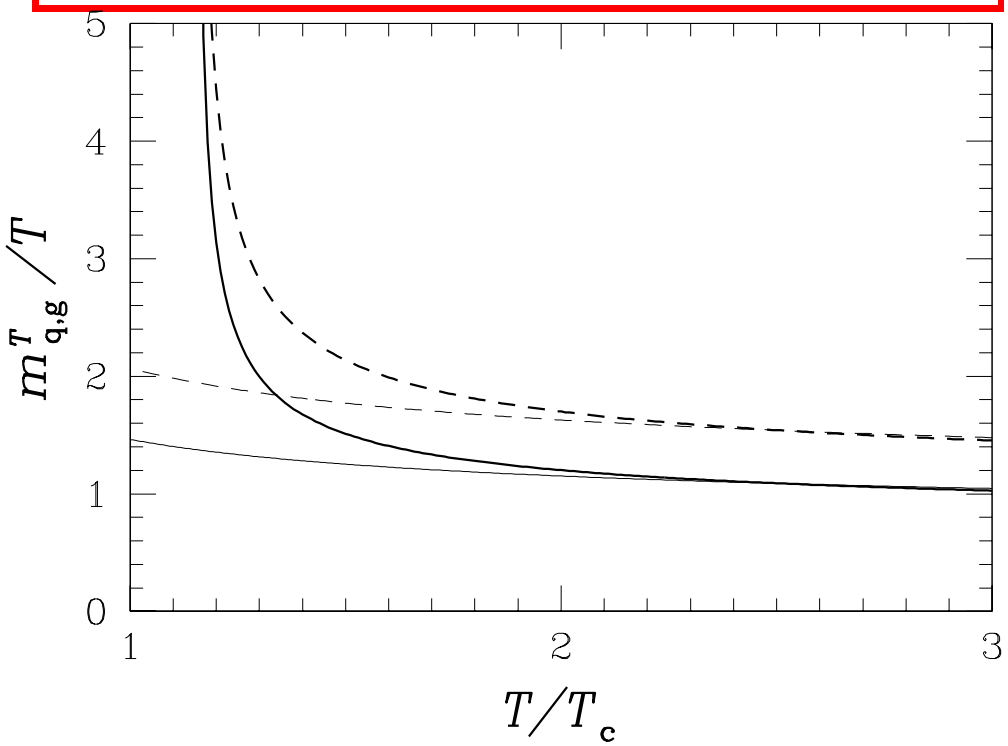

Thermal masses fitted to reproduce Lattice-QCD results
Thick solid line for quarks, and thick dashed line for gluons. Thin lines, perturbative QCD masses for $\alpha_s(\mu = 2\pi T)$.

$$(m_{\rm q}^{\rm T})^2 = \frac{4\pi}{3}\alpha_s T^2\,, \qquad (m_{\rm g}^{\rm T})^2 = 2\pi\alpha_s T^2\left(1+\frac{n_{\rm f}}{6}\right)\,,$$

The thermal masses required to describe the reduction of the number of degrees of freedom for $T > 2T_{\rm c}$ are outside of the range of the vacuum structure influence ($\mathcal{B}$) the perturbative QCD result. This means that thermal masses express, in a different way, the effect of perturbative QCD

Hadron Gas Phase

We can use the methods we proposed for quarks and gluons to describe the gas of pions, nucleons and all the rest! To be precise many thousand hadronic particles. Hadron Gas phase. A topic in itself, so I will just glance at it and its properties.

MISSING HADRON RESONANCES

Hagedorn mass spectrum is exponential, experimentally known resonances are exponential, within experimental limits:

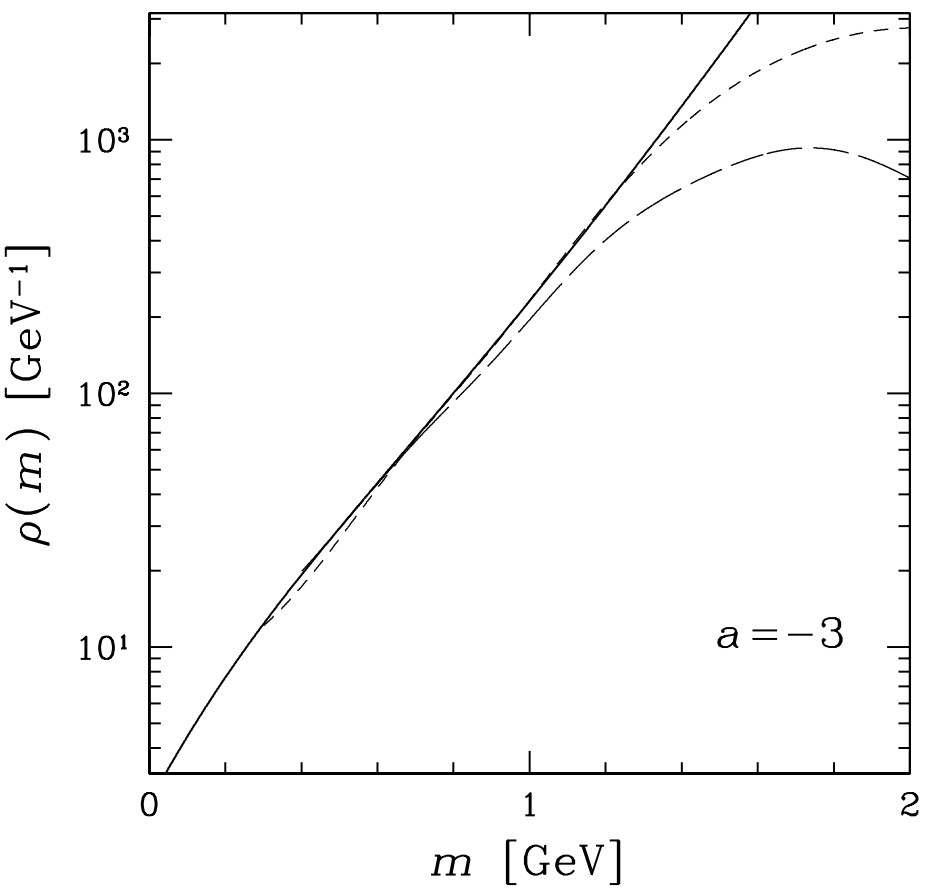

Dashed lines are the (smoothed) hadronic mass spectrum. The solid line represents the fit

$$\rho(m) \approx c(m_0^2 + m^2)^{a/2} \exp(m/T_0)$$

$T_0 = 0.158$ **GeV,** ($a = -3$ **preferred in the statistical bootstrap model,** $m_0 = 0.66$ **GeV).**

Long-dashed line:
1411 states of 1967.

Short-dashed line:
4627 states of 1996.

Exponential behavior related to critical behavior.

Lots of resonances missing above 1.4 GeV (log scale!)

How relevant an effect

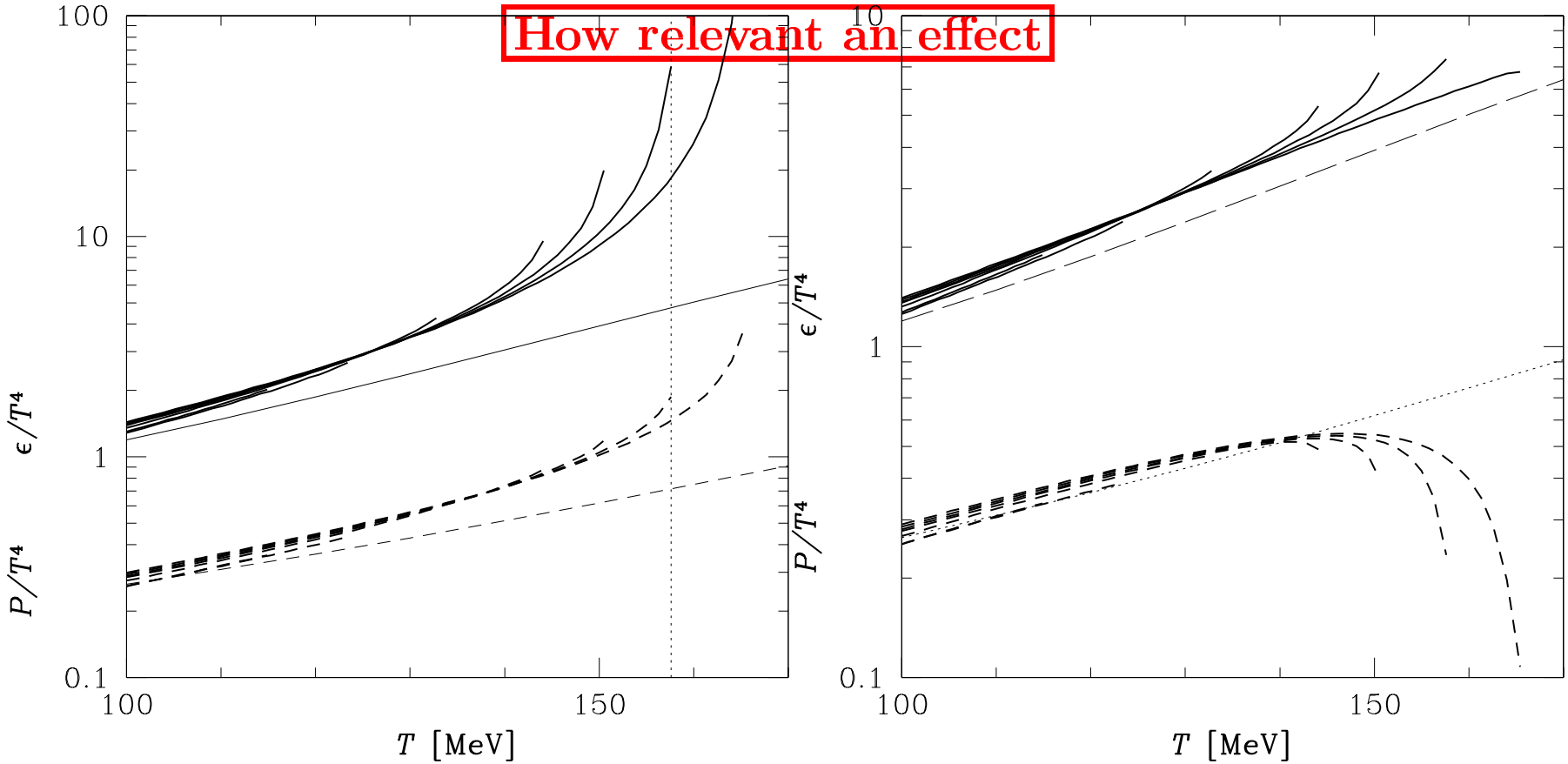

Point hadron gas **Hadrons of finite volume**

Thin lines from currently known experimental mass spectrum. All fugacities= 1. Thick: exponential mass spectrum with values of $a \in (-2.5, -7)$. Despite cancellation between two omissions hadron multiplicity e.g. π, h^- certainly 10–30% too low (fit 6%, if you believe fits).

A FEW EXAMPLES OF WHAT KNOWLEDGE OF EQUATIONS OF STATE ALLOW US TO THINK ABOUT

Inertia to Force Ratio

For study of flow of matter one of most relevant quantities is the rigidity of the matter. Hadrons are heavy thus their pressure is less, hence unlike for relativistic matter, $\epsilon/P > 3$ But there is a 'soft' point.

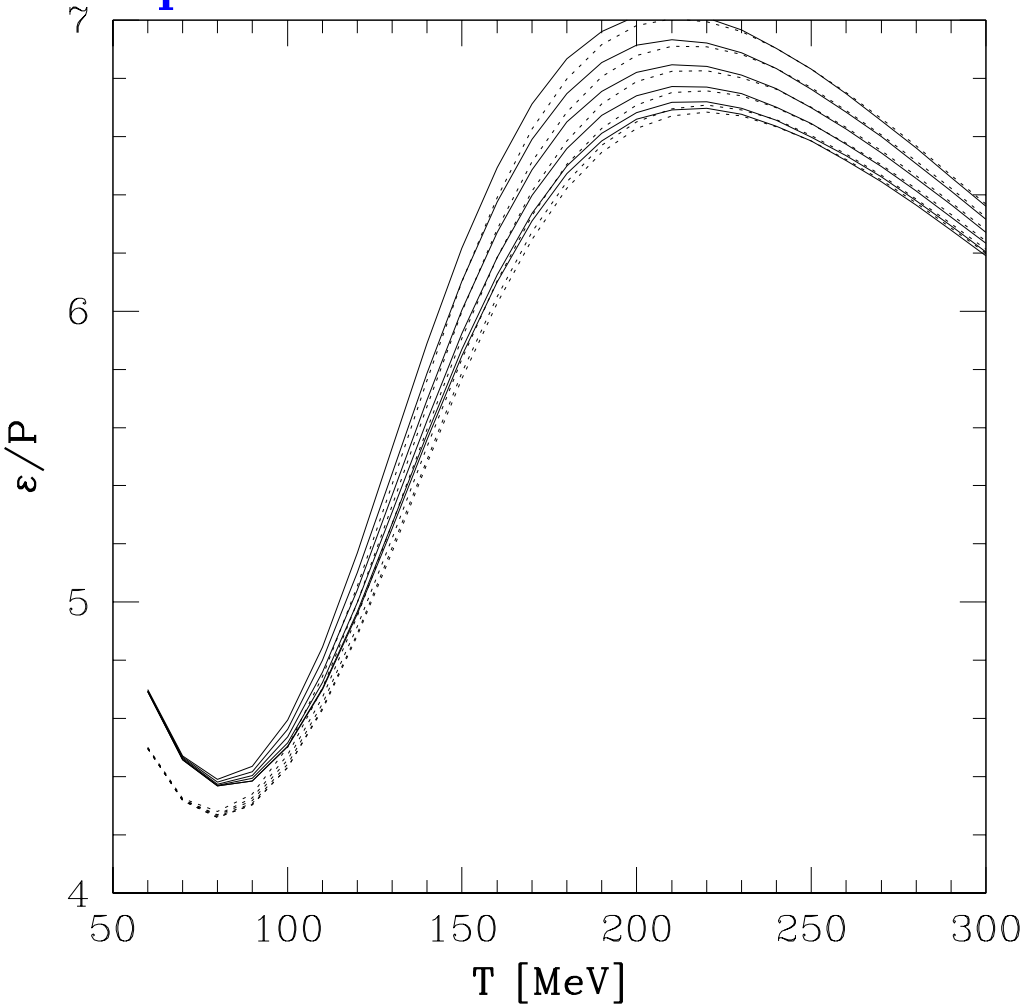

The energy density over pressure for a hadronic gas with statistical parameters $\lambda_s = 1.1$ and $\gamma_s/\gamma_q = 0.8$, with $\lambda_q = 1$ to 2 in steps of 0.2 from bottom to top and $\gamma_q = 1$ (dashed lines), or $\gamma_q = e^{m_\pi/(2T)}$ (full lines).

Hadronic gas flows very different from quark-gluon plasma.

Phase boundary

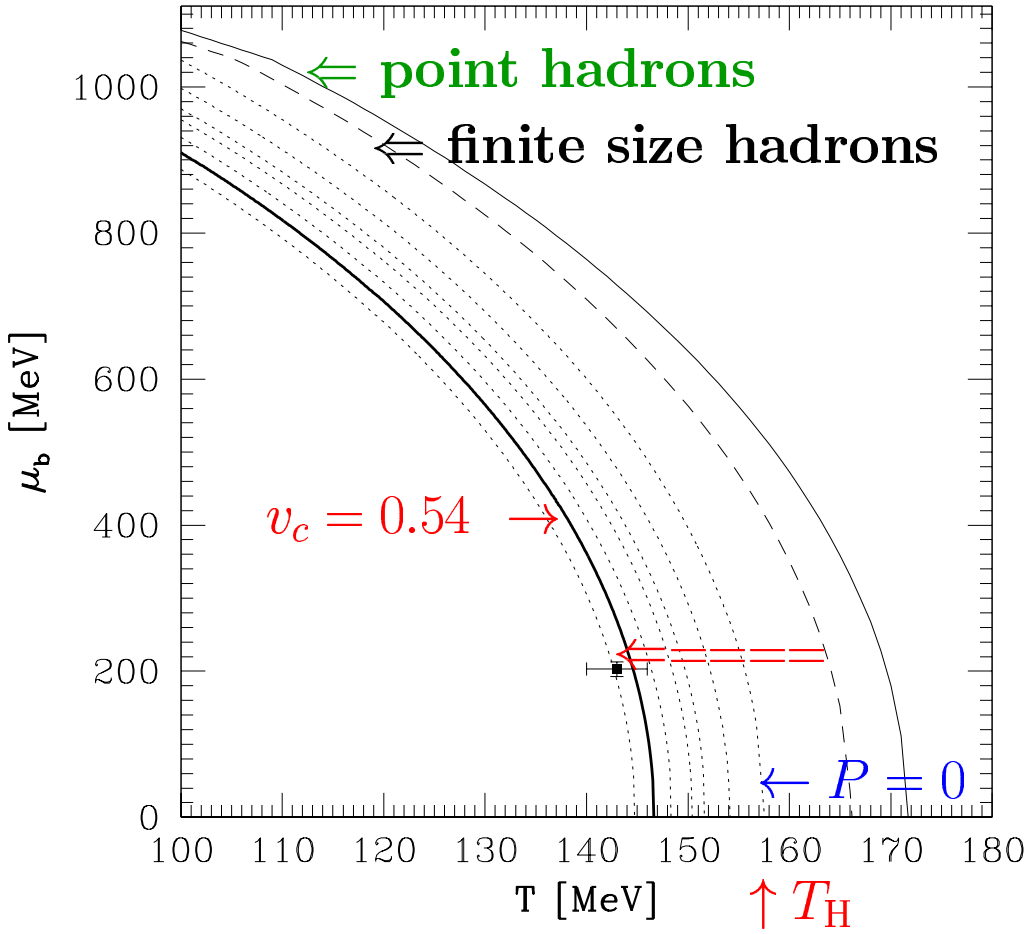

Solid: point hadrons T_p

Dashed: finite size

Dotted: $T_c(\mu_b)|_{P_{eff}-\mathcal{B}=0}$ for $v^2 = 0, 1/10, 1/6, 1/5, 1/4, 1/3$.

Thick solid: breakup with $v = 0.54$ ($\kappa = 0.6$)

PRL 85 (2000) 4695

DEEP SUPERCOOLING by 20 MeV

$T_H = 158$ MeV Hagedorn temperature where $P = 0$, no hadron P

$T_f \simeq 0.9 T_H \simeq 143$ MeV is where supercooled QGP fireball breaks up

equilibrium phase transformation is at $\simeq 166$.

Super-cooling of a fast expanding fireball

P and ε: local in QGP particle pressure, energy density, $\vec{v}$ local flow velocity. The pressure component in the energy-momentum tensor:

$$T^{ij} = P\delta_{ij} + (P+\varepsilon)\frac{v_i v_j}{1-\vec{v}^2}\,.$$

The rate of momentum flow vector $\vec{\mathcal{P}}$ at the surface of the fireball is obtained from the energy-stress tensor T_{kl} :

$$\vec{\mathcal{P}} \equiv \widehat{\mathcal{T}}\cdot\vec{n} = P\vec{n} + (P+\varepsilon)\frac{\vec{v}_{\rm c}\,\vec{v}_{\rm c}\cdot\vec{n}}{1-\vec{v}_{\rm c}^{\,2}}\,.$$

The pressure and energy comprise particle and the vacuum properties: $P = P_{\rm p} - \mathcal{B}$, $\varepsilon = \varepsilon_{\rm p} + \mathcal{B}$. Condition $\vec{\mathcal{P}} = 0$ reads:

$$\mathcal{B}\vec{n} = P_{\rm p}\vec{n} + (P_{\rm p}+\varepsilon_{\rm p})\frac{\vec{v}_{\rm c}\,\vec{v}_{\rm c}\cdot\vec{n}}{1-v_{\rm c}^2}\,,$$

Multiplying with $\vec{n}$, we find,

$$\mathcal{B} = P_{\rm p} + (P_{\rm p}+\varepsilon_{\rm p})\frac{\kappa v_{\rm c}^2}{1-v_{\rm c}^2}\,, \qquad \kappa = \frac{(\vec{v}_{\rm c}\cdot\vec{n})^2}{v_{\rm c}^2}\,.$$

This requires $P_{\rm p} < \mathcal{B}$: QGP phase pressure P must be NEGATIVE. A fireball surface region which reaches $\mathcal{P}\to 0$ and continues to flow outward is torn apart in a rapid instability. This can ONLY arise since matter presses again the vacuum which is not subject to collective dynamics.

MECHANISM OF SUDDEN HADRONIZATION

There is 'spinoidal' mechanical instability if the flow of the system outwards is continuing WHILE the pressure (force) has run out of strtength. The homogenouse surface 'fingers' out into the vacuum.

$$\sum_{i,j=1}^{3} n_i T_{ij} n_j = 0 = P + (P+\varepsilon)\frac{(\vec{v}_c \cdot \vec{n})^2}{1-v_c^2} \qquad \kappa = \frac{(\vec{v}_c \cdot \vec{n})^2}{v_c^2}$$

Combine this with Gibbs-Duham relation $P = T\sigma + \mu_b \nu_b - \varepsilon$ to derive the observable hadronization condition:

$$\frac{E}{S} = \left(T_h + \frac{\mu_b}{S/b}\right)\left\{1 + \kappa \frac{v_c^2}{1-v_c^2}\right\} \gtrsim T_h$$

We will see in the study of the hadronization properties how well this constraint is satisfied.

Initially there is no particle formation in the conventional sense but a breakup into small plasma fragments which finally give birth to particlesat drop temperature near $T = 150$ MeV.

END OF LECTURE 2

STRANGENESS

Primary production of strangeness in intial parton interactions produces the yield expected from 'wounded' nucleon model.

Additional strangeness is produced in 'soft' collision of thermalized constituents.

Dominant role of gluon based process (requires quark-gluon plasma).
Allows chemical equilibration of strangeness.

Multistrange hadrons produced in hadronization abundantly, (strange)an
have a small background.

Interpretation of hadronic production at SPS and RHIC produces properties expected from QGP.

Kinetic description of strangeness production

The generic angle averaged cross sections for (heavy) flavor s, $\bar{s}$ production processes $g+g \to s+\bar{s}$ and $q+\bar{q} \to s+\bar{s}$, are:

$$\bar{\sigma}_{gg\to s\bar{s}}(s) = \frac{2\pi\alpha_{\rm s}^2}{3s}\left[\left(1+\frac{4m_{\rm s}^2}{s}+\frac{m_{\rm s}^4}{s^2}\right)\tanh^{-1}W(s) - \left(\frac{7}{8}+\frac{31m_{\rm s}^2}{8s}\right)W(s)\right],$$

$$\bar{\sigma}_{q\bar{q}\to s\bar{s}}(s) = \frac{8\pi\alpha_{\rm s}^2}{27s}\left(1+\frac{2m_{\rm s}^2}{s}\right)W(s). \qquad W(s)=\sqrt{1-4m_{\rm s}^2/s}$$

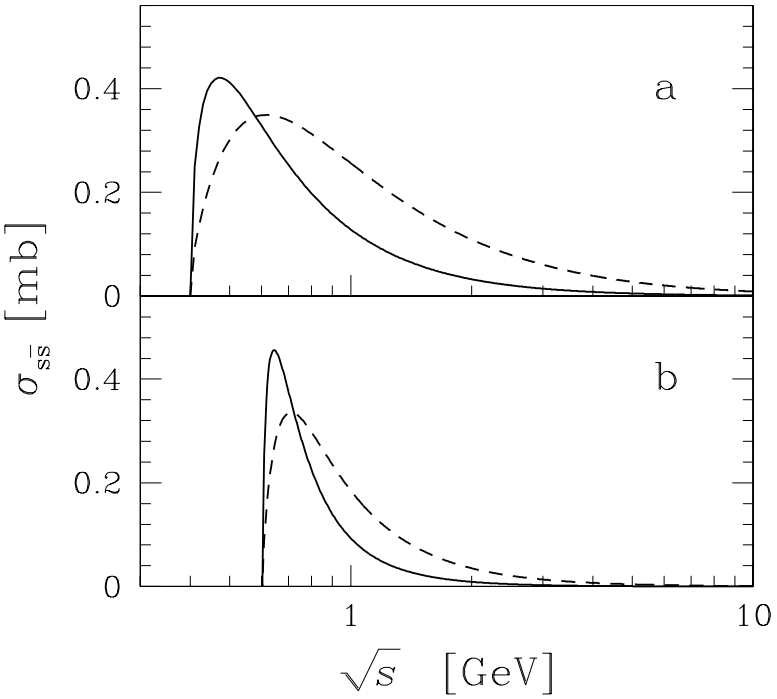

QGP Strangeness production cross sections:
Solid lines $q\bar{q} \to s\bar{s}$**; dashed lines** $gg \to s\bar{s}$**.**

a) TOP for fixed $\alpha_s = 0.6$**,** $m_{\rm s} = 200\,$**MeV;**
b) BOTTOM: for running $\alpha_s(\sqrt{s})$ **and** $m_{\rm s}(\sqrt{s})$**,**

with $\alpha_{s(M_Z)} = 0.118$**.** $m_s(M_Z) = 90 \pm 20\%$ **MeV,**
$m_s(1\,\mathbf{GeV}) \simeq 2.1 m_s(M_Z) \simeq 200\,\mathbf{MeV}$**.**

Collision rate

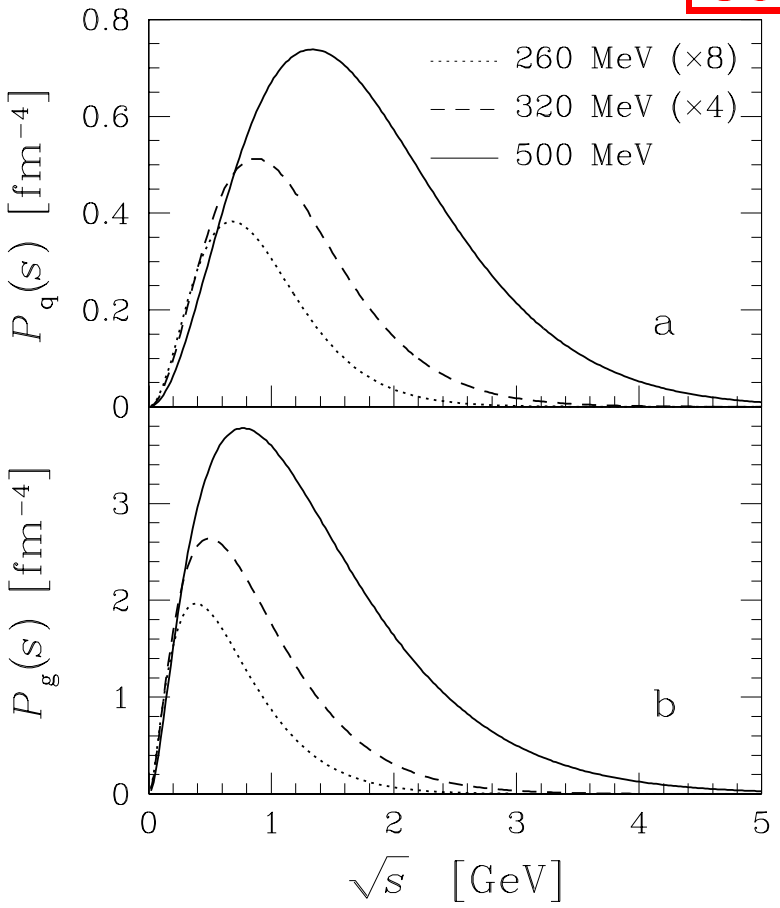

The collision distribution functions as function $\sqrt{s}$:

a) TOP: for quarks,
b) BOTTOM: for gluons.

Computed for temperature $T = 260\,\mathrm{MeV}$, $\lambda_q = 1.5$ (dotted lines, amplified by factor 8); $T = 320\,\mathrm{MeV}$, $\lambda_q = 1.6$ (dashed lines, amplified by factor 4); and $T = 500\,\mathrm{MeV}$, $\lambda_q = 1.05$ (solid lines). In all cases $\gamma_q, \gamma_g = 1$.

Gluon collisions dominate!

$$P_g = \frac{4Ts^{3/2}}{\pi^4}\sum_{l,n=1}^{\infty}\frac{1}{\sqrt{nl}}\,K_1\left(\frac{\sqrt{nl}\,s}{T}\right).$$

$$P_q|_{\mu_q=0} = \frac{9Ts^{3/2}}{4\pi^4}\sum_{l=1}^{\infty}(-)^{l+1}\frac{\gamma_q^l}{l\lambda_q^l}\int_0^{\infty}\frac{dp_1}{\sqrt{s}}\,\frac{e^{-l\frac{s}{4Tp_1}}}{\gamma_q^{-1}\lambda_q^{-1}e^{p_1/T}+1}.$$

Thermal average of reactions

Kinetic (momentum) equilibration is faster than chemical, use thermal particle distributions $f(\vec{p}_1,T)$ to obtain average rate:

$$\langle \sigma v_{\rm rel}\rangle_T \equiv \frac{\int d^3p_1 \int d^3p_2 \sigma_{12} v_{12} f(\vec{p}_1,T) f(\vec{p}_2,T)}{\int d^3p_1 \int d^3p_2 f(\vec{p}_1,T) f(\vec{p}_2,T)}\,.$$

Invariant reaction rate in medium:

$$A^{gg\to s\bar{s}} = \frac{1}{2}\rho_g^2(t)\,\langle \sigma v\rangle_T^{gg\to s\bar{s}}\,, \quad A^{q\bar{q}\to s\bar{s}} = \rho_q(t)\rho_{\bar{q}}(t)\langle \sigma v\rangle_T^{q\bar{q}\to s\bar{s}}\,, \quad A^{s\bar{s}\to gg,q\bar{q}} = \rho_s(t)\,\rho_{\bar{\rm s}}(t)\,\langle \sigma v\rangle_T^{s\bar{s}\to gg,q\bar{q}}.$$

$1/(1+\delta_{1,2})$ introduced for two gluon processescompensates the double-counting of identical particle pairs, arising since we are summing independently both reacting particles.

This rate enters the momentum-integrated Boltzmann equation which can be written in form of current conservation with a source term

$$\partial_\mu j_s^\mu \equiv \frac{\partial \rho_s}{\partial t} + \frac{\partial \vec{v}\rho_s}{\partial \vec{x}} = A^{gg\to s\bar{s}} + A^{q\bar{q}\to s\bar{s}} - A^{s\bar{s}\to gg,q\bar{q}}$$

Strangeness density time evolution

in local restframe ($\vec{v}$) we have :

$$\frac{d\rho_s}{dt} = \frac{d\rho_{\bar{s}}}{dt} = \frac{1}{2}\rho_g^2(t)\,\langle\sigma v\rangle_T^{gg\to s\bar{s}} + \rho_q(t)\rho_{\bar{q}}(t)\langle\sigma v\rangle_T^{q\bar{q}\to s\bar{s}} - \rho_s(t)\,\rho_{\bar{s}}(t)\,\langle\sigma v\rangle_T^{s\bar{s}\to gg,q\bar{q}}$$

Evolution for s and $\bar{s}$ identical, which allows to set $\rho_s(t) = \rho_{\bar{s}}(t)$.
Use detailed balance to simplify

$$\frac{d\rho_s}{dt} = A\left(1 - \frac{\rho_s^2(t)}{\rho_s^2(\infty)}\right), \qquad A = A^{gg\to s\bar{s}} + A^{q\bar{q}\to s\bar{s}}$$

The generic solution at fixed T ($\rho \propto \tanh$) implies that in all general cases there is an exponential approach to chemical equilibrium

$$\frac{\rho_s(t)}{\rho_s^\infty} \to 1 - e^{-t/\tau_s}$$

with the characteristic time constant τ_s:

$$\tau_s \equiv \frac{1}{2}\frac{\rho_s(\infty)}{(A^{gg\to s\bar{s}} + A^{q\bar{q}\to s\bar{s}} + \ldots)}$$

$$A^{12\to 34} \equiv \frac{1}{1+\delta_{1,2}}\rho_1^\infty\rho_2^\infty\langle\sigma_s v_{12}\rangle_T^{12\to 34}.$$

Characteristic time constant and γ_s-evolution

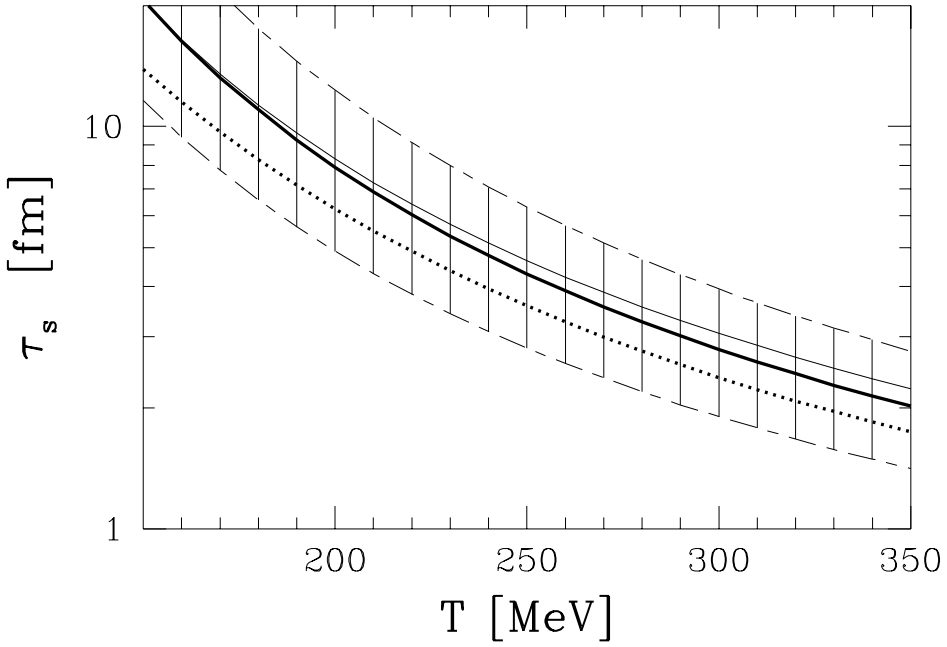

$\sigma_{\rm QCD}^{\to s\bar{s}}$ **gives** τ_s **similar to lifespan of the plasma phase!**
Strange quark pair production dominated by gluon fusion: $G+G\to s\bar{s}$**, also some (10%)** $q\bar{q}\to s\bar{s}$**, present; this is due to gluon collision rate.**
ENTROPY CONSERVING expansion i.e. at SPS T^3V **=Const. (not yet long. scaling):**

$$2\tau_s\frac{dT}{dt}\left(\frac{d\gamma_s}{dT}+\frac{\gamma_s}{T}z\frac{K_1(z)}{K_2(z)}\right)=1-{\gamma_s}^2\,,\quad \gamma_s(t)\equiv n_s(t)/n_s^\infty\,,\quad z=\frac{m_s}{T}\,,\quad K_i:\text{Besself.}$$

Once γ_s **known,** $\langle\rho_s(t)\rangle=\langle\bar{\rho}_s(t)\rangle=\int dx^3\rho_s^\infty(T(t,x))\gamma_s(T(t,x),\dot{T}(t,x))$;
evolution till $t\to t_f$**,but effectively production stops for** $T<180$ **MeV.**

What about charm? $m_s \to m_c$

We expect that thermal charm production is of relevance only for $T \to m_c(1\,\mathbf{GeV}) \simeq 1.5\,\mathbf{GeV}$, probably not accessible.

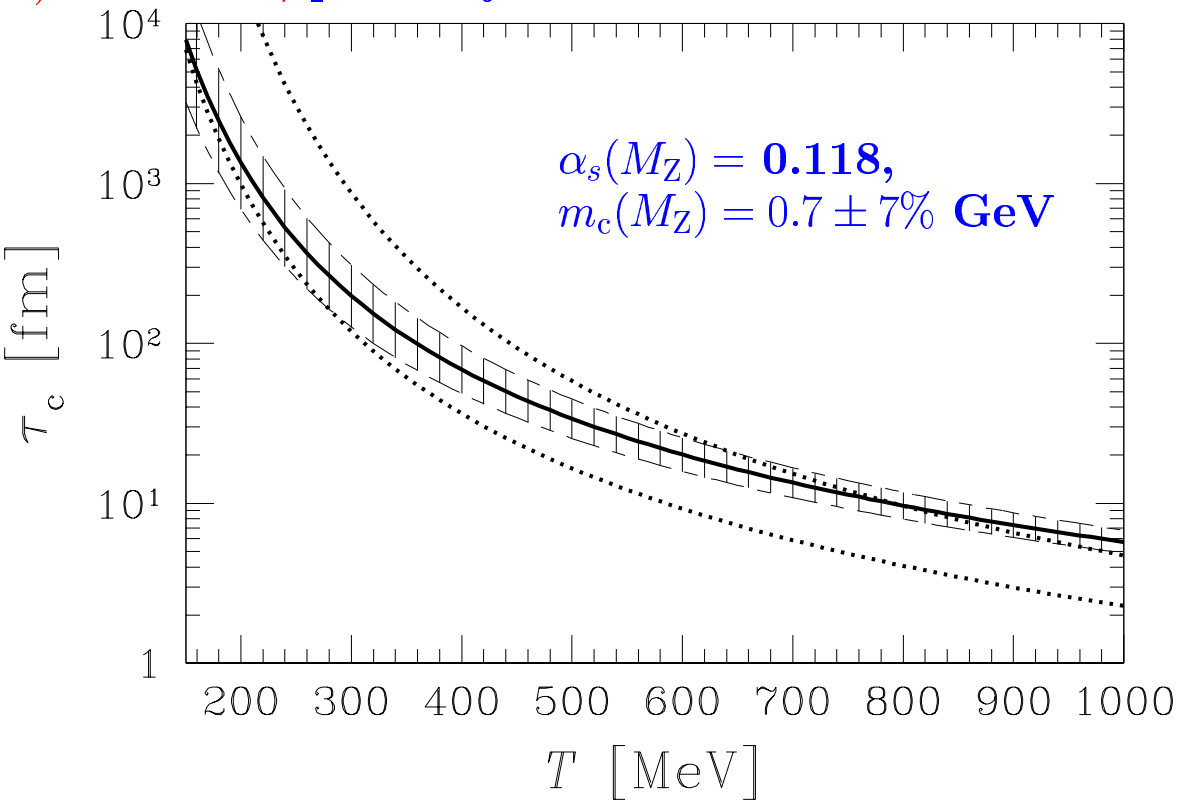

Lower dotted line: for fixed $m_c = 0.9\,\mathbf{GeV}$, $\alpha_s = 0.35$;
upper doted line: for fixed $m_c = 1.5\,\mathbf{GeV}$, $\alpha_s = 0.4$.
Equilibrium density for $\rho_c^\infty(m_c \simeq 1.5\,\mathbf{GeV})$.

Charm is produced relatively abundantly in first parton collisions. Benchmark: 10 $c\bar{c}$ pairs in central Au–Au at RHIC-200. This yield is greater than the expected equilibrium yield at hadronization of QGP.

OBJECTIVE: Physical properties of the source at hadronization

NEED the phase space of hadronic particles in great precision.

REFINED FERMI(STATISTICAL) HADRONIZATION MODEL

$T_{\rm f}$	Local rest frame chemical freeze-out temperature
v_h,$v_{\rm f}$	Hadronization, Local flow speed of emitting source
$\lambda_{\rm s}$, $\lambda_{\rm q}$	Chemical fugacities describe conserved quantum number
$\gamma_{\rm s}$, $\gamma_{\rm q}$	Phase space occupancies describe quark pair yield

We imply that locally thermal equilibrium can be established. However, chemical equilibrium is NOT ASSUMED (could be result of fit).

HOW DOES THE MODEL WORK?

The thermal emitted particles production yield dN_i within the time dt from a locally at rest surface element dS:

$$dN_i = \frac{dSd^3p}{(2\pi)^3}A_i v_i dt\,.$$

$v_i = dz/dt$ is the particle velocity normal to the surface element dS.

In a thermal quark-gluon source, phase space factor A_i is:

$$A_i = g_i\lambda_i\gamma_i e^{-E_i/T}\,, \qquad \lambda_i = \prod_{j\in i}\lambda_j\,, \quad \gamma_i = \prod_{j\in i}\gamma_j\,, \quad E_i = \sum_{j\in i}E_j\,,$$

$$\pi(q\bar{q}) \sim \gamma_q^2 \qquad N(qqq) \sim \gamma_q^3\lambda_q^3; \qquad \overline{N}(\bar{q}\bar{q}\bar{q}) \sim \gamma_q^3\lambda_q^{-3}$$

WITH QUANTUM STATISTICS

$$\frac{N_\pi}{V} = g_\pi\int\frac{d^3p}{(2\pi)^3}\frac{1}{\gamma_q^{-2}e^{\sqrt{m_\pi^2+p^2}/T}-1}, \qquad \gamma_q^2 < e^{m_\pi/T} \simeq (1.6)^2$$

$$\frac{N}{V} = g_N\int\frac{d^3p}{(2\pi)^3}\frac{1}{1+\gamma_q^{-3}\lambda_q^{-3}e^{E/T}} \qquad \frac{\overline{N}}{V} = g_N\int\frac{d^3p}{(2\pi)^3}\frac{1}{1+\gamma_q^{-3}\lambda_q^{+3}e^{E/T}}$$

$$\mu_N^{\rm eff} = 3T(\ln\lambda_q + \ln\gamma_q); \qquad \mu_{\overline{N}}^{\rm eff} = -3T(\ln\lambda_q - \ln\gamma_q)$$

---

in Boltzmann limit

$$R_\Lambda = \left.\frac{\overline{\Lambda}}{\Lambda}\right|_{m_\perp} = \frac{\overline{\Lambda}+\overline{\Sigma}^0+\overline{\Sigma}^*+\cdots}{\Lambda+\Sigma^0+\Sigma^*+\cdots} = \frac{\bar{s}\bar{q}\bar{q}}{sqq} = \lambda_{\rm s}^{-2}\lambda_{\rm q}^{-4} = e^{2\mu_{\rm S}/T}e^{-2\mu_b/T}\,.$$

$$R_\Xi = \left.\frac{\overline{\Xi^-}}{\Xi^-}\right|_{m_\perp} = \frac{\overline{\Xi^-}+\overline{\Xi^*}+\cdots}{\Xi^-+\Xi^*+\cdots} = \frac{\bar{s}\bar{s}\bar{q}}{ssq} = \lambda_{\rm s}^{-4}\lambda_{\rm q}^{-2} = e^{4\mu_{\rm S}/T}e^{-2\mu_b/T}\,.$$

This ratio is reliable, there is practically nothing that can influence it, constrains chemical potentials/fugacities strongly.

$$\left.\frac{\Xi^-(dss)}{\Lambda(dds)}\right|_{m_\perp} = \frac{g_\Xi\gamma_d\gamma_s^2\lambda_d\lambda_s^2}{g_\Lambda\gamma_d^2\gamma_s\lambda_d^2\lambda_s}\,.$$

g_i **are the spin statistical factors of the states considered.**

Judicial choice of compatible particle ratios reduces dependence on EXPLOSIVE flow,

For full phase space flow does not influence the observed yields. We allow fro flow in numerical studies

WHAT DO WE KNOW ABOUT PARAMETERS?

Assume exploding QGP-phase

1. **For given E/b, Equation of State relates the 5 parameters of state:**

   $$T_f,\ \lambda_q,\ \gamma_q,\ \lambda_s,\ \gamma_s$$

2. **Kinetic theory of strangeness production relates:**

   $$v_f,\ T_f \text{ and } \gamma_s$$

3. **Strangeness conservation in the source:**

   $$\langle s-\overline{s}\rangle = 0 \longrightarrow \lambda_s(T,\lambda_q;\gamma_s)$$

   for QGP: in S–Pb and at RHIC $\lambda_s = 1$

4. **Entropy/Baryon in source (QGP) $\leq$ in Final hadron** $\longrightarrow$ $\gamma_q \simeq 1.6$

   Explain below, also: Glue $\rightarrow q\bar{q}$ **adds quark pairs**

5. **Flow dynamics (e.g. Hydrodynamic): for bulk of matter** $v_f \simeq 1/\sqrt{(3)}$

WHY $\gamma_q \simeq 1.6$? **A striking feature of the data analysis is the maximization of entropy density in pion gas.** $E_\pi = \sqrt{m_\pi^2 + p^2}$

$$S_{\rm B,F} = \int \frac{d^3p\, d^3x}{(2\pi\hbar)^3} \left[\pm(1\pm f)\ln(1\pm f) - f\ln f\right], \qquad f_\pi(E) = \frac{1}{\gamma_q^{-2} e^{E_\pi/T} - 1}.$$

Pion gas properties: N**-particle,** E**-energy,** S**-entropy,** V**-volume as function of** γ_q**.**

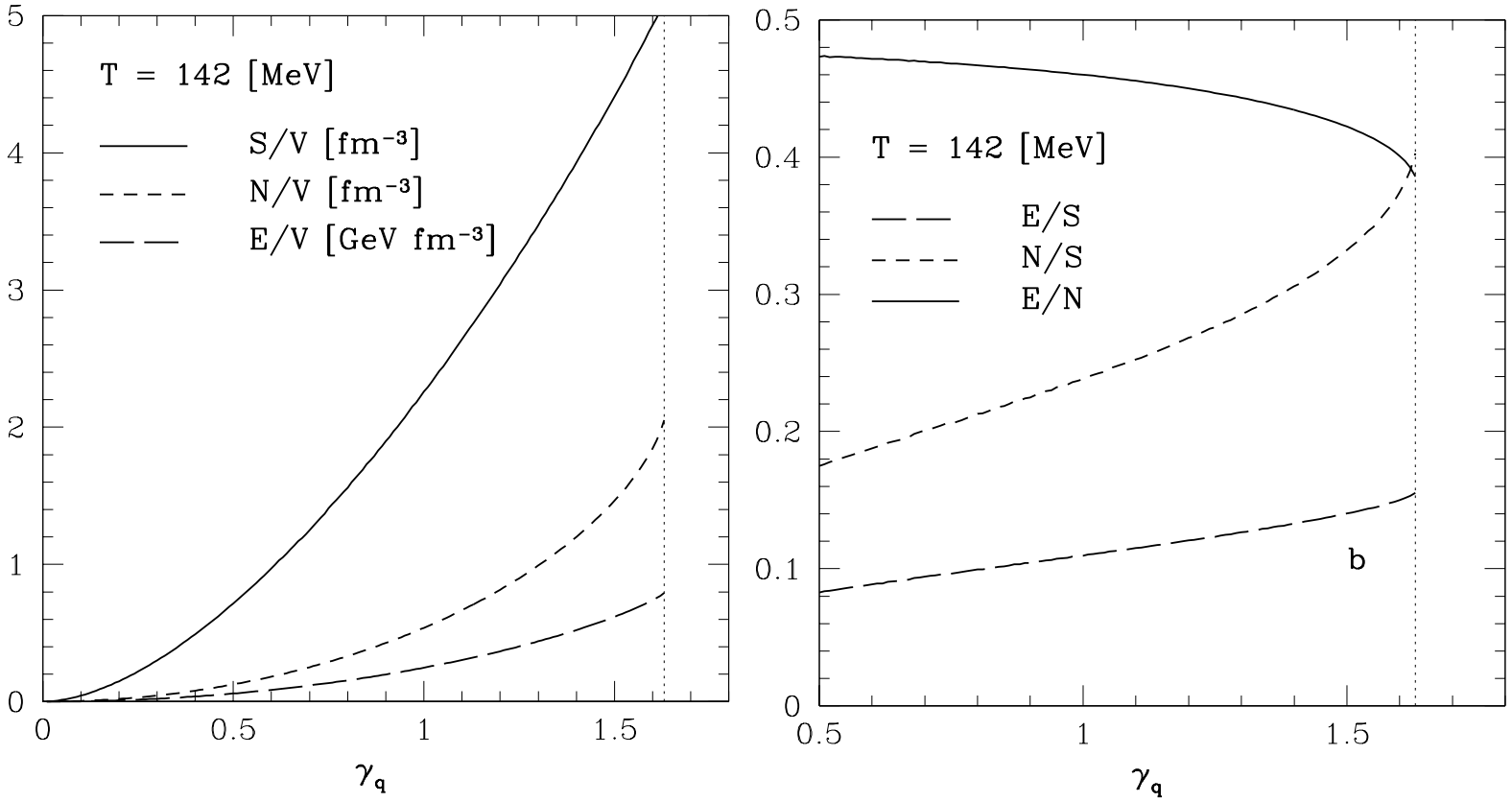

CONCLUSION: excess of QGP entropy pumped into pions

CAN WE ESTIMATE THE EXPECTED $\gamma_s^{\rm HG}$?

COMPUTE EXPECTED RATIO OF $\gamma_{\rm s}^{\rm HG}/\gamma_{\rm s}^{\rm QGP}$

In sudden hadronization, $V^{\rm HG} \simeq V^{\rm QGP}$, $T^{\rm QGP} \simeq T^{\rm HG}$, the chemical occupancy factors accommodate the different magnitude of particle phase space.

→

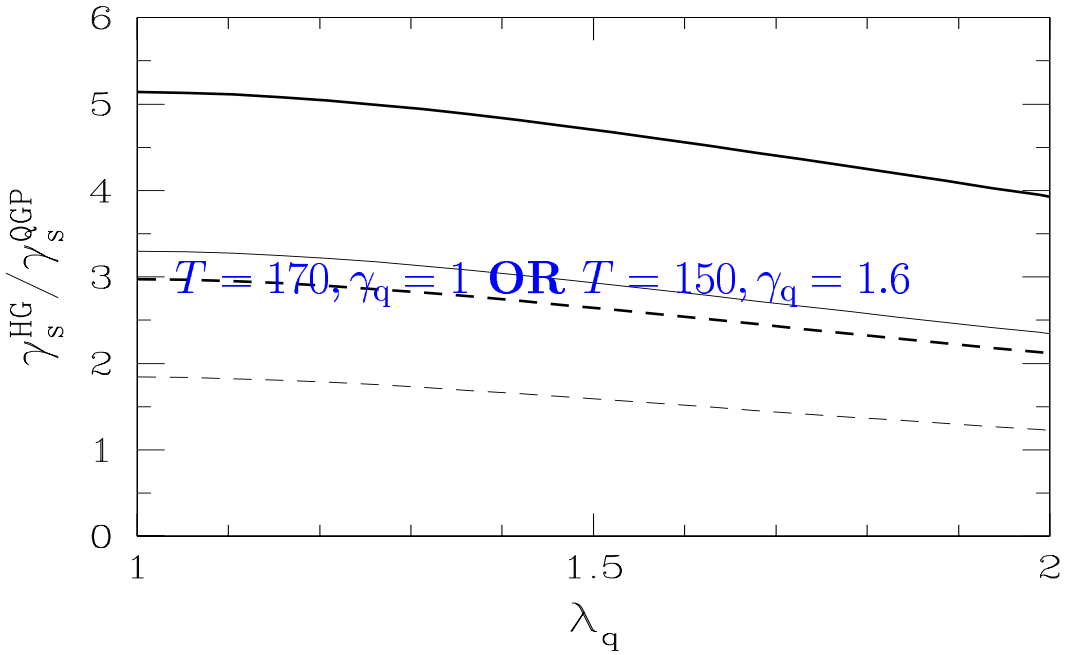

$\gamma_{\rm s}^{\rm HG}/\gamma_{\rm s}^{\rm QGP}$ in sudden hadronization as function of $\lambda_{\rm q}$. Solid lines $\gamma_{\rm q} = 1$, and short dashed $\gamma_{\rm q} = 1.6$. Thin lines for $T = 170$ and thick lines $T = 150$ MeV, common to both phases.

$$\gamma_s^{\rm HG} \simeq 3\gamma_s^{\rm QGP}$$

EXAMPLE: Pb–Pb ANALYSIS Fermi-2000 Model

Pb–Pb 158A GeV WA97 (top) and NA49 (bottom) S'2000 revised data

Ratios	Ref.	Exp. Data	$\mathrm{Pb}\vert_v^{\mathrm{s},\gamma_q}$	$\mathrm{Pb}\vert_v^{\gamma_q}$
Ξ/Λ	[1]	0.099 ± 0.008	0.098	0.096
$\bar{\Xi}/\bar{\Lambda}$	[1]	0.203 ± 0.024	0.199	0.201
$\bar{\Lambda}/\Lambda$	[1]	0.124 ± 0.013	0.122	0.121
$\bar{\Xi}/\Xi$	[1]	0.255 ± 0.025	0.248	0.253
$\frac{(\Xi+\bar{\Xi})}{(\Lambda+\bar{\Lambda})}$	[2]	0.13 ± 0.03	0.111	0.110
~~K_s^0/ϕ~~	~~[3]~~	~~11.9 ± 1.5~~	13.0	13.4
ϕ/π^-	[5]	0.0125 ± 0.0018	0.0127	0.0124
K^+/K^-	[4]	1.80 ± 0.10	1.757	1.790
$p/\bar{p}$	[6]	$18.1 \pm 4.$	16.00	16.50
~~$\bar{\Lambda}/\bar{p}$~~	~~[7]~~	~~$3. \pm 1.$~~	0.53	0.54
K^-/π^-		0.082 ± 0.012	0.81	0.080
K_s^0/B	[8]	0.183 ± 0.027	0.188	0.192
h^-/B	[9]	1.97 ± 0.1	1.782	1.829
	χ^2_{T}		2.25	1.36
	$N;p;r$		10;3;2	10;4;2
$\chi^2_{\mathrm{T}}/\mathrm{dof}$	LESS	than	0.25	0.15

References

[1] **I. Králik, WA97,** *Nucl. Phys.* **A 638,115, (1998).**

[2] **G.J. Odyniec, NA49,** *J. Phys.* **G 23, 1827 (1997).**

[3] **F. Pühlhofer, NA49,** *Nucl. Phys.* **A 638, 431,(1998).**

[4] **C. Bormann, NA49,** *J. Phys.* **G 23, 1817 (1997).**

[5] **S.V. Afanasiev, NA49,** *Phys. Lett.* **B 491 59 (2000).**

[6] **G.J. Odyniec,** *Nucl. Phys.* **A 638, 135, (1998).**

[7] **D. Röhrig, NA49, in EPS-HEP Conf. Jerusalem, Aug. 1997.**

[8] **P.G. Jones, NA49,** *Nucl. Phys.* **A 610, 188c (1996).**

[9] **H. Appelshäuser** *et al.*, **NA49,** *Phys. Rev. Lett.* **82, 2471 (1999).**

Chemical and Physical Properties for Pb–Pb (S'2000 data) and for S–Au/W/Pb

	$\mathbf{Pb}\vert_v^{\mathrm{s},\gamma_q}$	$\mathbf{Pb}\vert_v^{\gamma_q}$	$\mathbf{S}\vert_v$
$\chi^2_{\mathrm{T}};\ N;p;r$	**1.48; 11; 3; 2**	**0.76; 11; 4; 2**	**6.2; 16; 6; 6**
T_f [MeV]	151 ± 3	147 ± 5.5	144 ± 2
v_c	0.57 ± 0.05	0.52 ± 0.09	0.49 ± 0.02
λ_q	1.618 ± 0.026	1.625 ± 0.025	1.51 ± 0.02
λ_s	1.101^*	1.093 ± 0.02	1.00 ± 0.02
γ_q	$\gamma_q^{c*} = e^{m_\pi/2T_f}$=1.59	$\gamma_q^{c*} = e^{m_\pi/2T_f}$=1.62	1.41 ± 0.08
γ_s/γ_q	1.04 ± 0.05	1.05 ± 0.06	0.69 ± 0.03
E_f^{in}/S_f	0.163 ± 0.01	0.158 ± 0.01	0.186 ± 0.01
s_f/b	0.68 ± 0.05	0.69 ± 0.05	0.73 ± 0.05
$(\bar{s}_f - s_f)/b$	0^*	0.05 ± 0.05	0.17 ± 0.05

COMPARE TO RHIC-130 properties

Fireball Properties and Parameters of Fits to RHIC-130 results

	$100\%\,\Xi \to Y$ $40\%\ \ Y \to N$	$40\%\,\Xi \to Y$ $40\%\,Y \to N$	$40\%\,\Xi \to Y$ $40\%\,Y \to N$
T	140.1 ± 1.1	142.3 ± 1.2	164.3 ± 2.2
$\gamma_q^{\rm HG}$	1.64^*	1.63^*	1^*
λ_q	1.070 ± 0.008	1.0685 ± 0.008	1.065 ± 0.008
μ_b [MeV]	28.4	28.3	31.0
$\gamma_s^{\rm HG}/\gamma_q^{\rm HG}$	1.54 ± 0.04	$1.54 \pm 0.0.04$	1^*
λ_s	1.0136^*	1.0216^*	1.0196^*
$\mu_{\rm S}$ [MeV]	6.1	6.4	7.1
s/b	9.75	9.7	7.2
E/b [GeV]	35.0	34.6	34.8
S/b	234.8	230.5	245.7
E/S [MeV]	148.9	150.9	141.5
χ^2/dof	$7.1/(19-3)$	$19/(19-3)$	$177.2/(19-2)$

VERY large χ^2 originates in the inability to account for ratios of baryons and antibaryons for the chemical equilibrium assumption.

Specific strangeness content 9 times greater than at SPS.

Fireball energy content: internal thermal energy content $E/b \simeq 35$ GeV is 7+ times greater compared to top SPS result.

Laboratory energy contains kinetic energy associated with longitudinal and transverse flow of fireball matter. The energy of each particle is 'boosted' with the factor $\gamma_\perp^v \cosh y_\parallel$. Longitudinal flow $\Delta y = \pm 1.9$ (PHOBOS), on average we get $\int dy_\parallel \cosh y_\parallel / \int dy_\parallel \to \sinh(1.92)/1.9 = 1.7$. The transverse flow estimated with with $v_\perp = c/\sqrt{3} \to \gamma_\perp^v = 1.2$.

$$\gamma_\perp^v \langle \cosh y_\parallel \rangle = 2 \simeq \frac{65\,\mathbf{GeV}}{35\,\mathbf{GeV}}.$$

Richness of experimental results is still increasing....

	Data	100% $\Xi \to Y$ 40% $Y \to N$	40% $\Xi \to Y$ 40% $Y \to N$	40% $\Xi \to Y$ 40% $Y \to N$
$\bar{p}/p$	0.71 ± 0.06	0.672(0.4)	0.678(0.3)	0.689(0.1)
$\overline{\Lambda}_\Xi/\Lambda_\Xi$	0.71 ± 0.04	0.759(1.0)	0.748(0.9)	0.757(1.4)
$\overline{\Xi}/\Xi$	0.83 ± 0.08	0.794(0.2)	0.804(0.1)	0.816(0.0)
K^-/K^+	0.87 ± 0.07	0.925(0.6)	0.924(0.6)	0.934(0.8)
$K^-/\pi^\pm$	0.15 ± 0.02†	0.159(0.2)	0.161(0.3)	0.150(0.0)
$K^+/\pi^\pm$	0.17 ± 0.02†	0.172(0.0)	0.174(0.1)	0.161(0.2)
Λ_Ξ/h^-	0.059 ± 0.004†	0.057(0.3)	0.050(5.1)	0.045(11.9)
$\overline{\Lambda}_\Xi/h^-$	0.042 ± 0.004†	0.043(0.0)	0.037(1.3)	0.034(3.8)
Λ_Ξ/p	0.90 ± 0.12	0.832(0.3)	0.691(3.0)	0.491(11.6)
$\overline{\Lambda}_\Xi/\bar{p}$	0.93 ± 0.19	0.929(0.0)	0.763(0.8)	0.539(4.2)
$\pi^\pm/p_\Lambda$	9.5 ± 2	9.4(0.0)	9.2(0.5)	7.6(22.8)
$\pi^\pm/\bar{p}_\Lambda$	13.4 ± 2.5	13.7(0.1)	13.4(0.0)	10.9(7.9)
Ξ^-/π	0.0088±0.0008†	0.0096(1.0)	0.0103(3.6)	0.0067(7.1)
Ξ^-/h^-	0.0085±0.0015	0.0079(0.1)	0.0084(0.0)	0.0054(4.3)
$\overline{\Xi^-}/h^-$	0.0070±0.001	0.0063(0.5)	0.0068(0.1)	0.0044(6.7)
Ξ^-/Λ	0.193±0.009	0.195(0.1)	0.196(0.1)	0.132(45.2)
$\overline{\Xi^-}/\overline{\Lambda}$	0.221±0.011	0.213(0.6)	0.214(0.4)	0.144(48.7)
Ω/Ξ^-		0.205	0.21	0.18
$\overline{\Omega}/\overline{\Xi^-}$		0.22	0.23	0.20
$\overline{\Omega}/\Omega$	0.95±0.1	0.87(0.7)	0.88(0.5)	0.89(0.4)
$\bar{p}/h^-$		0.046	0.049	0.063
ϕ/K^-	0.15±0.03	0.178(0.9)	0.185(1.3)	0.146(0.0)
χ^2/dof		7.1/(19 − 3)	19/(19 − 3)	177.2/(19 − 2)

Fits of central-rapidity hadron ratios at $\sqrt{s_{\rm NN}} = 130$ GeV.

Columns: ratio considered, data value with reference, the non-equilibrium fit with 100% $\Xi \to Y$ cascading ($f_\Xi = 1$) and 40% $Y \to N$ ($f_\Lambda = 0.4$), the non-equilibrium fit with 40% $\Xi \to Y$ and 40% $Y \to N$, and in the last column, the chemical equilibrium fit with 40% cascading . The superscript * indicates quantities fixed by constrains and related considerations. The superscript † indicates the error is dominated by theoretical considerations. Subscripts Ξ, Λ mean that these values include weak cascading. In parenthesis we show the contribution of the particular result to the total χ^2.

Absolute Chemical Equilibrium EXCLUDED at RHIC

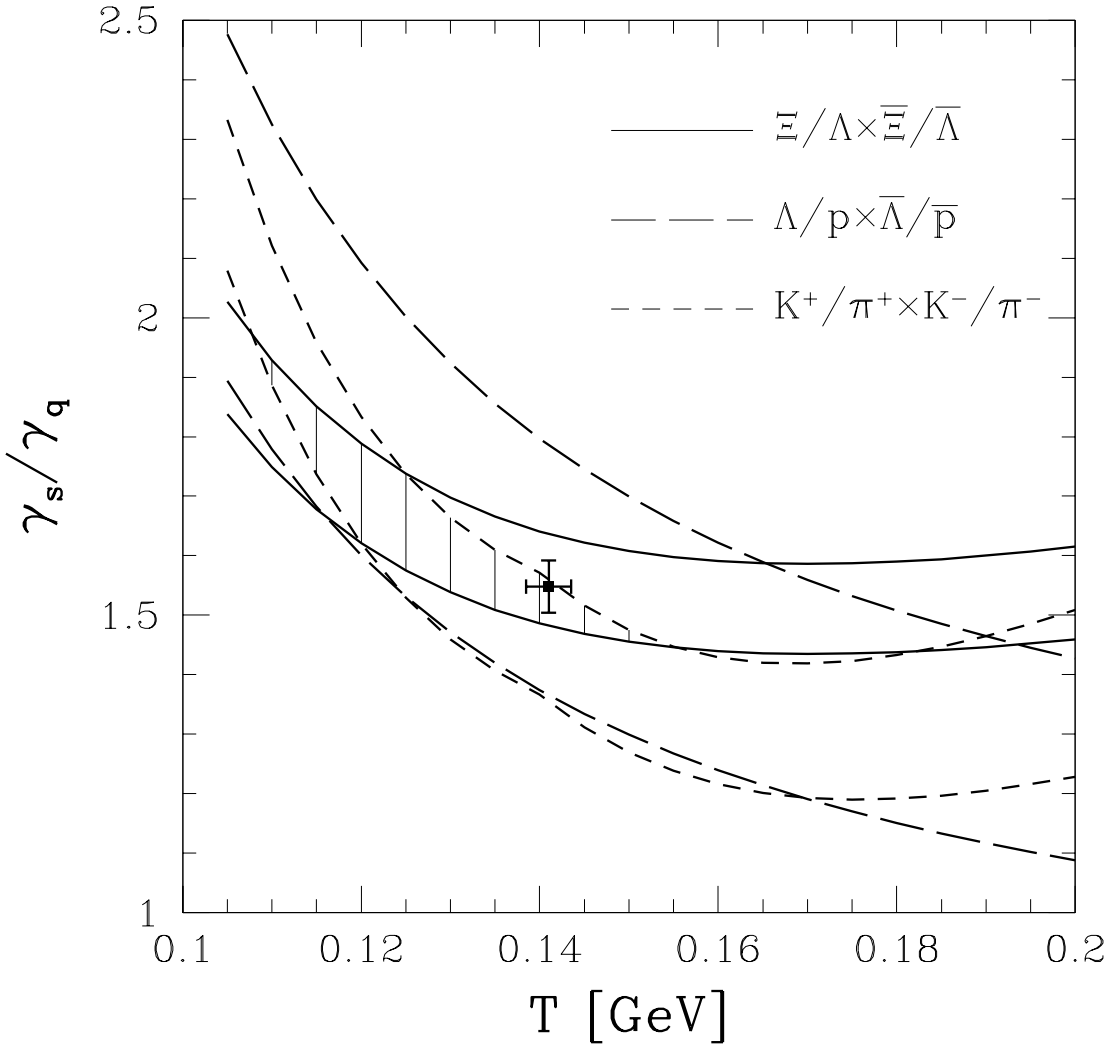

We show here products of particle ratios in which all chemical factors but the ratio of final state phase space occupancies cancel.

Equilibrium fit would need to be at the bottom of figure. Excluded STRONGLY by high yields of double strange CASCADES.

We show the current best fit to all data.

Note that best fit we have (next page) is for $\gamma_q \simeq 1.6$ (max in entropy) and a very large value $\gamma_s \simeq 2.5$, as would be expected from phase space arguments comparing QGP and HG phases.

Gibbs Duham Relation, freeze-out fits and SUPERCOOLING

$$\frac{E}{S} = \left(T_h + \frac{\mu_b}{S/b}\right)\left\{1 + \kappa \frac{v_c^2}{1-v_c^2}\right\} \gtrsim T_h$$

T [MeV]	140.1± 1.1	142.3± 1.2	164.3±2.2
E/S[MeV]	148.9	150.9	141.5

Chemical nonequilibrium results consistent with supercooling NO SUPERCOOLING FOR EQUILIBRIUM FIT, but fit physically consistent:

$$PV + E = TS + \mu_b b \quad \rightarrow \quad \frac{P}{\epsilon} = \frac{T - E/S}{E/S} + \frac{\mu_b}{E/b}$$

the baryon number term is insignificant: 30MeV/30GeV$\simeq 0.001$

For the non-equilibrium fit Gibbs-Duham relation implies supercooling $P/\epsilon = -1/22$

The equilibrium fit implies $P/\epsilon = 1/6.5$ **which is consistent with hadronic gas properties at this temperature (transparency 61).**

HOW IS THE THERMAL ENERGY DISTRIBUTED IN HADRONIZATION

RHIC−130 Hadronization

Primary Hadron Energy Yield

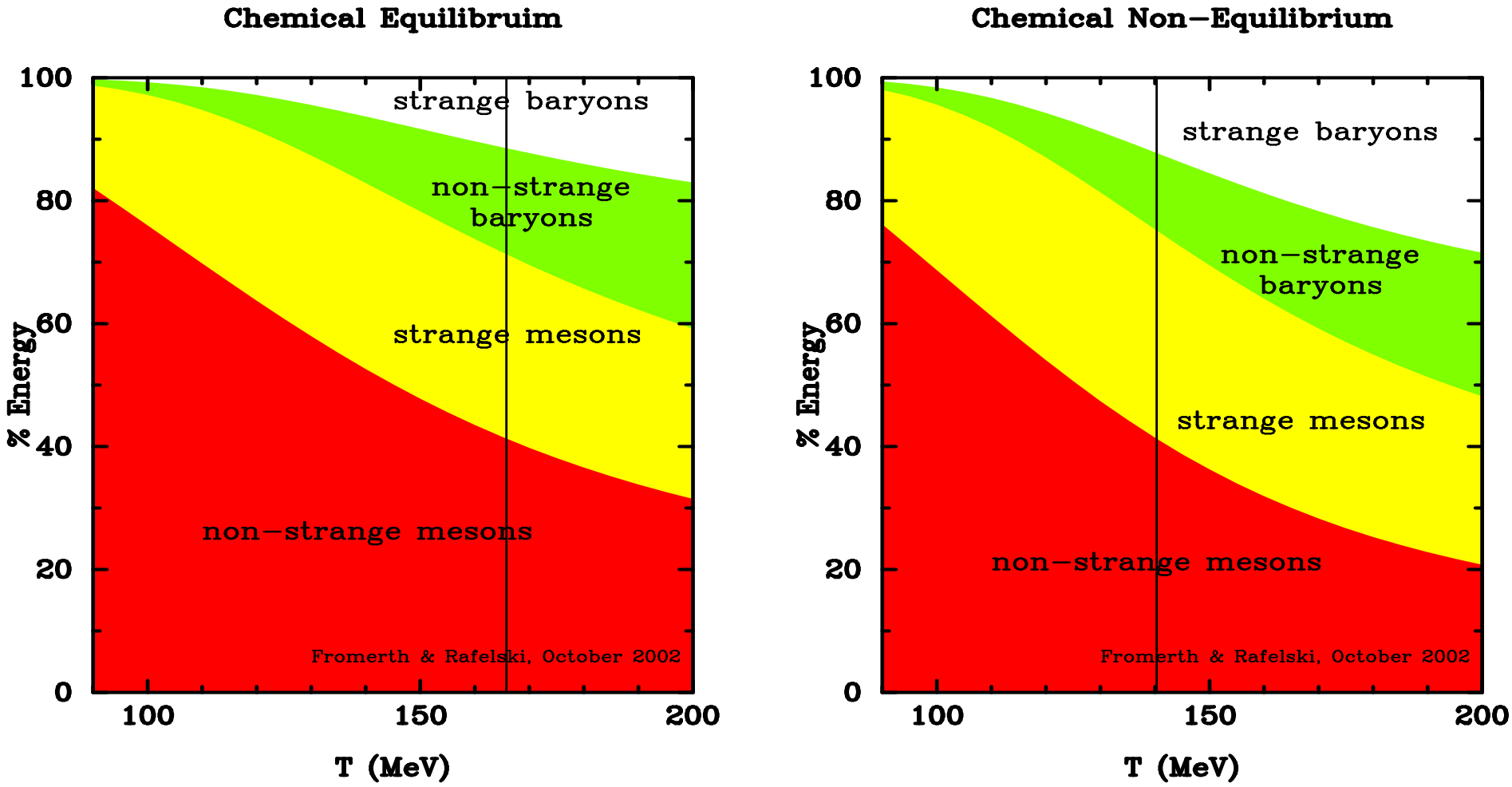

HOW ARE PRIMARY PARTICLES DISTRIBUTED IN HADRONIZATION

RHIC−130 Hadronization

Primary Hadron Particle Yield

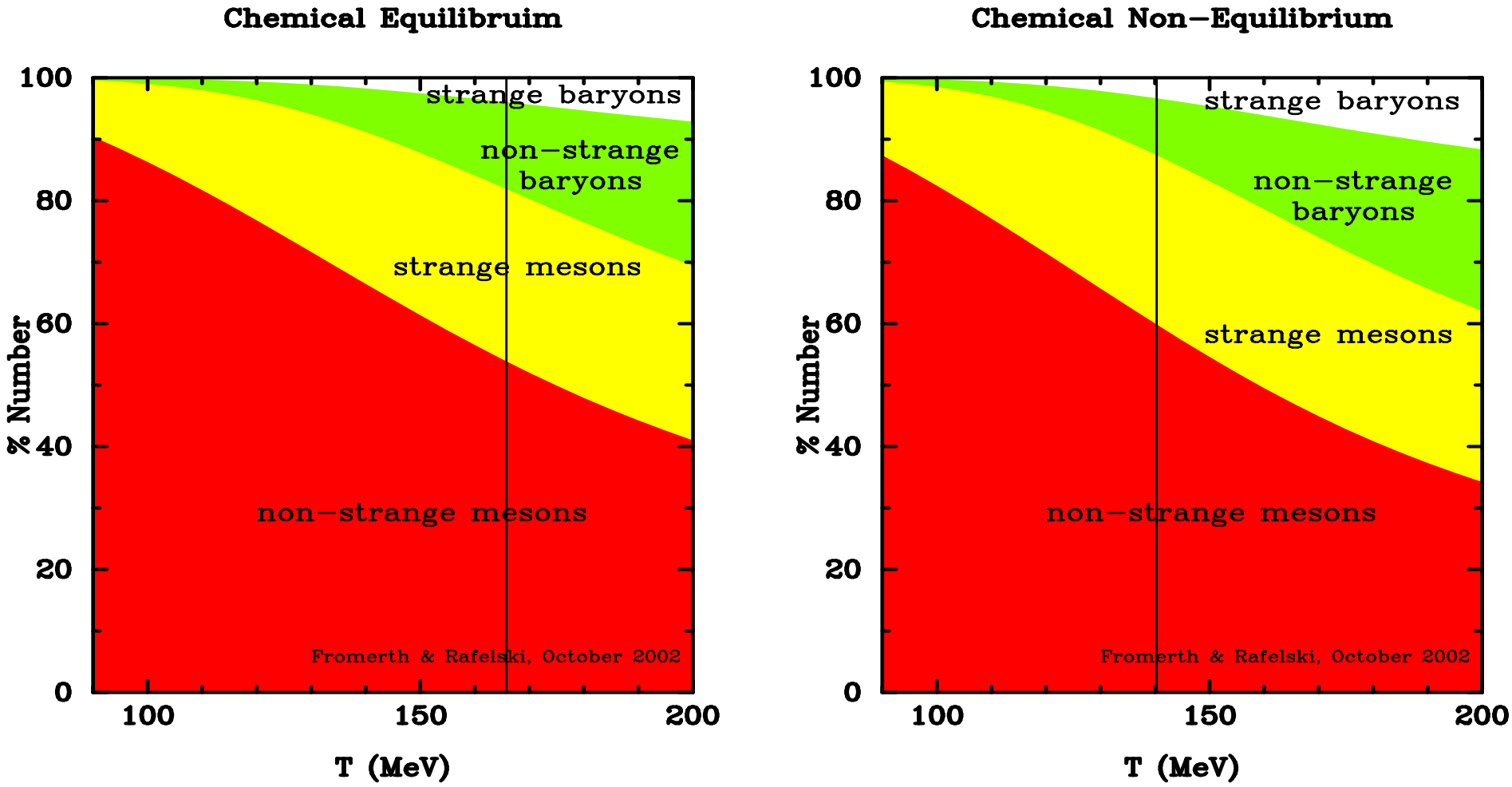

HOW ARE FINAL (after strong decays) PARTICLE YIELDS

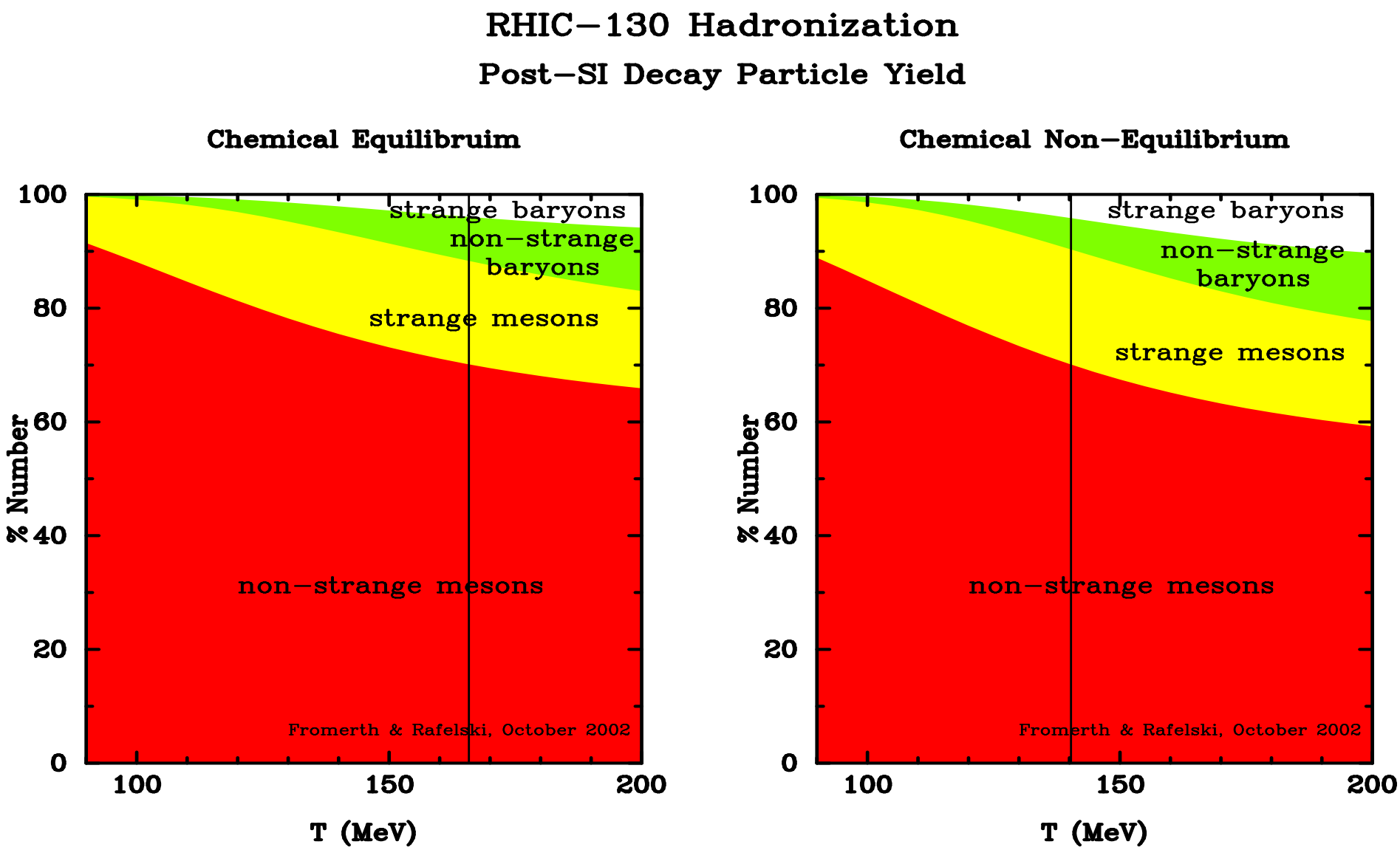

$m_\perp$ spectra **Hadron $m_\perp$-spectra are result of flow and thermal motion and are strongly influenced by resonance decays. The Flow-Boltzmann distribution we adapt with two velocities, one local temperature:**

$$\frac{d^2N}{dm_T dy} \propto \left(1 - \frac{\vec{v}_f^{-1}\cdot\vec{p}}{E}\right) \gamma\, m_T \cosh y\, e^{-\gamma\frac{E}{T}\left(1-\frac{\vec{v}\cdot\vec{p}}{E}\right)}\,, \quad \gamma = 1/\sqrt{1-v^2}$$

Resonance 2-body decay contribution:

$$\frac{dN_X}{dm_\perp} = \frac{dN_X}{dm_\perp}|_{\rm direct} + \sum_{\forall R\to X+2+\ldots} \frac{dN_X}{dm_\perp}|_{R\to X+2+\ldots}\,, \frac{dN_X}{dm_\perp^2 dy} = \frac{g_r b}{4\pi p^*}\int_{Y_-}^{Y_+} dY \int_{M_{T-}}^{M_{T+}} dM_T^2\, J\, \frac{d^2N_R}{dM_T^2 dY}\,.$$

$$J = \frac{M}{\sqrt{P_T^2 p_T^2 - \{M E^* - M_T m_T \cosh\Delta Y\}^2}}\,, \Delta Y = Y - y\,, E^* = (M^2 - m^2 - m_2^2)/2M\,,$$

$$p^* = \sqrt{E^{*2} - m^2}$$

$$Y_\pm = y \pm \sinh^{-1}\left(\frac{p^*}{m_T}\right)\,, \quad M_{T\pm} = M\frac{E^* m_T \cosh\Delta Y \pm p_T\sqrt{p^{*2} - m_T^2\sinh^2\Delta Y}}{m_T^2\sinh^2\Delta Y + m^2}$$

Λ and $\overline{\Lambda} - m_\perp$ SPS SPECTRA

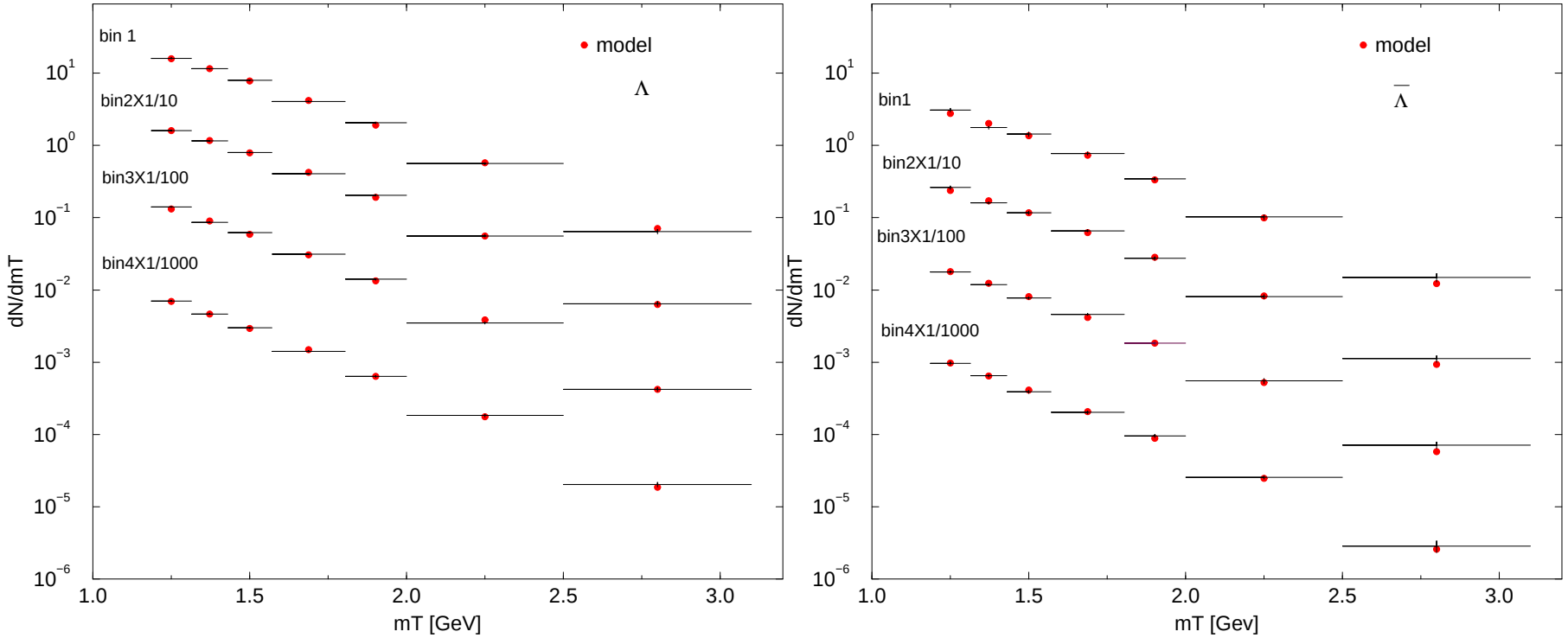

Thermal analysis m_T spectra: Λ (left) and $\overline{\Lambda}$ (right) for 4 different centralities.
'dots' theoretical values; HISTOGRAM: WA97 data in different centrality bins.

Ξ and $\overline{\Xi} - m_\perp$ SPECTRA

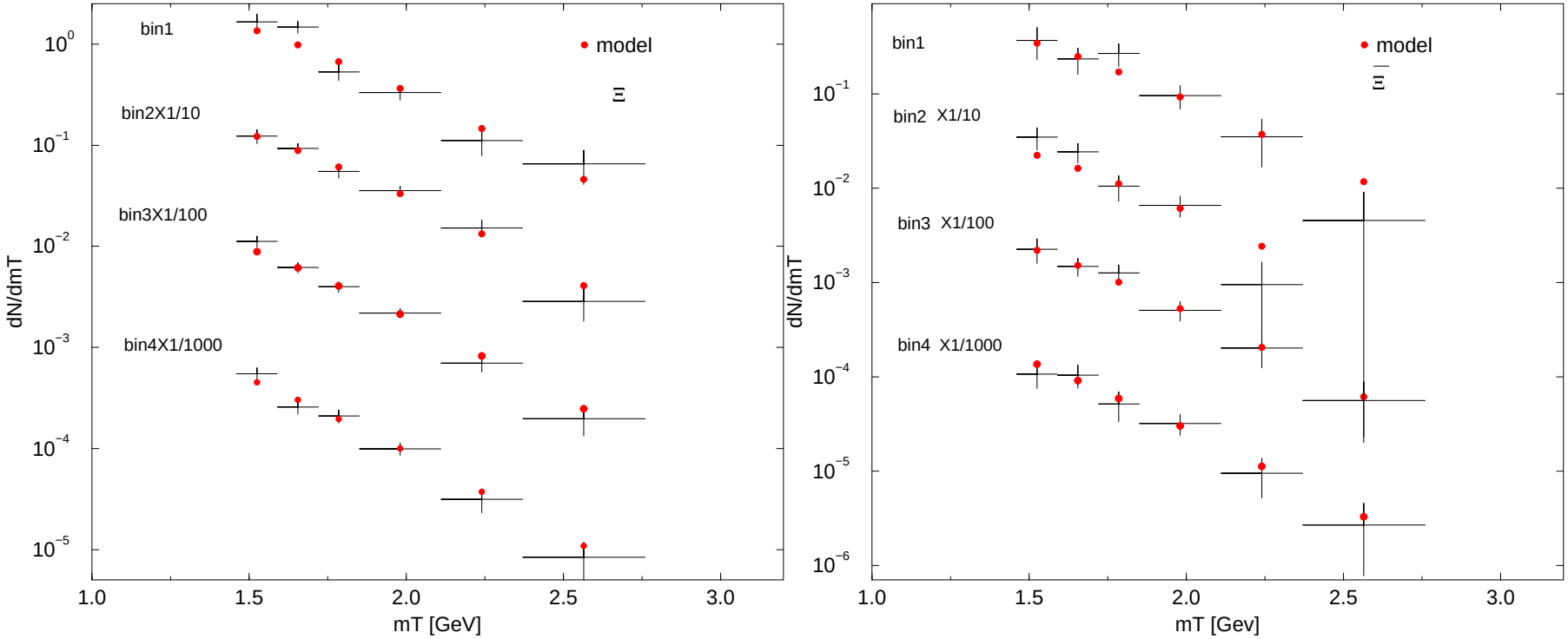

Thermal analysis m_T spectra: Ξ (left) and $\overline{\Xi}$ (right) for 4 different centralities.
'dots' theoretical values; Histogram lines: WA97 data in different centrality bins.

The χ^2 profiles show good significance,

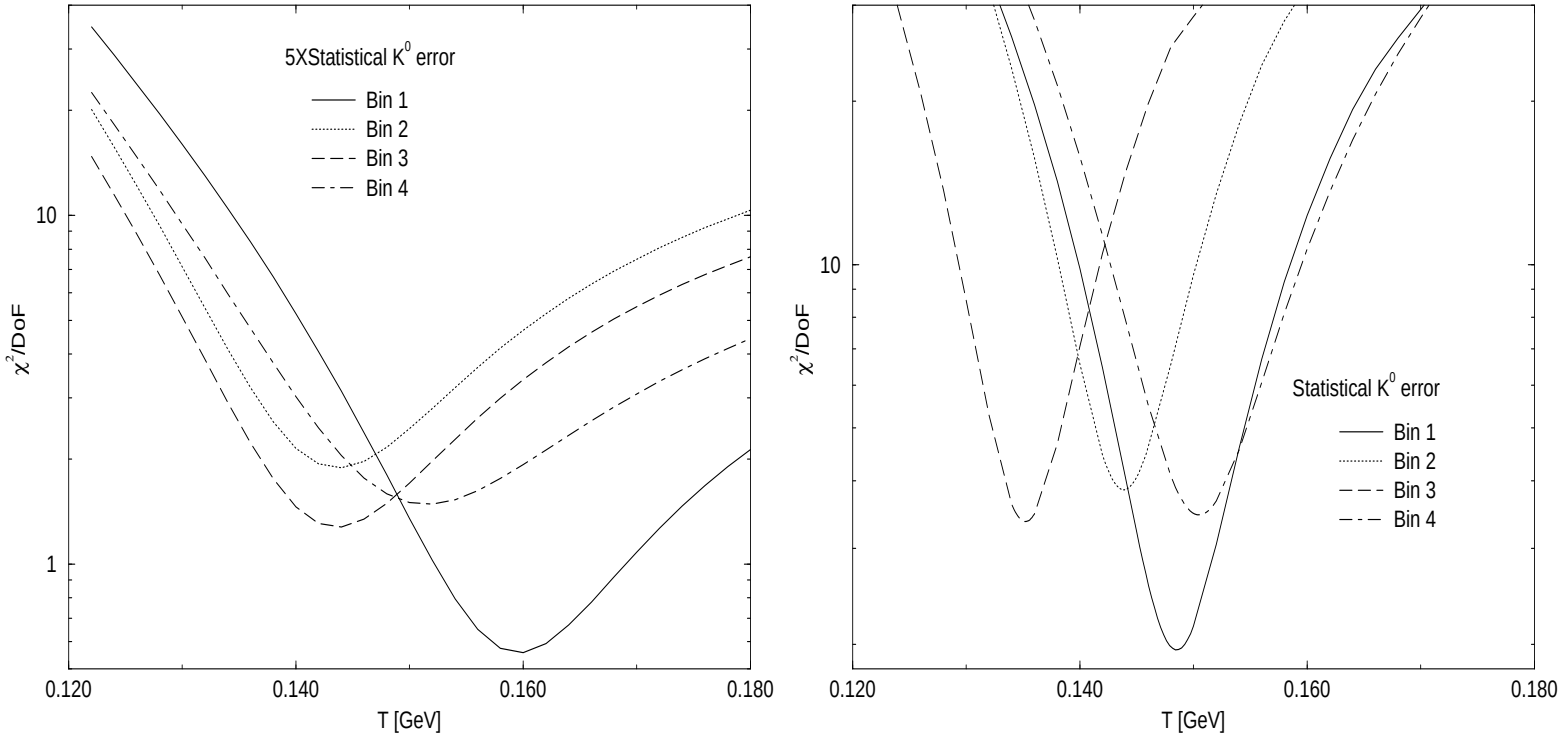

The total error divided by degrees of freedom for different centrality bins, shown as function of (fixed) freeze-out temperature T, RIGHT for the experimental value of the (statistical) K^0 error, LEFT for the 5 times enlarged kaon data statistical errors.

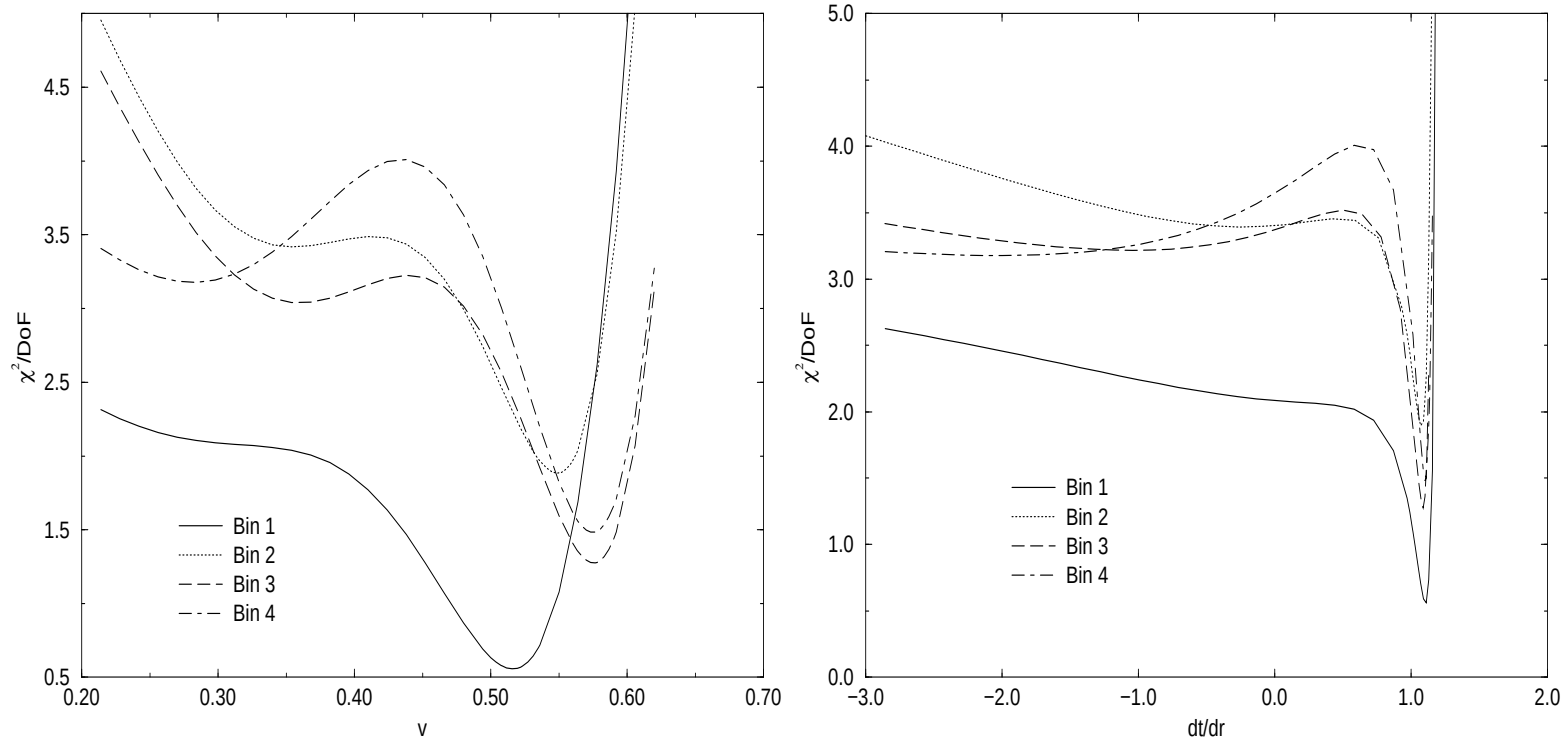

The total error divided by degrees of freedom for different centrality bins, shown as function of (fixed) flow velocity v on LEFT and for (fixed) freeze-out surface $\partial t_f/\partial r_f = 1/v_f$ dynamics on RIGHT.

NCE FOR SUDDEN BREAKUP? CHEMICAL AND THERMAL FREEZE-OUT T, v AGREE

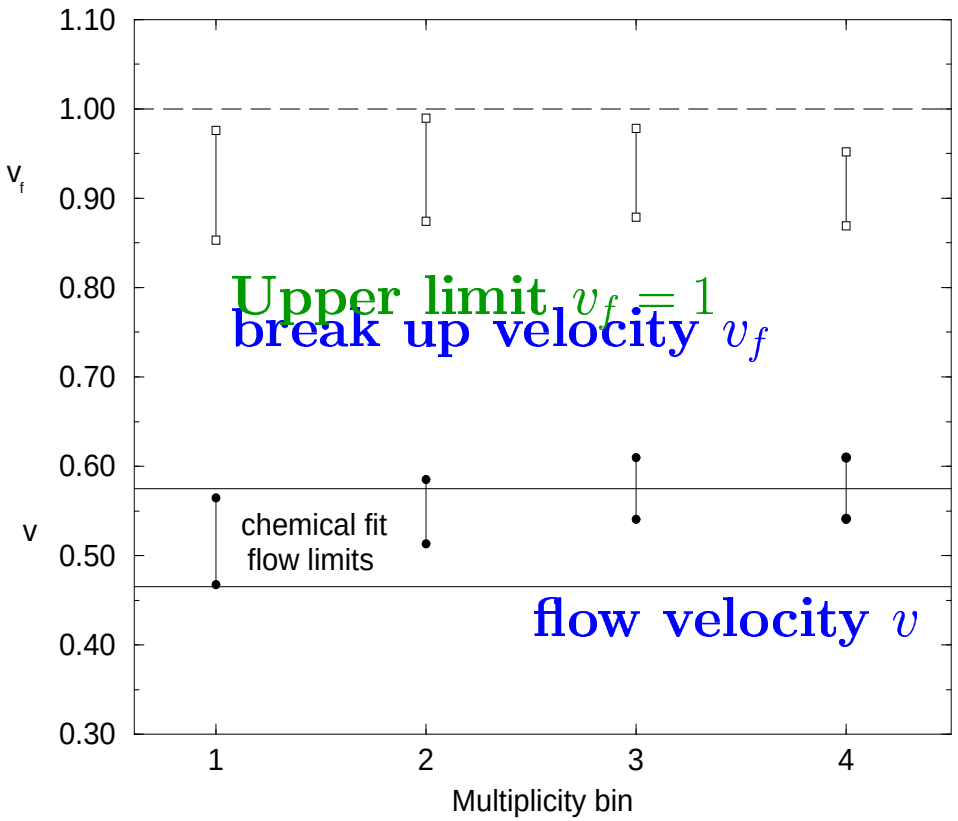

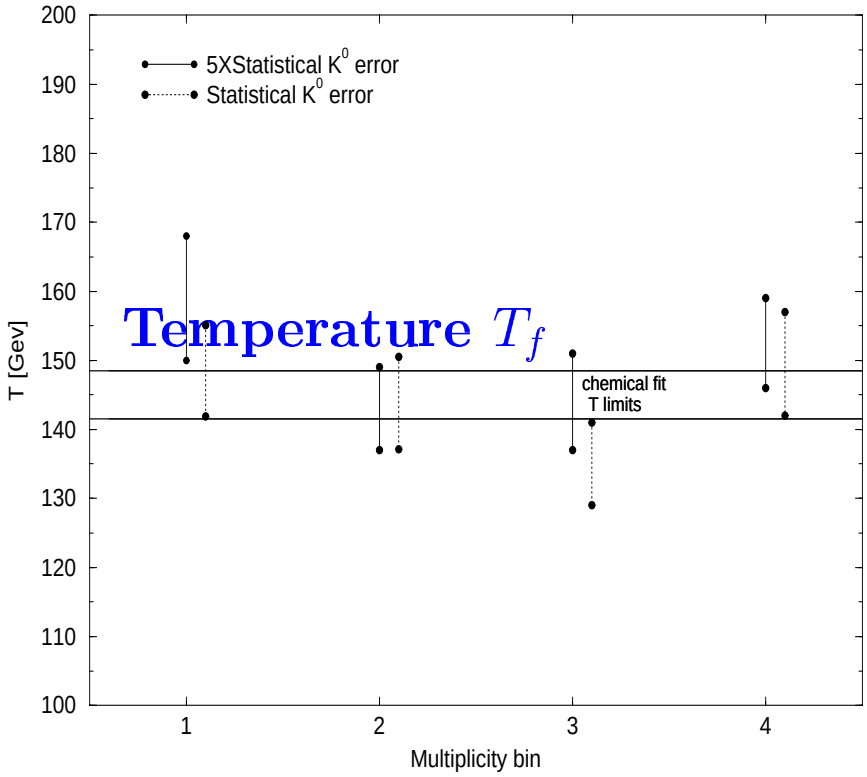

5 different collision centrality bins. We note flow velocity increase (within errors) with increasing size (centrality). Aside of this, there is no indication of a significant or systematic change of T, v, v_f with centrality, e.g. new state of matter is formed in all 4 centrality bins ($A > 100$). It will be interesting to see if the low centrality $A \simeq 50$ studied by experiment WA57 will show different freeze-out properties.

Strange hadron resonances PROBE sudden hadronization

direct experimental measurement!

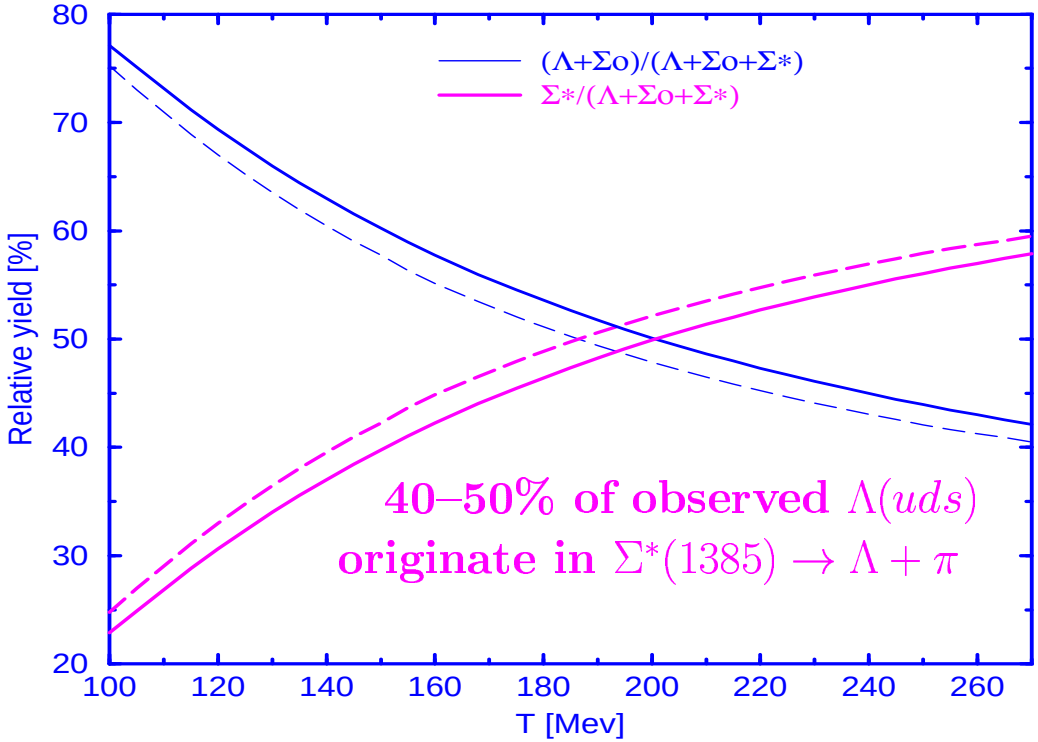

$\Sigma^*(1385) \to \Lambda + \pi$ **decay width of** $\Gamma_{\Sigma^*} = 35$ **MeV=1/(5.6 fm) assures that some decays occur within, and some outside the hadron matter – large fraction of decays within matter would be unreconstructable due to scattering of decay products. Same is true for observed** $\Gamma_{K^*(892)} = 50$ **MeV=1/(4 fm).**

Measured yields of $\Sigma^*(1385), K^*(892)$ **are IN GENERAL NOT the chemical freeze-out yields. Reduction by factor 2 for** K^* **probable. STAR results by P. Fachini .**

Other candidates for study $\Gamma_{\Lambda(1520)} = 15.6$**MeV=1/(12.6 fm). Complication: QUENCHING, metastable resonances such as** $\Lambda(1520)$ **may disappear.**

Direct Evidence for Resonance Free Space decay in Spectra Fits

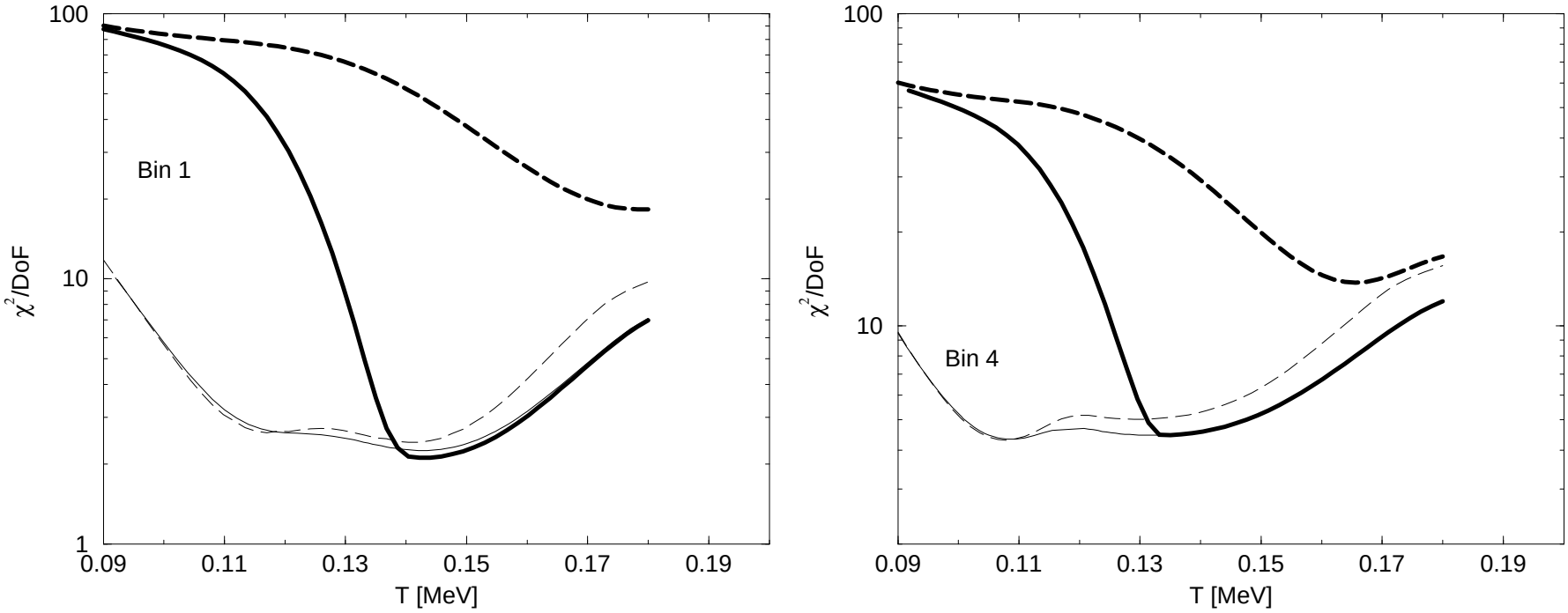

χ^2 profiles of fits to $m_\perp$ WA97 results for the four centrality bins, as function of temperature T. Solid lines are calculated assuming that the resonance decay products do not undergo rescattering, dashed lines assume the decay products rethermalize. Thin lines show profiles calculated without enforcing the limit $\gamma_q^2 \leq e^{\frac{m_\pi}{2T}}$, thick lines are obtained with this constraint enforced.

Problem: RESONANCE QUENCHING

IF DECAY IN FREE SPACE IS BLOCKED BY SUPERSELCTION RULE, QUENCHING IS EFFECTIVE! A possible explanation of $\Lambda(1520)$ suppression and/or nonobservation as reported by Ch. Markert for NA49 and STAR.

$$\pi + \Lambda(1520) \to \Sigma^* \to \pi + \Lambda\,,$$

Possible since $\Gamma_{\Lambda(1520)}$ is small due to need for angular $L = 2$ partial wave in its decay. If pion quenching is the right interpretation one can see the suppression increase with $d\pi/dy$ varying collision system, energy, and centrality.

Collisional quenching of a metastable state is a familiar phenomenon explored in several areas of physics. Elementary example: Stark mixing of metastable 2s state with 2p in atomic physics.

The decay of the $\phi(s\bar{s})$ has been the 'usual suspect' in search for such a quenching, given the proximity of the $K\overline{K}$ mass threshold ($m_\phi - 2m_K = 31,\ 23$ MeV), and the expected in medium modification of hadron masses.

Reconstructed line shape will sometimes know of the greater in-medium width, and sometimes not. In case of $\Lambda(1520)$ in-matter particle is 'different'. Thus effectively the production of normal $\Lambda(1520)$ is non-statistical, and the remaining small yield which is decaying outside of matter will be showing the natural width. In medium width can be observed ONLY if the in medium decay products can reach detectors.

Opaque scatterer and observable yields as function of t and T

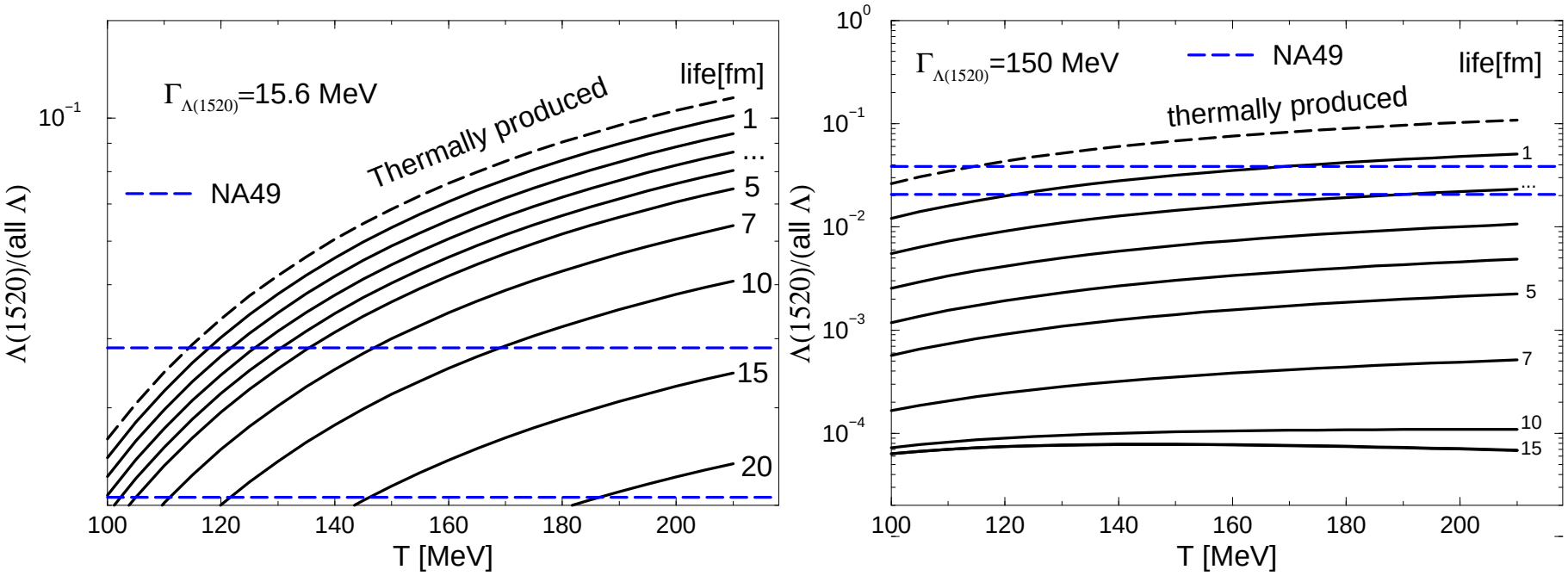

Relative $\Lambda(1520)/(\text{all }\Lambda)$ yield as function of freeze-out temperature T. Dashed - thermal yield, solid lines: observable yield for evolution lasting the time shown (1....20 fm) in an opaque medium. LEFT: natural $\Gamma_{\Lambda(1520)} = 15.6$MeV, RIGHT: quenched $\Gamma^*_{\Lambda(1520)} = 150$MeV. NA49 measures in $pp \simeq 0.11 \pm 0.02$, in Pb–Pb $\simeq 0.025 \pm 0.008$ (horizontal lines).

HOW TO FIX value of Γ^*?

Study TWO resonances; EXAMPLE

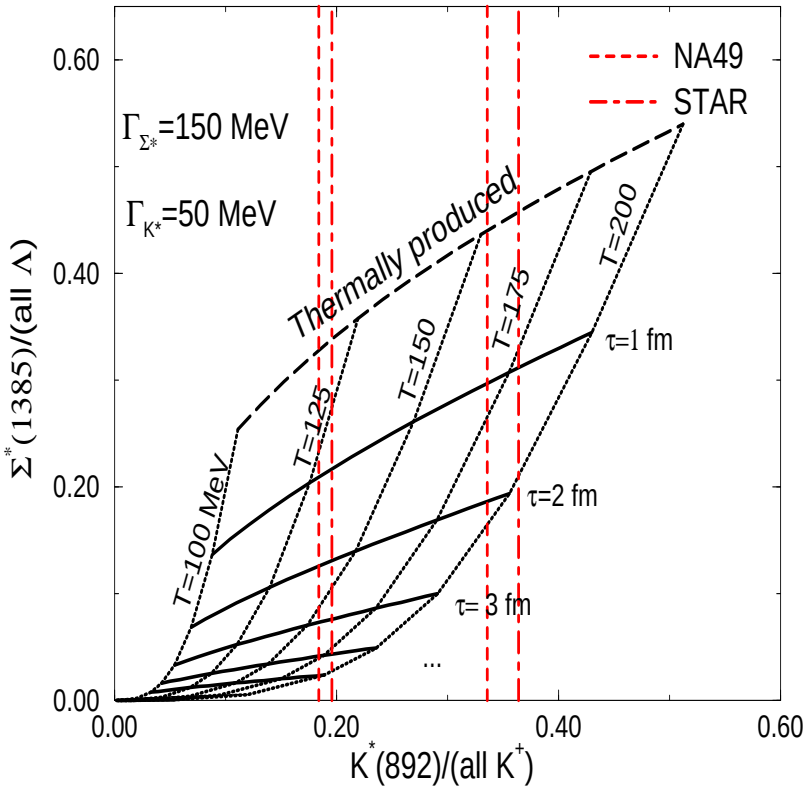

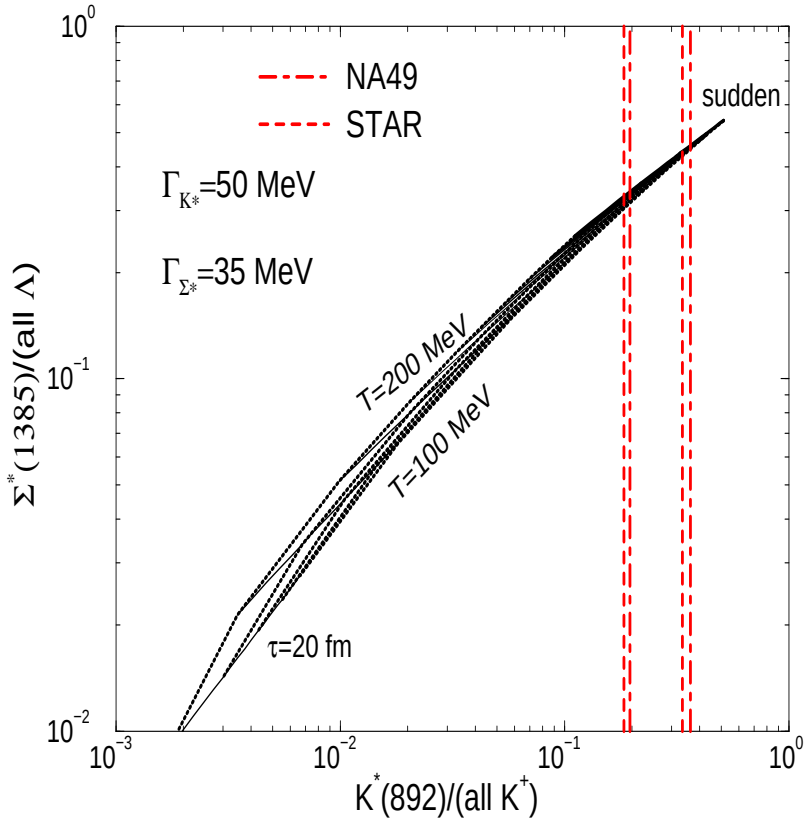

Dependence of the combined Σ^*/(all Λ) with $K^*(892)$/(all K) signals on the chemical freeze-out temperature and HG phase lifetime.
LEFT: quenched $\Gamma_{\Sigma^*} = 150$ **RIGHT natural widths**

END LECTURE 3

Quark-Hadron Universe

Our objective here is to study the Universe in the hadronic phase, in the range $300 < T < 5$ MeV in which the nearly free gas of quarks and gluons hadronizes and natimatter rich Universe annihilates into the final particle content as seen today.

Hadronization Point in the Universe

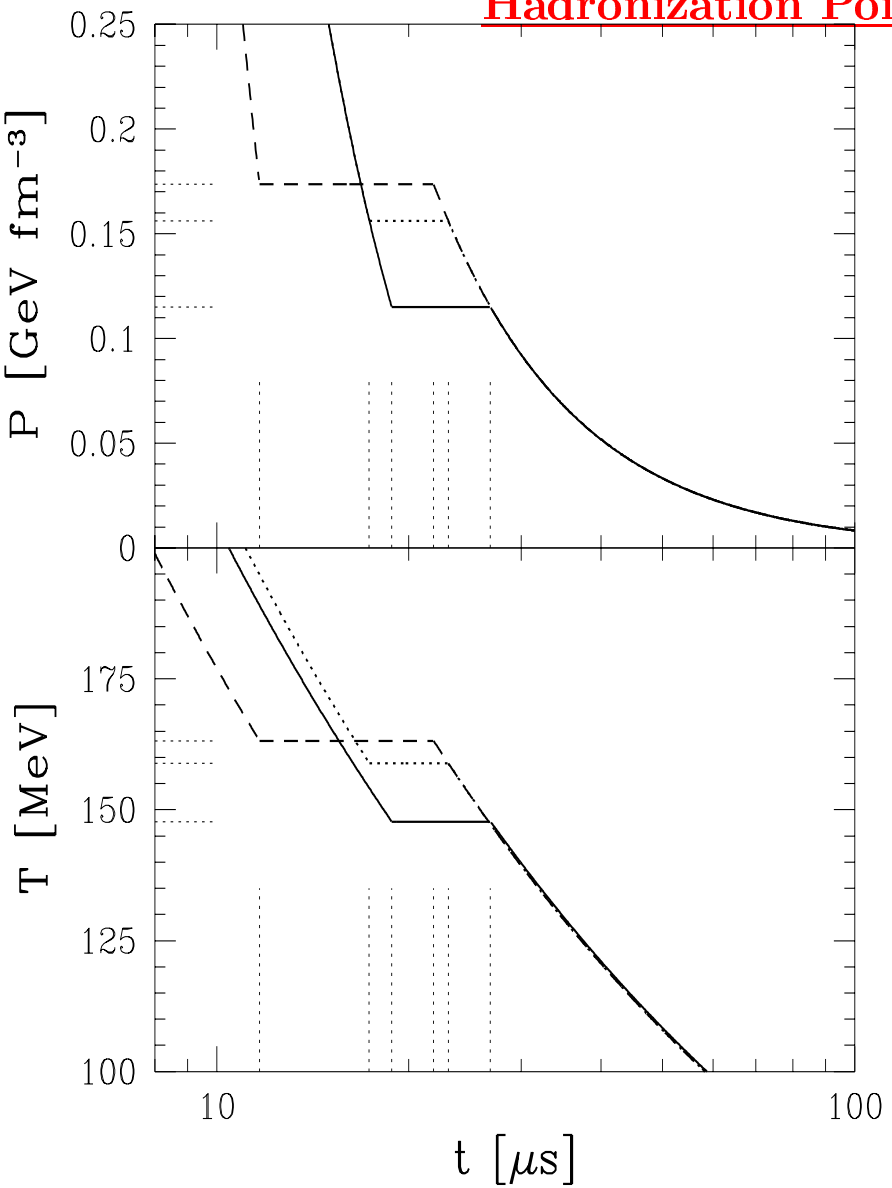

Two dynamical equations:

Entropy conserving expansion:

$$dE + P\,dV = T\,dS = 0, \quad dE = d(\epsilon V),$$

$$\frac{dV}{V} = \frac{3\,dR}{R}, \quad \frac{3dR}{R} = -\frac{d\epsilon}{\epsilon + P}.$$

Contraction of the Einstein equation in Freedman coordinates (Robertson-Walker Universe):

$$\mathcal{R}_{\mu\nu} - \tfrac{1}{2} g_{\mu\nu}\mathcal{R} + \Lambda_{\rm v} g_{\mu\nu} = 8\pi G T_{\mu\nu},$$

$$\epsilon = 3P + 4\mathcal{B}, \quad \dot{\epsilon}^2 = \frac{128\pi G}{3}\,\epsilon\,(\epsilon - \mathcal{B})^2,$$

Solution:

$$\epsilon_1 = \mathcal{B}\coth^2(t/\tau_{\rm U}),$$

TIME CONSTANT:

$$\tau_{\rm U} = \sqrt{\frac{3c^2}{32\pi G\mathcal{B}}} = 36\sqrt{\frac{\mathcal{B}_0}{\mathcal{B}}}\,\mu{\rm s}, \quad \mathcal{B}_0 = 0.19\,\frac{\rm GeV}{\rm fm^3}$$

Pressure (upper) and temperature (lower part) in the Universe, as function of time, in the vicinity of the phase transition from the deconfined phase to the confined phase. Solid lines, $\mathcal{B}^{1/4} = 195$ MeV; dotted lines, $\mathcal{B}^{1/4} = 170$ MeV (lower part) and $\mathcal{B}^{1/4} = 220$ MeV (upper part) all for $\alpha_{\rm s} = 0.6$.

TRACING μ IN THE UNIVERSE

Recent advances in the understanding of equations of state of QGP allow precise exploration of the conditions in which matter (protons, neutrons) formed. Neutrino osscilations essential!

Objective

1) Describe in quantitative terms the chemical composition of the Unvierse at hadronization:

$$T \simeq 160\,\mathbf{MeV} \qquad t \simeq 40\mu s,$$

2) Understand the quark-hadron phase transformation dynamics, baryon number distillation;

3) Describe the composition of the Universe during evolution towards the condition of neutrino decoupling

$$T \simeq 1\,\mathbf{MeV} \qquad t \simeq 10\,s$$

Chemical potentials

- **Photons in chemical equilibrium, assume the Planck distribution, implying a zero photon chemical potential; i.e., $\mu_\gamma = 0$.**
- **Because reactions such as $f + \bar{f} \rightleftharpoons 2\gamma$ are allowed, where f and $\bar{f}$ are a fermion – antifermion pair, we immediately see that $\mu_f = -\mu_{\bar{f}}$ whenever chemical and thermal equilibrium have been attained.**
- **More generally for any reaction $\nu_i A_i = 0$, where ν_i are the reaction equation coefficients of the chemical species A_i, chemical equilibrium occurs when $\nu_i \mu_i = 0$, which follows from a minimization of the Gibbs free energy.**
- **Weak interaction reactions assure:**

$$\mu_e - \mu_{\nu_e} = \mu_\mu - \mu_{\nu_\mu} = \mu_\tau - \mu_{\nu_\tau} \equiv \Delta\mu_l, \qquad \mu_u = \mu_d - \Delta\mu_l, \qquad \mu_s = \mu_d \ ,$$

- **The experimentally-favored "large mixing angle" solution is correct, the neutrino oscillations $\nu_e \rightleftharpoons \nu_\mu \rightleftharpoons \nu_\tau$ imply that:**

$$\mu_{\nu_e} = \mu_{\nu_\mu} = \mu_{\nu_\tau} \equiv \mu_\nu,$$

and the mixing is occurring fast in 'dense' matter.

- **There are three chemical potentials which are 'free' and we choose to follow the following: μ_d, μ_e, and μ_ν.**

- **Quark chemical potentials can be used also in the hadron phase, e.g. $\Sigma^0\,(uds)$ has chemical potential $\mu_{\Sigma^0} = \mu_u + \mu_d + \mu_s$**

- **The baryochemical potential is:**

$$\mu_b = \frac{1}{2}(\mu_p + \mu_n) = \frac{3}{2}(\mu_d + \mu_u) = 3\mu_d - \frac{3}{2}\Delta\mu_l = 3\mu_d - \frac{3}{2}(\mu_e - \mu_\nu).$$

Chemical Conditions

Three chemical potentials obtained solving the three available constraints:

i. *Charge neutrality* $(Q = 0)$ **is required to eliminate Coulomb energy. This implies that:**

$$n_Q \equiv \sum_i Q_i \, n_i(\mu_i, T) = 0,$$

where Q_i and n_i are the charge and number density of species i.

ii. *Net lepton number equals net baryon number* $(L = B)$ **is required in baryogenesis:**

$$n_L - n_B \equiv \sum_i (L_i - B_i) \, n_i(\mu_i, T) = 0,$$

iii. *Constant in time entropy-per-baryon* (S/B) **i.e. the Universe evolves adiabatically,**

$$\frac{\sigma}{n_B} \equiv \frac{\sum_i \sigma_i(\mu_i, T)}{\sum_i B_i \, n_i(\mu_i, T)} = 4.5^{+1.4}_{-1.1} \times 10^{10}$$

Entropy per Baryon in the Universe

$$\eta \equiv n_{\rm B}/n_\gamma = 5.5 \pm 1.5 \times 10^{-10}$$

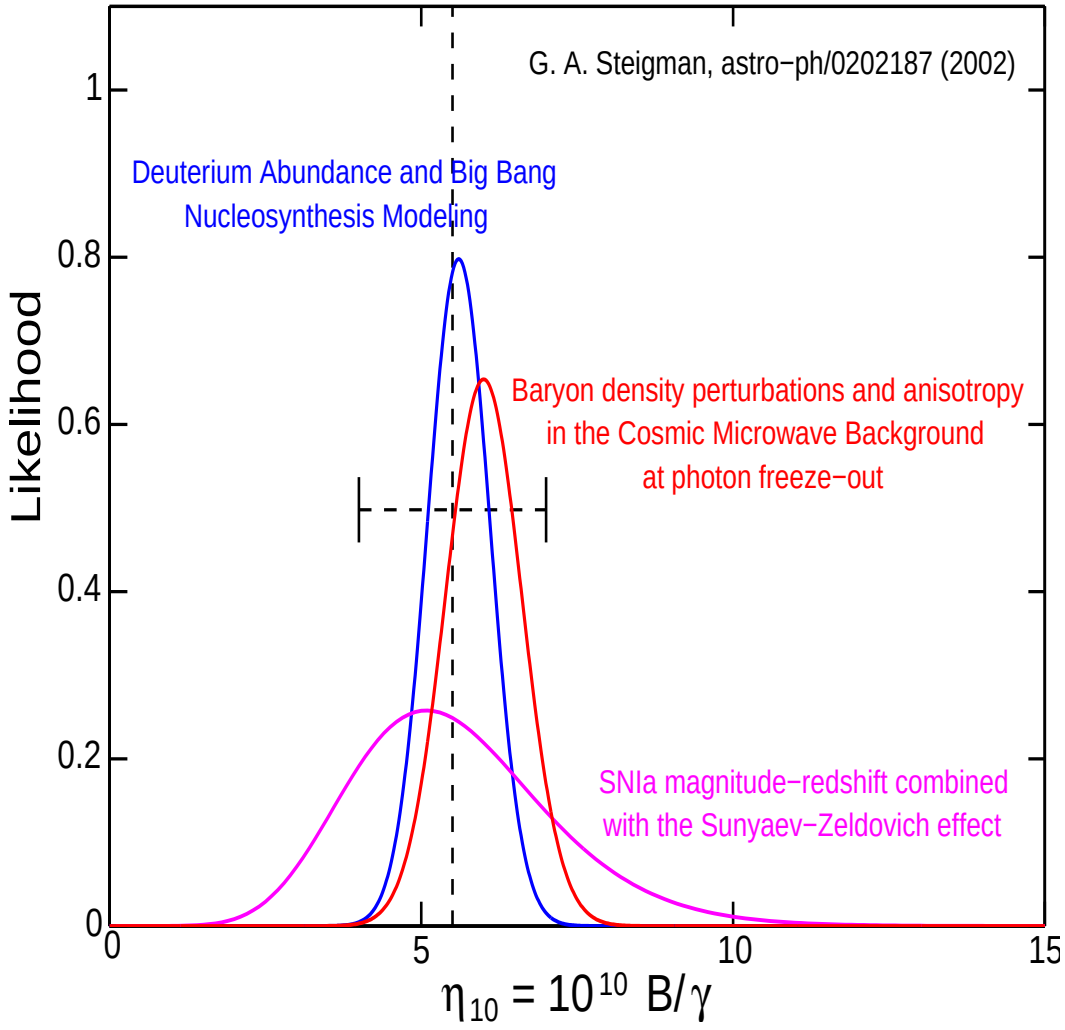

This yields $S/b \simeq 4.5\,10^{10}$

TRACING μ_d IN THE UNIVERSE

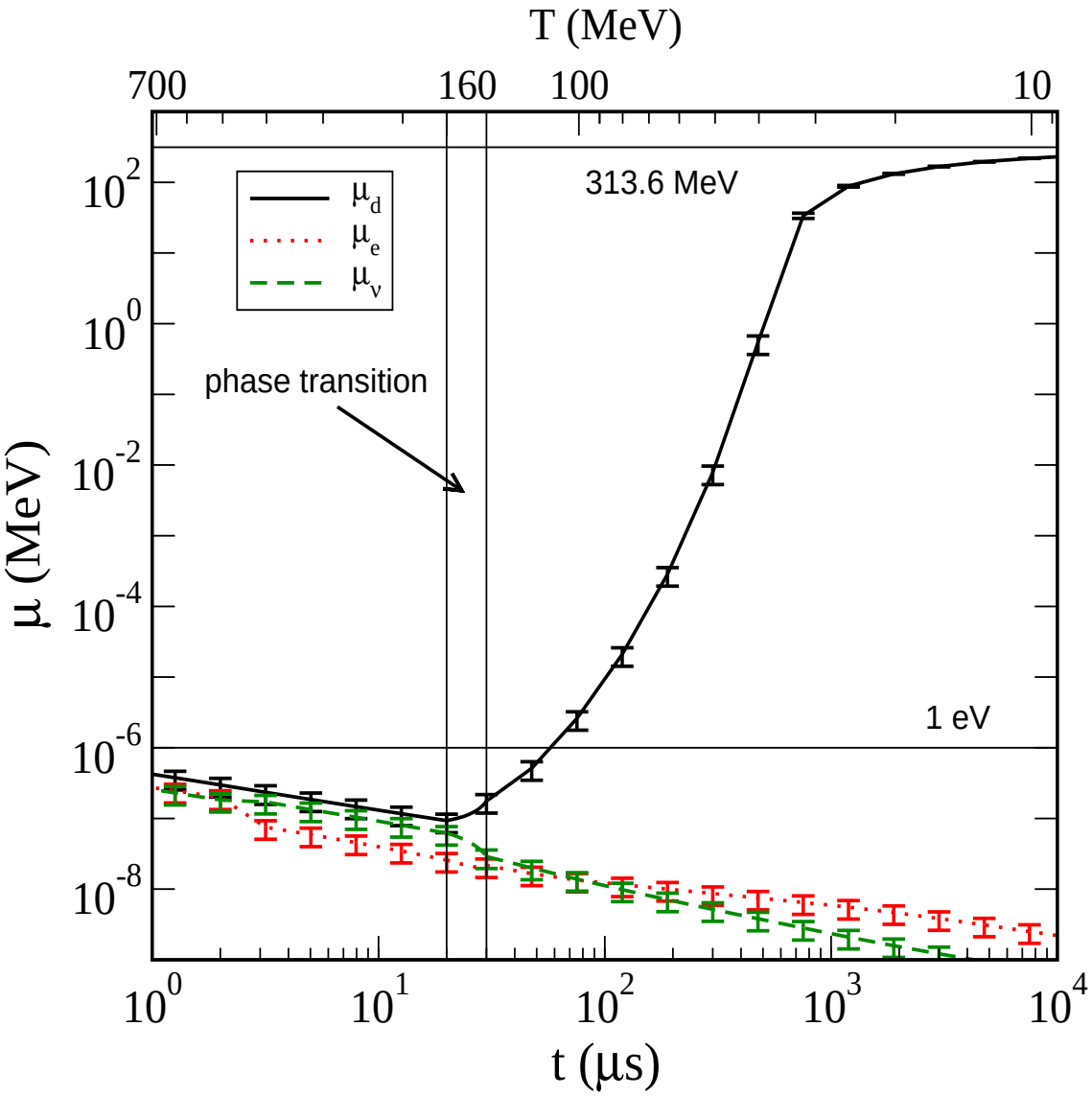

Minimum $\mu_b = 0.33^{+0.11}_{-0.08}$ eV.
μ_b relevant at final hadron $(\pi, \overline{N})$ freeze-out.

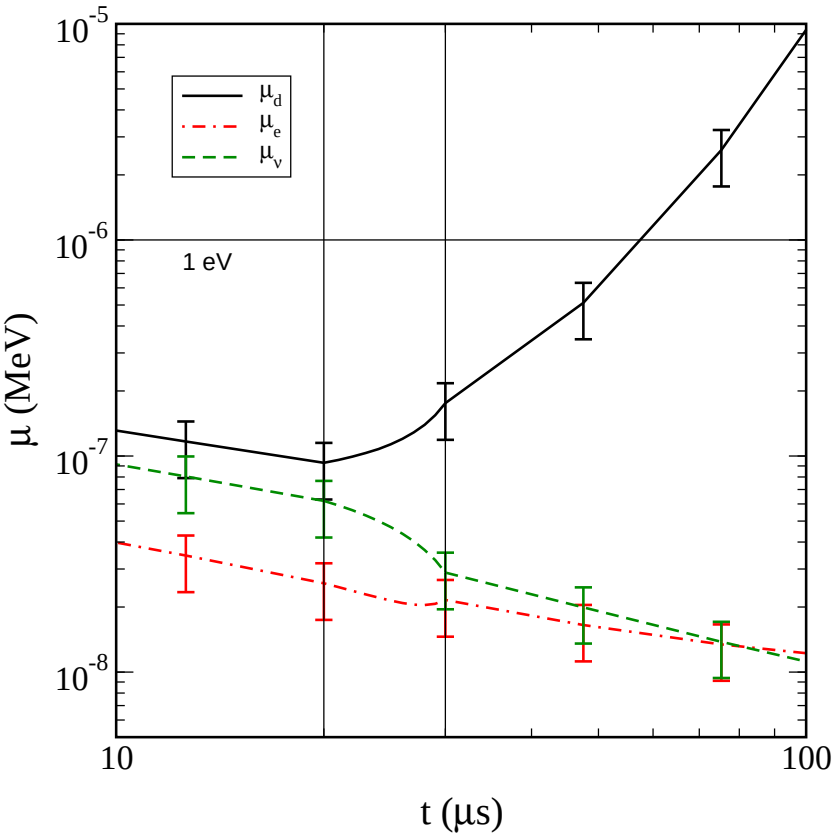

TRACING μ_d IN A UNIVERSE

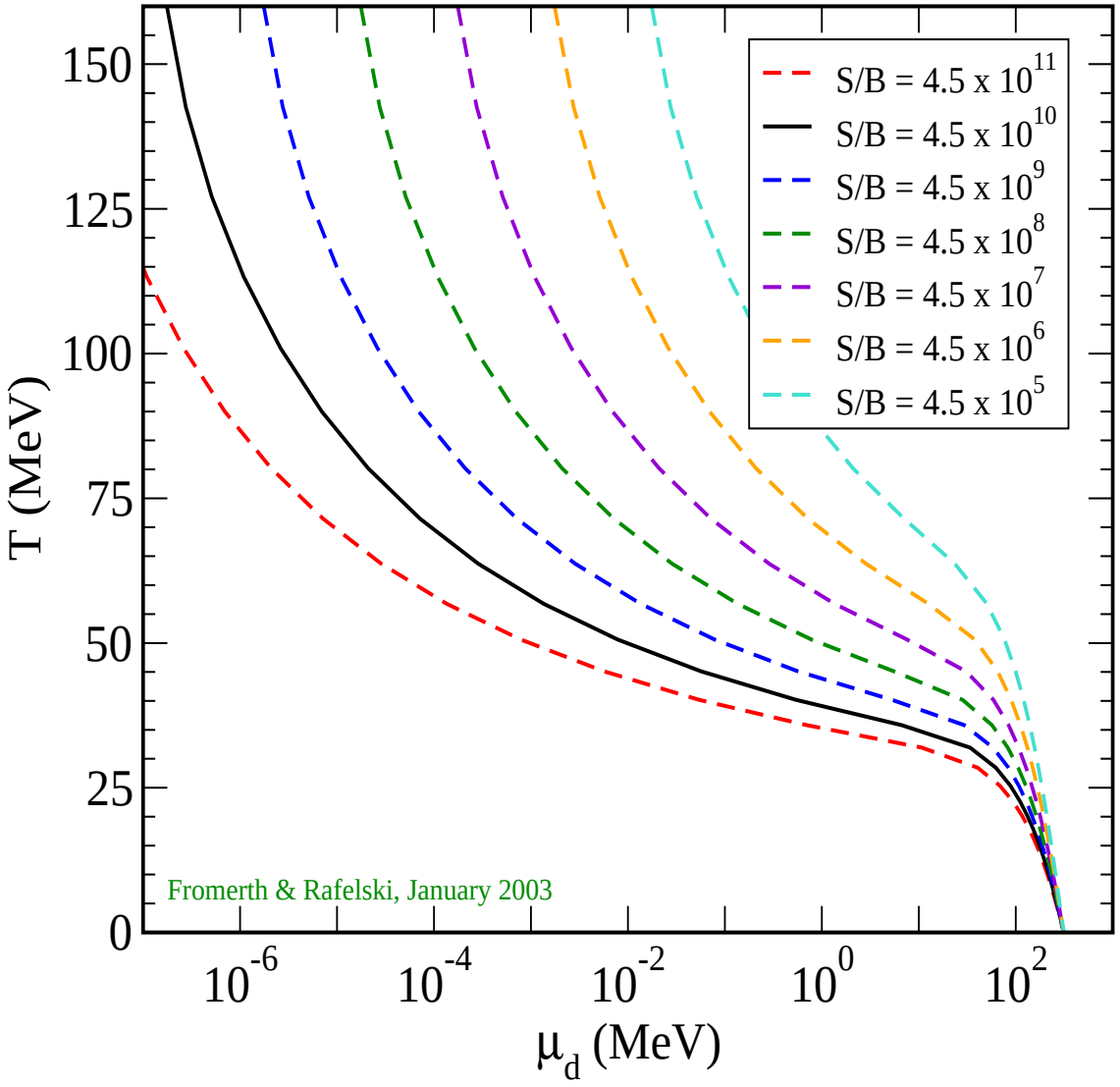

Mixed Phase

Many properties of the Universe jump as one compares QGP with Hadron Phase. Thus we introduce the mixed hadron-quak phase and parameterize the partition function during the phase transformation as

$$\ln Z_{\rm tot} = f_{\rm HG} \ln Z_{\rm HG} + (1 - f_{\rm HG}) \ln Z_{\rm QGP}$$

$f_{\rm HG}$ represents the fraction of total phase space occupied by the HG phase.

The three constraints are accordingly modified, e.g.:

$$Q = 0 = n_Q^{\rm QGP} V_{\rm QGP} + n_Q^{\rm HG} V_{\rm HG} = V_{\rm tot} \Big[(1 - f_{\rm HG}) n_Q^{\rm QGP} + f_{\rm HG} n_Q^{\rm HG} \Big[$$

where the total volume $V_{\rm tot}$ is irrelevant to the solution. Analogous expressions can be derived for $L - B$ and S/B constraints.

We assume that mixed phase exists $10\,\mu s$ and that $f_{\rm HG}$ changes linearly in time. Actual values wil require dynamic nucleation transport theory description.

Charge and baryon number distillation

Initially at $f_{\rm HG} = 0$ all matter in QGP phase, as hadronization progresses with $f_{\rm HG} \to 1$ the baryon component in hadronic gas reaches 100%.

The constraint to a charge neutral universe conserves charge in both fractions. Charge in each fraction can be finite.

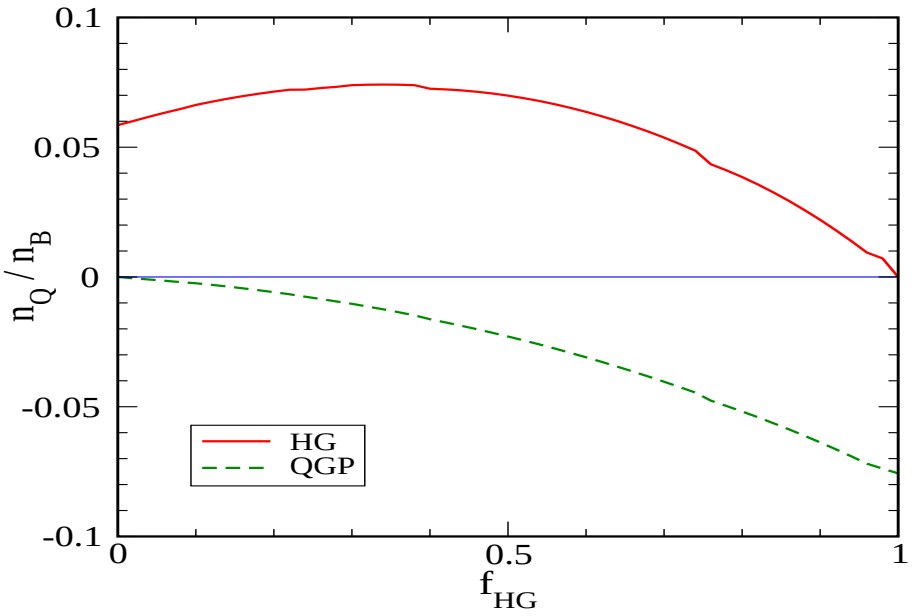

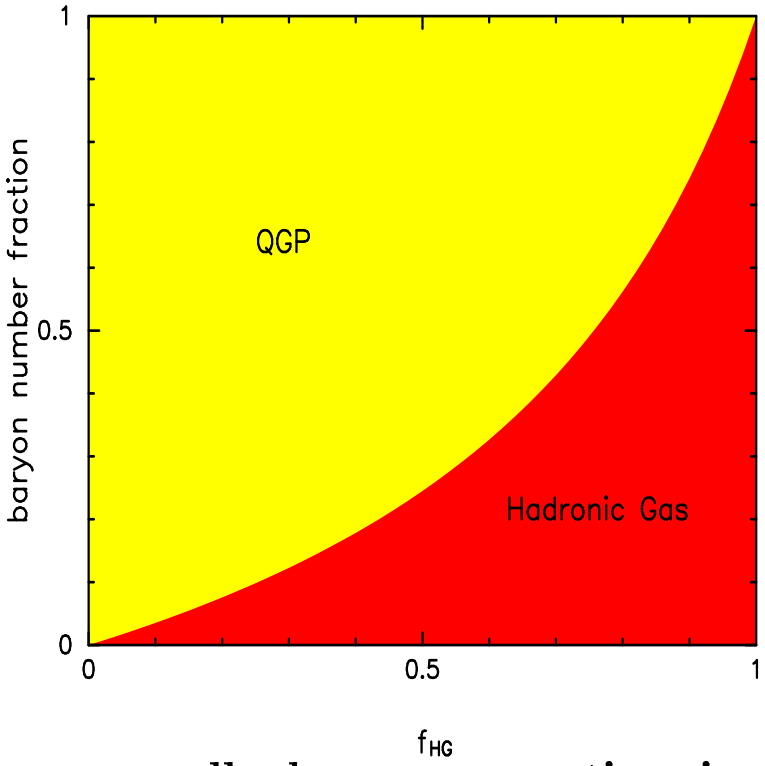

Even a small charge seperation introduces a finite non-zero Coulom potential and this amplifies the existnet baryon asymmetry. This mechanism noticed by Witten in his 1984 paper, and exploited by A. Olinto for generation of magnetic fields.

Hadronic Universe Particle Densities

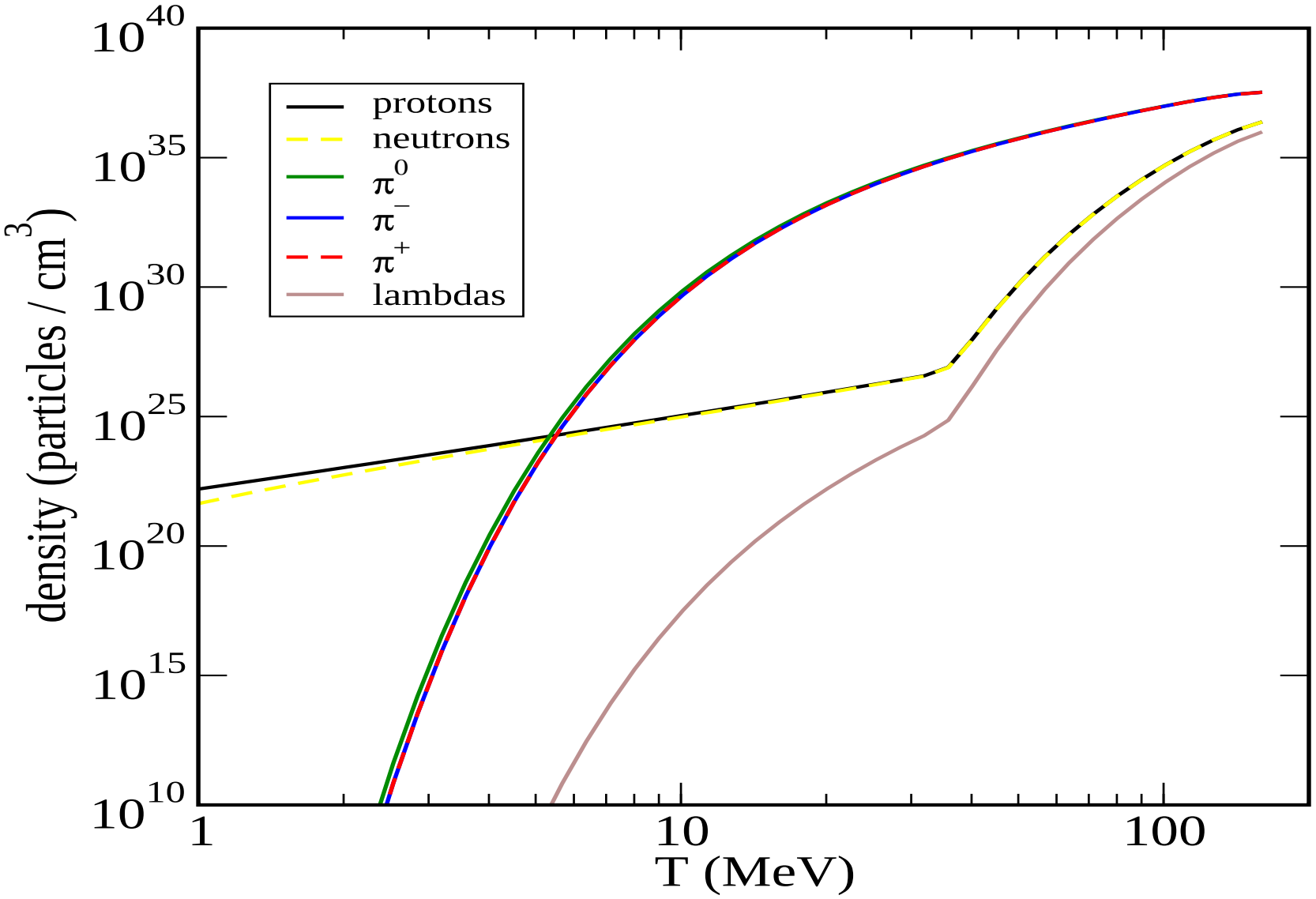

Energy in luminous hadronic Universe

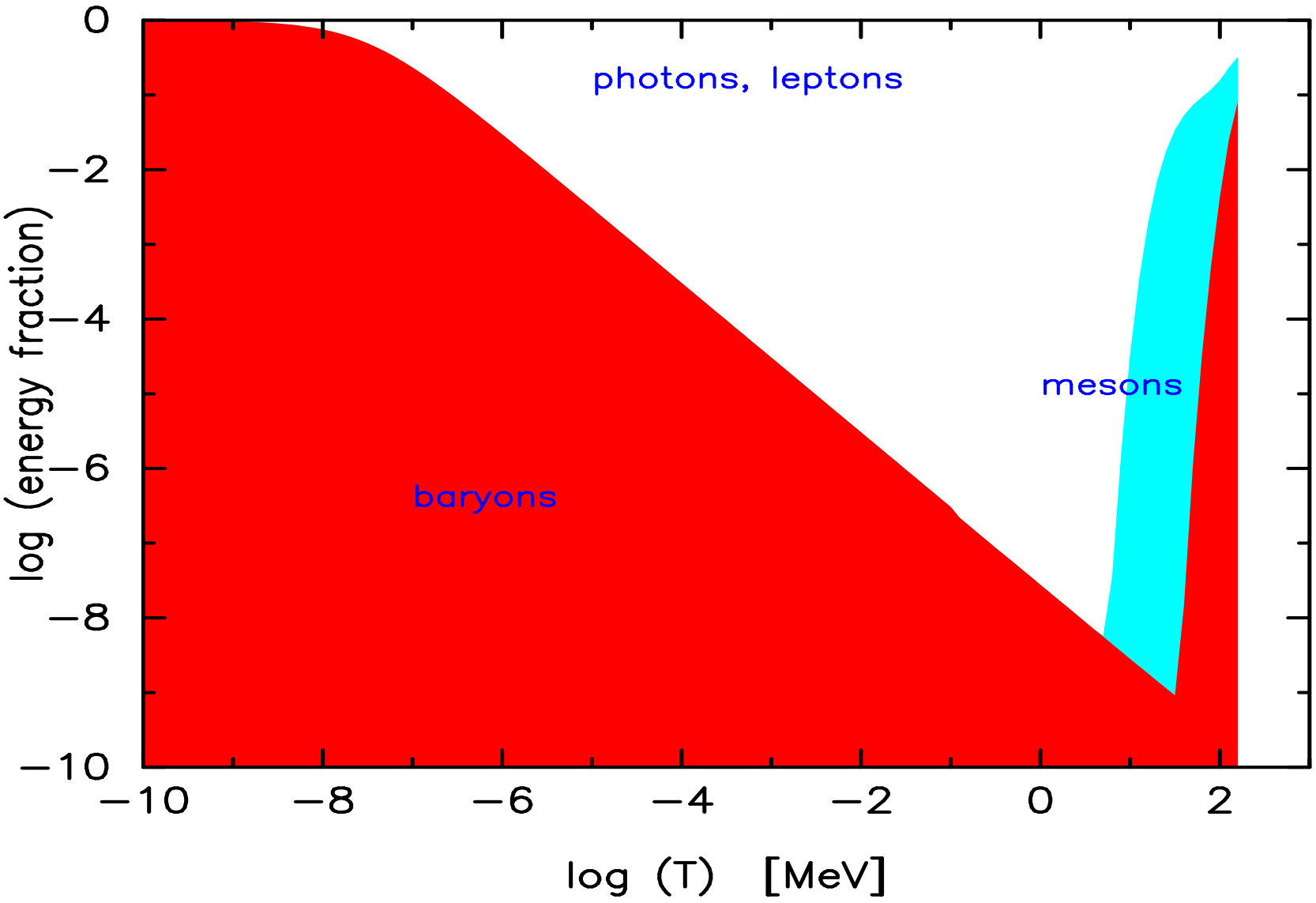

Other source of baryon asymmetry

What if the CPT is broken, the finite baryon number is supported by resulting particle-antiparticle mass asymmetry. In PDG the limit on mass differences is at the level of many eV. This is larger than the baryochemical potential required to sustain the asymmetry near phase transfromation. We explore this assuming that quark-anti-quark mass difference possible, is expresed as hadron mass difference and we found:

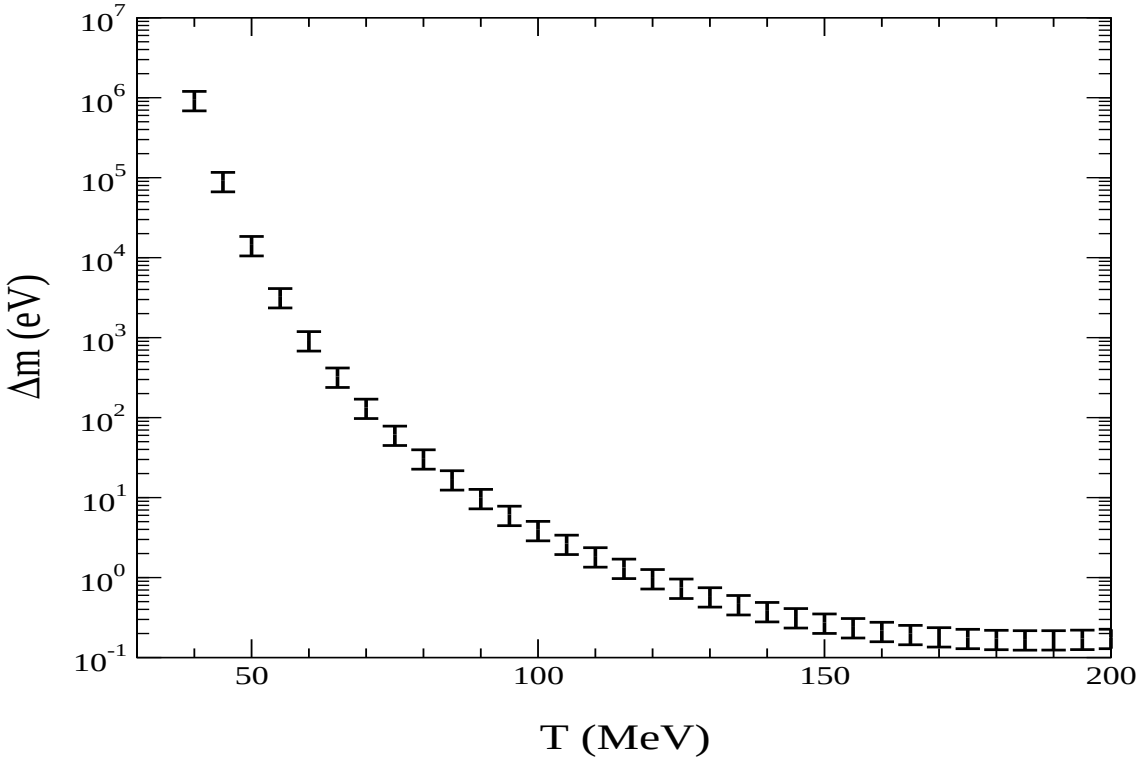

We found a better CPT limit on $m - \overline{m}$

We define the K_L and K_S states in the standard formalism (see e.g. Perkins):

$$K_L = \frac{1}{\sqrt{2+2\epsilon^2}}\left[(1+\epsilon)K^0 + (1-\epsilon)\bar{K^0}\right] \ , \ K_S = \frac{1}{\sqrt{2+2\epsilon^2}}\left[(1-\epsilon)K^0 - (1+\epsilon)\bar{K^0}\right] \ ,$$

where $K^0 = |d\bar{s}\rangle$, $\bar{K^0} = |\bar{d}s\rangle$, and $\epsilon = 2.07 \pm 0.28 \times 10^{-3}$ is the direct CP violation parameter.

We express the (assumed) CPT-violating mass difference between quarks and antiquarks as:

$$m_{s,\bar{s}} = m_s^0 \pm \frac{\delta m_s}{2} \qquad m_{d,\bar{d}} = m_d^0 \pm \frac{\delta m_d}{2} \ ,$$

where the signs of δm_s and δm_d are undetermined. The mass difference between K_L and K_S becomes:

$$\Delta m = \Delta m_w \ + \ 2\,\epsilon f\,\left[(m_{\bar{s}} - m_s) - (m_{\bar{d}} - m_d)\right]$$

where Δm_w is the second order WI mass difference which explains the known mass differnce in K_S–K_L, $\Delta m \equiv m_{K_L} - m_{K_S} = 3.463 \pm 0.010 \times 10^{-6}$ eV. $f \simeq 1$ expresses the response of Kaon mass to a small change in quark masses.

This means:

$$|(m_{\bar{s}} - m_s) - (m_{\bar{d}} - m_d)| \ \ll \ \frac{\Delta m}{2\epsilon f} \ \approx \ 10^{-3}\,\mathrm{eV}\ .$$

We find that the current upper limit to the mass difference between quarks and antiquarks in the d and s flavors is $\ll 10^{-3}\,\mathrm{eV}$ if the magnitude of the CPT violation is uncorrelated across flavors. In this case, the relative precision with which the strange quark mass difference is determined appears to be by far the most precise such value presently known:

$$\left|\frac{m_s - m_{\bar{s}}}{m_s + m_{\bar{s}}}\right| \ll 10^{-11}\,,$$

providing a strong constraint for any CPT model considered. Also, we excluded the possibility that the quark mass differnce is associated with baryon asymmetry in the early Universe.

FINAL REMARKS

First CERN-SPS and now BNL-RHIC offer laboratory tool to study the early Universe at $t = 10\,\mu s$

Strangeness: a fingerprint a new state of matter

SUPERCOOLED QGP FIREBALL BREAKS SUDDENLY

We begin to transfer the 'know-how' from the study of nuclear collisions to the study of the early Universe

---